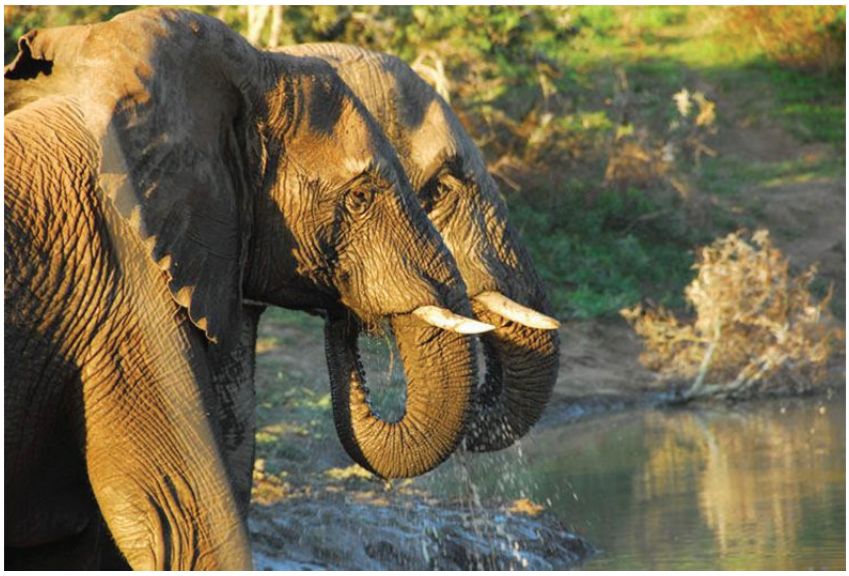

6th South African Conference on Photonic Materials

4 - 8 May 2015

Mabula Game Lodge, South Africa

Programme & Book of Abstracts

Fisika by KOVSIES/ Physics at KOVSIES
Moenie ophou droom nie!/ Don't stop dreaming!

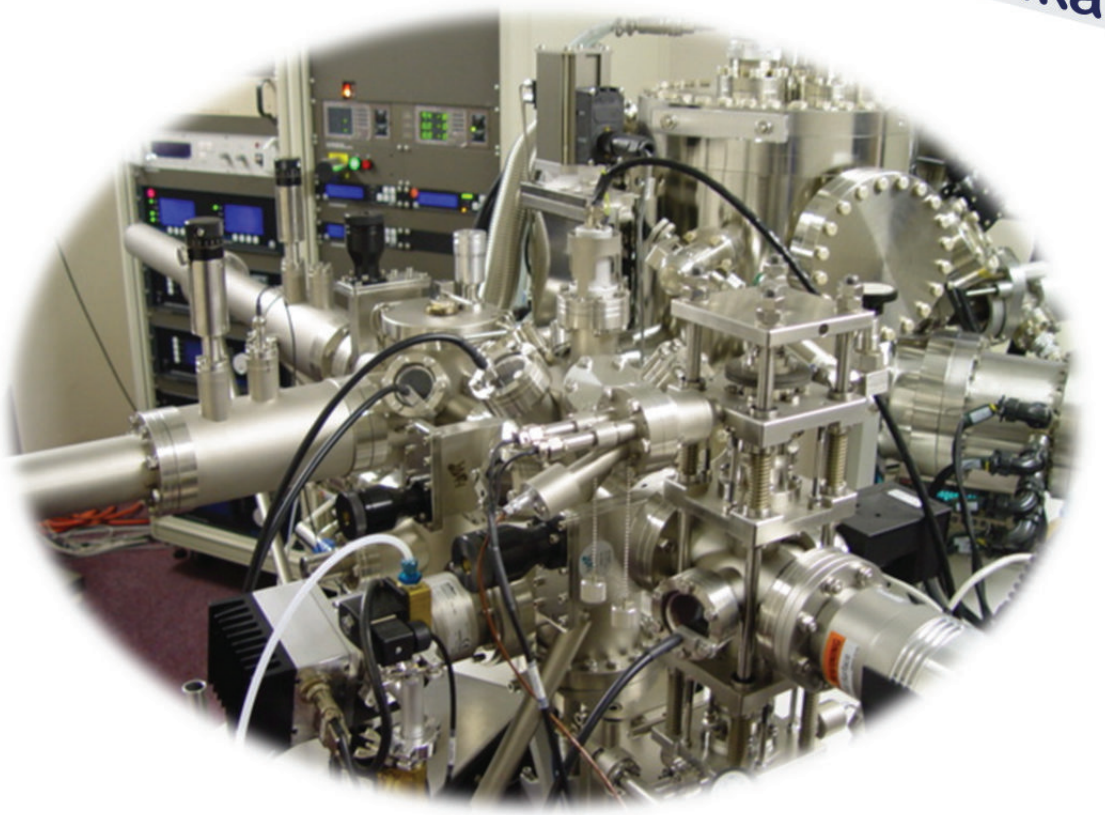

UNIVERSITY OF THE
FREE STATE
UNIVERSITEIT VAN DIE
VRYSTAAT
YUNIVESITHI YA
FREISTATA

UFS·UV
NATURAL AND
AGRICULTURAL SCIENCES
NATUUR- EN
LANDBOUWETENSKAPPE

Posbus 339, Bloemfontein, 9300 ● Tel: (051) 401 2321 ● E-pos: swarthc@ufs.ac.za ● www.ufs.ac.za/physics

Sponsors

UNIVERSITEIT VAN PRETORIA
UNIVERSITY OF PRETORIA
YUNIBESITHI YA PRETORIA
Denkleiers • Leading Minds • Dikgopolo tša Dihlalefi

Nelson Mandela Metropolitan University
for tomorrow

UNIVERSITY OF THE FREE STATE
UNIVERSITEIT VAN DIE VRYSTAAT
YUNIVESITHI YA FREISTATA

UFS·UV
NATURAL AND AGRICULTURAL SCIENCES
NATUUR- EN LANDBOUWETENSKAPPE

South African Institute of PHYSICS
THE VOICE OF PHYSICS IN SOUTH AFRICA

african laser centre

SMM INSTRUMENTS (PTY)LTD

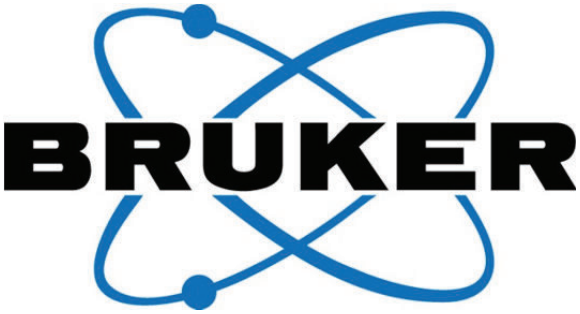

BRUKER

ZEISS

Hitech Lasers
Leading with Quality

VACUTEC

Table of Contents

Organising Committee

Conference Chair	Dr. Jackie Nel	UP
Conference Co-chair	Prof Hendrik Swart	UFS
Finance	Prof. Walter Meyer	UP
Programme	Johan Janse van Rensburg	UP
Proceedings Editor	Prof Hendrik Swart Dr. Jackie Nel Prof. Reinhardt Botha	UFS UP NMMU
Transport	Mr. Matshisa Legodi	UP
Advertising & Sponsors	Dr. Jackie Nel Prof Japie Engelbrecht	UP NMMU
Website	Prof. Ted Kroon Johan Janse van Rensburg	UFS UP
Additional Members	Prof Koos Terblans Prof Martin Ntwaeaborwa Prof Japie Engelbrecht Prof Ernest van Dyk Dr. Mmantsae Diale	UFS UFS NMMU NMMU UP

South African Institute of Physics

Mr. Brian Masara (Executive officer)
Mr. Roelf Botha (Indico system)

List of Sponsors & Advertisers

Sponsor	Website
African Laser Centre	www.africanlasercentre.com
Bruker South Africa	www.bruker.com/za
Department of Physics, Nelson Mandela Metropolitan University	physics.nmmu.ac.za
Department of Physics, University of Pretoria	www.up.ac.za/physics
Department of Physics, University of the Free State	www.ufs.ac.za/physics
Hitech Lasers	www.hitechlasers.co.za
SMM Instruments	www.smmafrica.com
Vacutec	www.vacutec.co.za
Zeis South Africa	www.zeiss.co.za

Message from SAIP President

Remarkable progress is being made across South Africa in photonic materials at present. What makes this tick?

First of all, the presence of top researchers and bright students is clearly essential. Their exertions must be underpinned by a sound national science infrastructure and also by stable, intelligent universities which display foresight and initiative. In the present climate, it is essential that both university administrators and government decision-makers recognise the importance of an attractive environment for top researchers. It is too easy for university work to become one-half research, one-half teaching, and one-half administration. Likewise, the temptation to funding agencies to demand reports at decreasing intervals places a burden on thinkers and inventors that is not associated with pushing back the frontiers of useful human knowledge.

Why are photonic materials important to South Africa and Africa? It has been demonstrated throughout Africa that this is a challenging and very productive research field, and also a sector of Applied Physics with high-value-added business potential, particularly for small high-tech firms in fields from materials processing and coating, to diagnostics and imaging. Photonics is the field closest to solving the potential internet crunch, estimated to be in about 2020. Entanglement and encryption are realities that are being exploited already. Surface functionalization of optical fibres has implications for diagnostics from the biosciences and health sciences, to diesel degradation sensors. It's a field with so much excitement and novel application that it is almost pyrotechnic.
The study of light has fortunately remained as a topic in the chaotic South African school curriculum, and the hope is that this syllabus and its surrounding processes will stabilise in time towards a useful preparation for university. Most demonstrations using light and lasers are entrancing to students and certainly give rise to "Aha!" phenomena associated with many career choices – here is mathematics, sometimes at a seemingly abstruse level, at its most beautiful.

I'm glad that the SAIP Division for Physics of Condensed Matter and Materials and the Applied Physics Forum, with the Photonics Division, form a co-hosting basis for this very important event in the Physics Calendar of the region. On behalf of the South African Institute of Physics, welcome to the 6th South African Conference on Photonic Materials, and I wish you a meeting filled with leaps of enlightenment, multiple modes of thought, detanglement of issues, Delightfully Functional Theories, and the stimulated emission of ideas.

Irvy (Igle) Gledhill
SAIP President

Invited Plenary Speakers

André Vantomme

Instituut voor Kern- en Stralingsfysica, Leuven, Belgium

André Vantomme obtained his PhD degree from KU Leuven, Belgium, in 1991 after which he spent two years as a postdoctoral researcher at the California Institute of Technology, Pasadena. Since 1997, he is a professor in nuclear solid state physics in Leuven, where he built up his research group. His research focuses on unravelling the intimate link between the structure and the functional properties of low-dimensional materials – down to the atomic level.
Besides using 'conventional' characterization techniques to investigate these systems, his research has greatly benefited from applying nuclear techniques, which provide complementary information on structure or functionality, often down to the single atom. These techniques are either based on (stable or radioactive) ion beams or on hyperfine interactions. He is leading the Ion and Molecular Beam Laboratory in Leuven, a unique facility where 3 accelerators are in situ coupled to two molecular beam epitaxy set-ups as well as to a wide scala of (surface-sensitive) characterization techniques. This experimental facility is complemented by frequent experiments at large scale facilities such as ESRF, ISOLDE-Cern, APS, ILL and iThemba LABS.
Throughout the past 25 years, André Vantomme has been active in the field of thin film growth mechanisms (with emphasis on silicide and germanide thin films, including ternary systems), magnetic, superconducting and optical properties of thin films and nano structures, and doping of semiconductors, including investigating the lattice site of implanted species.
Besides conducting research, he also enjoys teaching physics, including training young researchers. So far, he has been promotor of 37 finished or ongoing PhD students. Furthermore, he is serving the international scientific community via membership in or chairing of various councils, boards and commissions.

Talk: Lattice location of dopants in group-III nitrides and ZnO
Abstract p. 2

Adi Salomon

Chemistry Department, Institute of Nanotechnology, Bar-Ilan University, Israel

Adi Salomon obtained her B.Sc. in Chemistry from Tel Aviv University and received her PhD from the department of Materials and Interfaces at Weizmann Institute of Science with David Cahen. There she got a scientific background on surface chemistry, semiconductors and electron transport through organic molecules. Then she went to ISIS, Strasbourg, working with Thomas Ebbesen on Interaction between molecules and surface plasmons. Her research was the first to demonstrate the dynamics of interaction between surface plasmons and molecules throughout the development of a new surface photochemistry. Later on, at the WIS, together with Yehiam Prior, Tamar Seideman, Robert Gordon and Maxim Shukaharev, they have developed a new model to explain interactions between molecules which are immersed in the 'plasmonic field'. Current research in Salomon's lab is on interaction between molecules at light at the nano scale, and real time imaging of electrodes surfaces as part of INREP group.

Talk: Plasmonic systems and their Interaction with Molecules
Abstract p. 7

Valentin Craciun

National Institute for Laser, Plasma and Radiation Physics, Romania

Valentin Craciun obtained his Diplomat Engineer degree from the Physics Faculty, University of Bucharest in 1984 with a thesis on Laser annealing of semiconductors and a PhD degree from the Polytechnic University Bucharest in 1991 with a thesis on Surface studies with laser for microelectronic applications. After a post-doc stage at University College London in Prof. I. W. Boyd's group studying low temperature UV-assisted oxidation of semiconductors and a visiting scientist position at the University of Orleans in Prof. Chantal Leborgne's group he returned in 1995 to the National Institute for Laser, Plasma and Radiation Physics in Bucharest where he continued his work on laser processing and characterization of thin films. He was a graduate faculty and associate research scientist in the Materials Science and Engineering Department, University of Florida, USA from 2003 till 2012, when he returned back to NILPRP, where now he is the head of the Laser Department and the President of the Scientific Council. He has more than 30 years' experience in the area of laser processing of materials, pulsed laser deposition of thin films, synthesis and characterization of carbide, nitride and oxide thin films, nanostructures and devices. He has acquired international recognition in these areas, by publishing more than 170 articles in ISI-indexed journals with high impact factors that have been cited more than 1600 times (h index = 27), delivering more than 50 invited talks and seminars, organizing 12 international conferences, chairing sessions and being member of numerous international conferences scientific committees. He has been the principal investigator for 5 national and international projects totalling more than 2,000,000 Euro research funds in the last two years in the area of transparent and conductive oxides, thin carbide films for nuclear applications, high emissivity optical coatings, hard and protective coatings, 1 bilateral project and mentor for 2 postdoctoral national projects.

Talk: Characteristics of amorphous transparent and conductive oxides grown by combinatorial pulsed laser deposition
Abstract p. 10

Rienk van Grondelle

Vrije Universiteit Amsterdam, Netherlands

Rienk van Grondelle received his PhD 1978 in the Biophysics group of Leiden University under the supervision of Lou Duysens. After a postdoc at the University of Bristol (with Owen Jones) he returned to Leiden and became involved in ultrafast spectroscopy. In 1982 he moved to VU Amsterdam where in 1987 he was appointed as full professor in Biophysics. He is one of the most influential experimental physicists working on the primary physical processes of photosynthesis world-wide. Using the tools of ultrafast spectroscopy he has made major contributions to elucidate the fundamental physical mechanisms that underlie photosynthetic light harvesting and charge separation. He has developed theoretical tools to infer the effective electronic and molecular structure and dynamics from complex spectroscopic data. His work recently led to a fundamental new understanding of light-driven charge separation in the oxygen evolving photosynthetic reaction center of plants. Using multi-dimensional electronic spectroscopy he was able to show that in photosynthesis ultrafast charge separation is driven by specific molecular vibrations that allow electronic coherences to stay alive. Five years ago he proposed an explicit molecular model for photoprotection and demonstrated that the major plant light harvesting complex operates as a nanoswitch, controlled by its biological environment. These results, of utmost importance for our understanding of photosynthesis, inspire technological solutions for artificial and/or redesigned photosynthesis, as a possible route towards sustainable energy production on a global scale. He has published 532 papers in international, peer reviewed journals that in total have attracted over 22 thousand citations (h-index 77). In addition he is the co-author of three textbooks: Environmental Physics (3rd edition), Environmental Science and Photosynthetic Excitons. The latter has attracted close to 750 citations.

Talk: The Quantum Design of Photosynthesis
Abstract p. 15

Tjaart Krüger

Department of Physics, University of Pretoria, South Africa

Tjaart completed his M.Sc at Potchefstroom University and then went to Amsterdam where he obtained his PhD in Biophysics cum laude in 2011 from the Vrije Universiteit Amsterdam. His specialization is on the primary steps of photosynthesis and in particular the spectroscopic characterization of Light-Harvesting complexes of various photosynthetic organisms. He has 20 journal publications, a couple of chapters in books and a number of invited keynote lectures amongst his many conference presentations. Tjaart joined the University of Pretoria in 2013, where he currently heads the Biophysics research group at the University of Pretoria, and he is also currently the Chair of the South African Institute of Physics (SAIP) Biophysics Initiative.

Talk: Making every photon count - optical nanoscopy and single molecule spectroscopy applied to natural light-harvesting materials
Abstract p. 16

David Cahen

Weizmann Institute of Science, Israel

David Cahen's main research interests lie in exploring chemical means to control the electronic and optical properties of materials. He has had a keen interest in solar energy conversion ever since participating in the first Earth Day as a beginner PhD student, and in earlier studies co-invented and developed a solar cell, a device that uses solar energy to generate electrical power, of a new type – one that also stores electricity. He also contributed to the understanding and assessing the efficiency of the photosynthetic apparatus of plants and algae. His atomic-level research has helped to define the chemical limits of semiconductor miniaturization and contributed significantly both to the basic understanding and the practical use of several types of solar cells. His current research is aimed at understanding how simple organic molecules and complex biomolecules, such as proteins, can function as optical-electronic materials, how they can work in devices such as solar cells and sensors, and how to improve solar cells, in terms of materials and use of light.

Talk: Proteins as opto-electronic materials?
Abstract p. 17

Eduard Hulicius

Institute of Physics, Czech Republic

Eduard Hulicius obtained his diploma in physics from the Czech Technical University in Prague in 1973 and his CSc. (PhD. equivalent), in the Semiconductor Dept. of the Institute of Solid State Physics, later Institute of Physics of the Czechoslovak (later Czech) Academy of Sciences in 1981. He is currently Research Professor in the Department of Semiconductors and is head of MOVPE laboratory at the same institution. He has authored and co-authored 340 publications in scientific journals and also has several popular articles in newspapers, journals, radio and TV. He has also been on numerous scientific and organising committees for conferences and is a member and was both Vice chairperson and Chairperson of the Scientific Council of Institute of Physics of Czech Acad. of Sci. a few years back. He has been contractor or co-ordinator of more than 30 Grant projects and has been a participant in 11 other projects in the last 21 years. The projects are from three fields: Semiconductor lasers, LEDs and laser structures; Porous-Si and MOVPE technology, AIIIBV layers, nanostructures and devices. Eduard Hulicius has more than 50 industrial collaborations in Czech Rep., Europe, and USA - these are mainly in the field of semiconductor lasers and diodes.

Talk: Preparation and measurements of MOVPE multiple InAs/GaAs/GaAsSb quantum dot structures for the telecom wavelength region emitted from 1.3 to 1.8 μm
Abstract p. 18

Francis Chi-Chung Ling

University of Hong Kong,China

Francis Chi-Chung Ling received his Ph.D. degree from The University of Hong Kong in 1996, with the thesis title “Positron Annihilation Spectroscopic Studies of GaAs and InP Related Systems”. He then joined the same university as a Lecturer, and became the Assistant Professor in 2000. He is now the Associate Professor of The University of Hong Kong. Ling was elected a Fellow of The Institute of Physics (F. Inst. P.), U.K. in 2006. His research activities fall in the regime of semiconductor physics, which include optoelectronic and defects in semiconductors. In recent years, particular emphasis is placed in understanding the defects in oxide-based semiconductors, and their relations with the materials electrical, optical and magnetic properties. He has supervised 7 Ph.D. and 18 M.Ph. students. Ling has published 116 peer-reviewed papers in international journals.

Talk: Defects in Zinc Oxide Grown By Pulsed Laser Deposition
Abstract p. 23

Jens Birch

Linköping University,Sweden

Jens Birch is professor in Thin Film Physics at Linköping University (LiU). His research has focused at understanding the physics and materials science behind creation of new, previously unknown materials, with unique properties, in the form of artificial nanometer sized layers and 3D nanostructures. Typical dimensions of the structures range from sub-nm to a few tenths of nm. The materials range from amorphous metals to group III-nitride semiconductors, with diverse applications such as X-ray optics, piezoelectric devices, and optoelectronics. Recent research, in collaboration with the European Spallation Source (ESS), aiming at enabling novel thin film 10B-based neutron detector technology, is receiving much appreciation within the neutron scattering community. Birch was director of the Center for Nanoscience and Technology at LiU in 2003-2007. He is active in building up research infrastructures for structural characterization, locally, nationally as well as internationally. He has built and maintains a state-of-the-art thin film X-ray diffraction (XRD) lab in Linköping, an XRD end-station at MAX-II in Lund and he is working actively with the new Swedish materials science beamline at PETRA III in Hamburg through his commitment in the steering committee for the Röntgen-Ångström Cluster. He has published more than 145 peer-reviewed articles in well renowned Physics Journals and he has been the main supervisor for 5 PhDs and co-supervisor for 11 PhD students. His research is funded through both large collaborative and smaller focused project research contracts.

Talk: Structural and optical properties of group-III nitride nanorods grown by reactive magnetron sputter epitaxy
Abstract p. 26

Programme Overview
Morning Sessions

Time	Monday	Tuesday	Wednesday	Thursday	Friday
	4 May	5 May	6 May	7 May	8 May
5:30				GAME DRIVE	
7:00		BREAKFAST	BREAKFAST	BREAKFAST	BREAKFAST
8:00					
8:30		SESSION 1 Opening	SESSION 4 Notices		
8:40		André Vantomme	Rienk v Grondelle		
8:50					
9:00				SESSION 6 Notices	DEPARTURE
9:10		Kabongo	Tjaart Kruger	Ling	
9:20					
9:30		Carvalho			
9:40			David Cahen	Coelho	
9:50		Holtz			
10:00				Vinod Kumar	
10:10		Diale	DISCUSSION		
10:20				DISCUSSION	
10:30		DISCUSSION	TEA		
10:40				TEA	
10:50		TEA	SESSION 5 Hulicius	SESSION 7 Birch	
11:00					
11:10		SESSION 2 Adi Salomon			
11:20			Akande	Engelbrecht	
11:30					
11:40		Koao	Wamwangi	Aissa	
11:50					
12:00		Lee	Urgessa	Van Dyk	
12:10					
12:20		DISCUSSION	DISCUSSION	DISCUSSION	
12:30					
12:40		LUNCH	LUNCH	LUNCH	
12:50					
13:00					
13:10					

Programme Overview
Afternoon Sessions

Time	Monday	Tuesday	Wednesday	Thursday	Friday
	4 May	5 May	6 May	7 May	8 May
12:40		LUNCH	LUNCH	LUNCH	
12:50					
13:00					
13:10					
13:20					
13:20					
13:30		SESSION 3 Craciun	POSTER SESSION 2	SESSION 8 Hölsä	
13:40					
13:50				Abbass	
14:00	REGISTRATION	Janzén			
14:10				Pandey	
14:20		Omotoso			
14:30				Ayabei	
14:40		Tankio Djiokap			
14:50				DISCUSSION	
15:00		DISCUSSION	TEA	TEA	
15:10		TEA			
15:20		POSTER SESSION 1	POSTER SESSION 2 (Continued) 14:00 – 16:00	SESSION 9 Visser	
15:30					
15:40				Duvenhage	
15:50					
16:00				Mulwa	
16:10					
16:20			GAME DRIVE / Sundowners	Munyati	
16:30					
16:40				DISCUSSION	
16:50					
17:00					
15:20					
18:00	WELCOME (Restaurant)				
19:00	DINNER	DINNER	DINNER	DINNER	
20:30					

Scientific Programme
Tuesday 5 May

Time	Activity	Speaker	Abstract Page
Session 1 Chair: Prof Danie Auret			
8:30	**Opening and Welcome**	Jackie Nel	
8:40	Lattice location of dopants in group-III nitrides and ZnO	André Vantomme	2
9:10	Effective doping of ZnO quantum dots with Rare Earth ions for opto-electronic applications	G. L. Kabongo	3
9:30	The Role of Titanium Valence on the Luminescence of ZrO_2 Materials	José Carvalho	4
9:50	Polarization Controlled Light Emitters Based on Elongated Pyramidal Quantum Dots	Per Olof Holtz	5
10:10	Effects of temperature on current-voltage characteristics of Au/Ni/AlGaN Schottky barrier diodes	Mmantsae Diale	6
10:30	Discussion		
10:50	TEA		
Session 2 Chair: Dr Mmantsae Diale			
11:10	Plasmonic systems and their Interaction with Moleucles	Adi Salomon	7
11:40	Annealed Ce-doped ZnO nanoparticles synthesized by chemical bath deposition method	Lehlohonolo Koao	8
12:00	Characterization of crystallite morphology for doped strontium fluoride nanophosphors by TEM and XRD	M.E. Lee	9
12:20	Discussion		
12:40	Lunch		
Session 3 Chair: Prof Hendrik Swart			
13:30	Characteristics of amorphous transparent and conductive oxides grown by combinatorial pulsed laser deposition	V. Craciun	10
14:00	Chloride-based SiC growth on a-axis 4H-SiC substrates	Erik Janzén	11
14:20	Response of Ni/4H-SiC Schottky barrier diodes to alpha-particle irradiation at different fluences	E. Omotoso	12
14:40	Transport characteristics of n-ZnO/p-Si heterojunction as determined from temperature dependent current-voltage measurements	Stive Roussel Tankio Djiokap	13
15:00	Discussion		
15:10	TEA		
15:20 - 17:00	Poster Session 1 (All odd numbered posters presented)		
19:00	Dinner		

Lattice location of dopants in group-III nitrides and ZnO

André Vantomme

Inst. voor Kern- en Stralingsfysica, KU Leuven, Leuven, Belgium
Corresponding author e-mail address: andre.vantomme@fys.kuleuven.be

The properties (electric, optic, and magnetic) of impurities and dopants in semiconductors are strongly dependent on the lattice sites which they occupy. Although the main occupied site, for a given impurity-host combination, can often be predicted based on chemical similarities between impurity and host elements, such expectations fail in many cases. Furthermore, minority sites (in case of multiple-site occupancy) are even more difficult to predict, detect and identify. In this talk, we give an overview of recent lattice location studies for impurities and dopants in ZnO and GaN, as representative wide-gap semiconductors. These experiments are based on the emission channeling (EC) technique, using radioactive isotopes produced at the ISOLDE facility at CERN. EC makes use of the charged particles emitted by a radioactive isotope upon decay. The screened Coulomb potential of atomic rows and planes determines the anisotropic scattering of the particles emitted isotropically during the radioactive decay. Along low-index directions of single crystals and epitaxial films, this anisotropic scattering results in well defined channeling or blocking effects. Because these effects strongly depend on the initial position of the emitted particles, they result in emission patterns which are characteristic of the lattice site(s) occupied by the probe atoms. In this talk, we present some particular cases that illustrate the strengths of emission channeling when studying systems exhibiting multiple-site occupancy.

Effective doping of ZnO quantum dots with Rare Earth ions for opto-electronic applications

G. L. Kabongo[1,2,3], G. H. Mhlongo[2,*], B. M. Mothudi[1], K. T. Hillie[2,4], M. S. Dhlamini[1,2,*]

[1]Department of Physics, University of South Africa, PO Box 392, 0003, South Africa
[2]CSIR-National Centre for Nano-structured Materials, PO Box 395, 0001, South Africa
[3]Département de Physique, Université Pédagogique Nationale, 8815, République Démocratique du Congo
[4]Department of Physics, University of the Free State, Bloemfontein 9300, South Africa
[*]dhlamini@unisa.ac.za, gmhlongo@csir.co.za

1. Introduction

ZnO is among the most widely investigated semiconductor for opto-electronic applications. The need of enhancing optical properties led scientists to engineer its band-gap through various processes such as doping. We demonstrate a successful rare earth (RE) doped ZnO process which was achieved under an elaborated facile sol-gel method using analytical grade reactants and ethanol as a solvent. We present morphological, optical and surface property results obtained using transmission electron microscopy (TEM), photoluminescence (PL) spectroscopy and x-ray photoelectron (XPS) spectroscopy under room temperature conditions. We observe an effective modification of the band-gap with RE doping which was effectively detected during luminescence investigation. Through this study we introduce a facile cost-effective substitute process to produce highly crystalline RE-doped ZnO quantum dots with average diameters ranging from 2 to 7 nm which could be applied in various optical devices. The size and morphology of the particles together with the mechanism of energy transfer from the matrix (ZnO) to the dopant (Tb^{3+} ions) are shown in figure 1.

Keywords: ZnO, Rare earth, photoluminescence, band-gap, doping, Opto-electronic, XPS

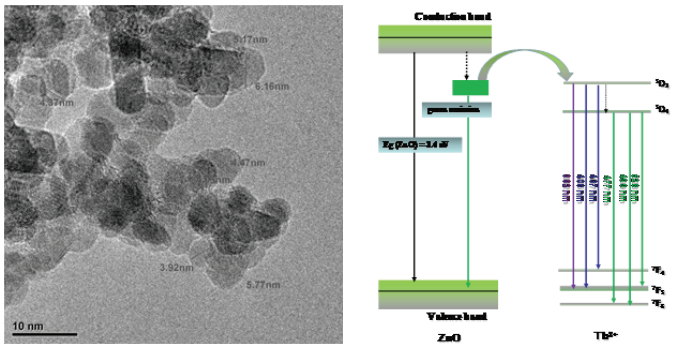

TEM micrographs and schematic representation of energy transfer process from ZnO to Tb^{3+} [1].

2. Reference

[1] G.L. Kabongo, G.H. Mhlongo, T. Malwela, B.M. Mothudi, K.T. Hillie, M.S. Dhlamini. J. Alloys Comp. 591 (2014) 156-163.

The Role of Titanium Valence on the Luminescence of ZrO_2 Materials

José M. Carvalho[1], **Jorma Hölsä**[1-3], **Mika Lastusaari**[2,3], **Hermi F. Brito**[1]

[1]*University of São Paulo, Institute of Chemistry, São Paulo-SP, Brazil*
[2]*University of Turku, Department of Chemistry, FI-20014 Turku, Finland*
[3]*Turku University Centre for Materials and Surfaces (MatSurf), Turku, Finland*
Corresponding author e-mail address: jmc@iq.usp.br

1. Introduction

The optical properties of zirconia materials have received much attention though no outstanding applications have been established so far. The advantage of combining the efficient luminescence of the trivalent rare earths (R^{3+}) and the stable and versatile zirconia host has finally been ruined by the incompatibility of these two systems: the charge compensation defects created by the aliovalent substitution of the tetravalent zirconium with trivalent (or divalent) rare earths have jeopardized the luminescence efficiency [1]. So far, no efficient tetravalent luminescent rare earth has been found and, undoubtedly, will not be in the future either. The room temperature UV excited luminescence of the non-doped ZrO_2 or zirconates or even hafnates have been noted in several reports. In addition to Ti impurity luminescence, defects as oxygen vacancies and colour centers have been offered as origins to luminescence. The Ti impurities were mentioned as the luminescence center and a mechanism to the persistent luminescence was proposed recently [2]. Regarding the details of the luminescence mechanism, synchrotron radiation techniques such as X-ray absorption and vacuum UV (VUV) spectroscopy can unveil more details on the elements' valences as well as energy transfer processes.

2. Results

The monoclinic ZrO_2 nanomaterials were prepared using the sol-gel route followed with annealing at 1000 °C for 5 h. The typical VUV excited luminescence was observed as a broad band centred at 500 nm (Fig. 1, left). Starting with opposite hypotheses to explain this emission, the materials were doped either with Ti^{3+} or Lu^{3+} (both 0.5 mole-%) supposed to enhance the Ti^{3+} or defect emission, respectively. The emission spectra at room temperature show clearly that the 500 nm luminescence is due to a Ti^{3+} impurity, albeit at a trace element level [2]. The analogy between $Ti^{3+/IV}$ and $Tb^{3+/IV}$ suggests the dopant can exist in both oxidation states in ZrO_2 depending on the post-preparation treatment of the material. The XANES measurements (Fig. 2) on the Ti K edge proved inconclusive due to complicated pre-edge structure, however. Low temperature emission spectra with VUV excitation agree with the emission of both Ti^{IV} and Ti^{3+} species in the Lu^{3+} doped and non-doped material. Lu^{3+} doping enhances slightly the Ti^{3+} emission. The Ti^{IV} charge transfer emission centered at 390 nm agrees with the UV-vis absorption edge of TiO_2. The broad bands at 750 nm may be attributed to Ti^{IV}-Ti^{3+} polarons [3] supporting the presence of both ions. The Ti doped materials reveal only the 520 nm transition due to the $e_g \rightarrow t_{2g}$ transition of Ti^{3+} splitting when symmetry lowers from O_h. The UV-VUV excitation spectra (Fig. 1, right) show energy transfer from the ZrO_2 host to $Ti^{3+/IV}$ with E_g at 5.25 eV which decreases with increasing temperature as usual.

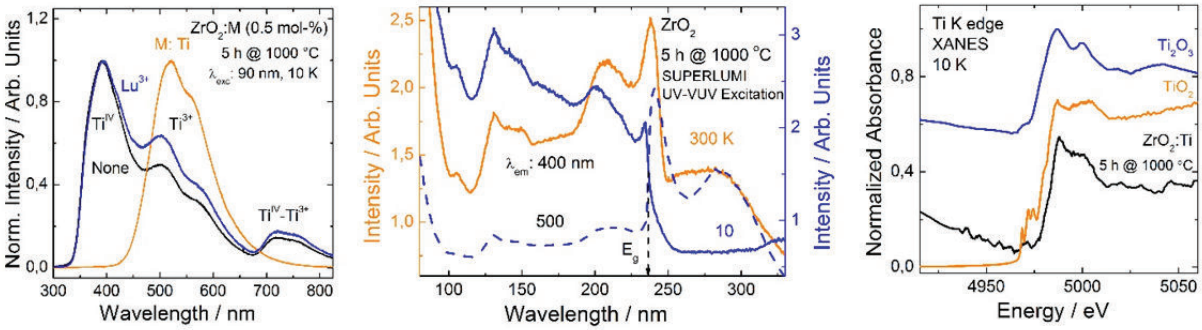

Fig. 1: VUV excited visible emission spectra (left) of the non-doped as well as the Ti and Lu doped ZrO_2 nanomaterials at 10 K. UV-VUV excitation spectra (right) of the non-doped ZrO_2 nanomaterial at 10 and 300 K.

Fig. 2: Ti K edge XANES spectra of ZrO_2:Ti (black), TiO_2 (orange) and Ti_2O_3 (blue curve) nanomaterials at 10 K

3. References

[1] I. A. A. Terra, L. J. Borrero-González, J. M. Carvalho, M. C. Terrile, M. C. F. C. Felinto, H. F. Brito, and L. A. O. Nunes. *J. Appl. Phys.* **113** (2013) 073105.
[2] J. M. Carvalho, L. C. V. Rodrigues, J. Hölsä, M. Lastusaari, L. A. O. Nunes, M. C. F. C. Felinto, O. L. Malta and H. F. Brito. *Opt. Mater. Express*. **2** (2012) 331.
[3] L. H. C. Andrade, S. M. Lima, A. Novatski, P. T. Udo, N. G. C. Astrath, A. N. Medina, A. C. Bento, M. L. Baesso, Y. Guyot and G. Boulon. *Phys. Rev. Lett.* **100** (2008) 027402.

Polarization Controlled Light Emitters Based on Elongated Pyramidal Quantum Dots

Per Olof Holtz, Chih-Wei Hsu, Martin Eriksson, H. Machhadani, T. Jemson, K. Fredrik Karlsson, Anders Lundskog, and Erik Janzén

Department of Physics, Chemistry and Biology (IFM), Linköping University, S-581 83, Linköping, Sweden
E-mail address, corresponding author: poh@ifm.liu.se

1. Introduction

Polarized light is the basis for a manifold of optoelectronic technologies ranging from telecommunication and LCD-displays to quantum cryptography. However, it is challenging to efficiently attain a strong polarization of spontaneously emitted light, in particular for the generation of single photons. In solutions of today, mainly filtering of unpolarized light is employed. In this process, a higher light transmission rate larger than 50 percent from the source can never be achieved. Such a loss is particularly devastating for quantum information technologies, in which each single quantum of light, i.e. each photon, literally counts.

2. Results

Our approach is based on the unique properties of the III-nitride materials, known to be efficient light emitters in the blue and UV part of the spectrum. We have employed μm-sized GaN pyramids with six facets, formed in etched circular holes in a patterned substrate by Selective Area Growth (SAG). The holes are made in a SiN film on top of the substrate by means of standard UV lithography and RIE etching. The tips of the pyramids are made slightly truncated, as has been demonstrated to be advantageous for quantum dot (QD) formation. The pyramids are subsequently overgrown by a thin optically active InGaN quantum well and finally capped with a thin GaN layer. Due to the accumulated strain caused by the lattice mismatch between the GaN and InGaN well, InGaN QDs will evolve on the microscopic c-plane area in the apex of the pyramid. Well-defined single emission lines with a sub-meV line width have been monitored by means of μ-photoluminescence (μPL) from these deterministic QDs. So far, emission wavelengths have been demonstrated in the blue range, around 400 nm, but can be pre-defined by altering the growth conditions, such as the growth temperature, the well width and/or the In composition, for the InGaN layers.

In a subsequent step, the circular holes in the patterned substrate have been replaced by elongated holes in a specified direction. As a result, elongated pyramids are formed with ridges characterized by typical dimensions of 1.0 μm length and 100 nm width on top of these asymmetric pyramids. The elongation directions 0°, 60°, and 120° are preferable due to the six-fold symmetry of the wurtzite crystal structure.

The primary emission lines monitored are originating from electron-hole pairs, i.e. single neutral excitons, but also biexcitons and charged excitons have been monitored. Interestingly, the excitonic emission from the extended InGaN QDs on top of the elongated pyramids exhibit a strong degree of linear polarization, with a typical polarization ratio of about 85% achieved for the case of an elongation of the pyramid base by 1μm.

For investigations of the exciton lifetime, μ-PL with a high spatial resolution combined with a streak-camera detector for recording the time spectral evolution under pulsed excitation with ps pulse duration was employed. The exciton lifetimes have been demonstrated to vary between 100 ps to 1 ns, with shortest lifetimes measured for the negatively charged QDs.

In order to demonstrate the single photon characteristics of the dots, temporal photon correlation spectroscopy has been performed. These correlation measurements have been done in a setup of a Hanbury-Brown and Twiss interferometer equipped with sensitive single photon detectors. The excitonic single photon emission and biexcitonic photon bunching from the pyramidal dots are reported, confirming the sound single photon properties of these dots.

3. References

1. C.W.Hsu, A. Lundskog, K. F. Karlsson, U. Forsberg, E. Janzén and P.O.Holtz, Nano Letters Volume **11**, **2415** (April 28, 2011)
2. A. Lundskog, C.W. Hsu, D. Nilsson, U.Forsberg, K. F. Karlsson, P.O. Holtz and E. Janzén, Nature: Light, Science & Applications (2014) 3, Article:139; doi:10.1038/lsa.2014.20
3. A. Lundskog, J. Palisaitis, C. W. Hsu, M. Eriksson, K. F. Karlsson, L. Hultman, P.O.Å. Persson, U.Forsberg, P. O. Holtz, E. Janzen, Nanotechnology 23, 305708 (2012)
4. A.Lundskog, C.W. Hsu, D. Nilsson, U. Forsberg, P.O. Holtz and E. Janzén, Journal of Crystal growth 363, 287 (2013)
5. A. Lundskog, U. Forsberg, P.O. Holtz and Janzén, Crystal growth and design 12, 5491 (2012)
6. S. Amloy, K. Fredrik Karlsson, P. O Holtz arXiv: 1311.5731
7. T. Jemsson, H. Machhadani, P.O. Holtz and K. F. Karlsson, Nanotechnology 26, 065702 (2015)

Effects of temperature on current-voltage characteristics of Au/Ni/AlGaN Schottky barrier diodes

Mmantsae Diale

University of Pretoria, Department of Physics, Private Bag X20, Hatfield, 0028, South Africa
Corresponding author e-mail address: Mmantsae.diale@up.ac.za

1. Abstract

GaN has attracted considerable attention because of its potential in the fabrication of high-power and high-frequency optoelectronic devices. In particular, AlGaN/GaN heterostructures are capable of handling current densities differently, as compared to other III-V heterostructures because of the higher density of the two-dimensional electron gas (2DEG) accumulated at the heterojunction [1]. In different device structures, GaN metal-insulator semiconductor (MIS) structures are promising because of the large gate forward voltage swing, small gate leakage current, and surface passivation effect suppressing the drain current collapse [2]. Recently, Nakamura was awarded a 2014 Physics Nobel prize for his invention of efficient blue light-emitting diode, enabling bright and energy-saving white light source. The importance of metal-contacts and surface/interface states issues on the AlGaN devices remains an important focus for the success of these material structures [3].

In this study, Au/Ni Schottky barrier contacts have been fabricated on AlGaN grown by hydride vapor-phase epitaxy (HVPE). After ohmic and Schottky contacts fabrication, the contacts were annealed at 500. The electrical characteristics of the diodes were investigated by using current-voltage measurements. The results show that the diodes characteristics improved after annealing, with reverse leakage current dropping to less than 10^{-8} A. Furthermore, the analysis of the temperature dependent electrical characteristics shows that the reverse current of the diodes increases with increasing temperature. The barrier height and ideality factors increased and decreased with increasing temperature respectively.

2. Results

The fabricated diodes show that the unannealed diodes exhibit multiple current-transport mechanism. In Figure 1, the diodes in the 0-1 V range are characterized by tunneling and thermionic currents while diffusion current and series resistance dominates the 1-2 V range. After annealing at 500, all forward current curves shows pure thermionic current in the 0-0.6 V range while the effects of series resistance are seen in the higher temperatures. Figure 2 shows the normal trend by Schottky barrier diodes where the barrier height increases with increasing temperature and ideality factor decreases.

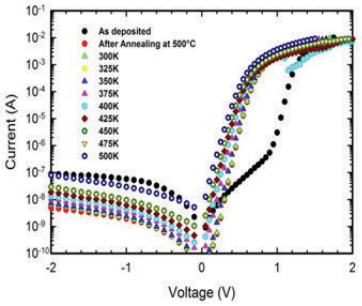

Fig. 1: Current-voltage characteristics of the as deposited, annealed and temperature variation of the diodes

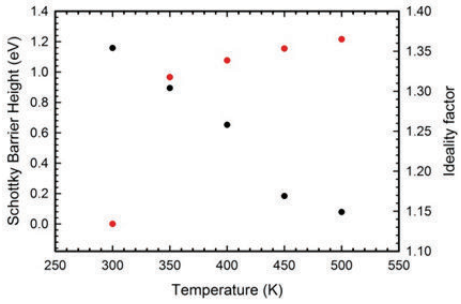

Fig. 2: I-V-T results of the Schottky barrier height and ideality factor

3. References

[1] Mohammad S. N., Salvador A. A. and Morkoc H., Emerging gallium nitride based devices, Proceeding IEEE 83 (1995) 1306.
[2] A. Bauknecht, S. Siebentritt, J. Albert and M. C. Lux-Steiner. *J. Appl. Phys.* **89** (2001) 4391.
[3] Monroy E., Calle F., Munoz E., Omnes F., Gibart P. and Munoz J. A., Applied Physics Letters **73** (1998) 2146.
[4] Diale M., Auret F. D., Van der Berg N. G., Odendaal R. Q. and Roos W. D., Applied Surface Science **246** (2005) 279.

Plasmonic systems and their Interaction with Molecules

Adi Salomon

Chemistry Department, Insitute of Nanotechnology, Bar-Ilan University, 5290002, Israel
Email: adi.salomo@biu.ac.il

We look on interaction between molecules and light at the nanoscale, by fabrication of metallic nanostructures (plasmonic systems). The interaction (coupling) is interesting both in the effect the molecules have on the plasmons and in the effect the plasmons have on the molecular transitions. Thus, molecules which are immeressed is the plasmonic field, may undergo photochemical processes which otherwise suppressed.
We further discussed the coupling between localized plasmonic modes of metallic nano structures and their nonlinear properties, such as second harmonic generation (SHG). We show that when strongly coupled the equilateral triangular nanocavities lose their individual three-fold symmetry to adopt a lower symmetry of the coupled system. The coupled system then responds like a single dipolar entity, and the SHG signal is either enhanced or suppressed depending on the incoming beam polarization.

References

[1] From Individual to coupled metallic nanocavities. Salomon, A.;Prior, Y.; Kolkowski, R.; Zyss, J. ; Journal of optics 2014
[2] Role of mode degeneracy in molecule-surface plasmon strong coupling. Salomon A. Wang, S. Hutchison, J.A., Genet, C. Ebbesen, T.W. *J. Phys. Chem. C*, 2013, 117 (43), pp 22377–22382
[3] Collective Plasmonic-Molecular Modes in the Strong Coupling Regime. Salomon, A et al. .; *Phys. Rev. Lett* 109, 073002, 2012
[4] Molecule – light complex: dynamics of hybrid molecule – surface plasmon states. Salomon, A. Genet, C. and Ebbesen, TW. Angewandte Chemie, 48, Pages: 8749-8751, 2009.

Annealed Ce-doped ZnO nanoparticles synthesized by chemical bath deposition method

Lehlohonolo F. Koao[1], **Francis B. Dejene**[1], **Moges Tsega, Hendrik C. Swart**[2]

[1]*Department of Physics, University of the Free State (Qwaqwa campus), Private Bag X13, Phuthaditjhaba, 9866, South Africa*
[2]*Department of Physics, University of the Free State, P.O. Box 339, Bloemfontein, 9300 South Africa*
Corresponding author e-mail address: koaolf@qwa.ufs.ac.za

1. Introduction

Zinc oxide (ZnO) is representative of II-VI group inorganic semiconductor materials, which has been investigated in terms of preparation and characterization of its properties based on its potential application in the fabrication of solar cells, photoelectronic devices and photocatalysis. Udoped ZnO exhibits a direct band gap of 3.37 eV which corresponds to absorption edge at around 370 nm. The extrinsic doping can greatly influence the morphology, structure, optical and luminescence properties of ZnO. Cerium (Ce) is a major element which has excellent luminescent properties when doped into matrix materials. As a dopant, Ce has received great attention due to its peculiar optical and catalytic properties arising from availability of the 4f levels [1]. The emission from Ce^{3+} is in either the UV or the visible region. Ce-doped ZnO nanoparticles have been synthesized by many methods. However, to the best of our knowledge, there is no report on synthesises of Ce-doped ZnO nanoparticles synthesized by chemical bath deposition method (CBD). The CBD is a large area production process, simple in instrumental operation [2], cheap and convenient process to prepare semiconducting materials. The more recent interest in all things 'nano' has provided a boost for CBD, since it is a low temperature, solution (almost always aqueous) technique, crystal size is often very small and it gives better homogeneity. The CBD process has been used extensively to synthesize semiconductor powders and thin films.

2. Results

The X-ray diffraction results showed that All the ZnO samples possess a typical wurtzite structure for non-annealed and annealed. It was observed that the XRD diffraction intensities decrease with annealing temperature as shown in Fig. 1. This behaviour may be due the estimated crystallite size that decreased with annealing temperature. In Fig. 2 The XRD spectra of the annealed ZnO:Ce^{3+} nanostructures correspond to the various planes of a single hexagonal ZnO phase for the lower and higher Ce concentration samples. At higher Ce molar concentration there is secondary phase. The estimated average crystallite sizes decay exponential with an increase in the amount of Ce. Scanning electron microscopy observations showed the presence of flower-like for non-annealed samples and spherical nanoparticles for annealed samples. Doping the annealed samples with Ce it was observed that the nanoparticles increase in size with an increase in the amount of Ce. At higher molar concentration of Ce there was a mixture of spherical and hexagonal particles. The UV-Vis spectra showed that the absorption edges red shift slightly with an increase in the molar concentration of Ce. The photoluminescence results showed that the maximum intensity is obtained for udoped ZnO nanoparticle and doping with Ce there was decrease in luminescence intensity.

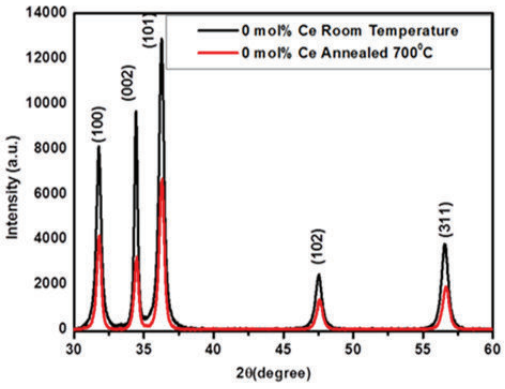

Fig.1: X-ray powder diffraction patterns for non-annealed and annealed ZnO nanostructures.

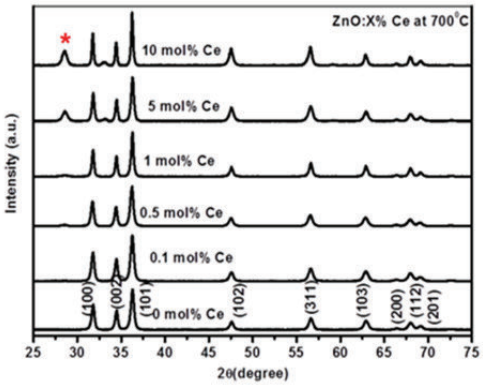

Fig. 2: X-ray powder diffraction patterns for undoped and Ce-doped ZnO nanostructures annealed at 700º C

3. References

[2] L. Liao, H.X. Mai, Q. Yuang, H.B. Lu, J.C. Li, C. Liu, C.H. Yan, Z.X. Shen, T. Yu, J. Phys. Chem. C **112** (2008) 9061
[3] T. P. Niesen, M. R. De Guire, J. Electroceram. **6** (2001) 169-207.

Characterization of crystallite morphology for doped strontium fluoride nanophosphors by TEM and XRD

M.E. Lee[1], J.H. O'Connell[1], M.Y.A. Yagoub[2], H.C. Swart[2] and E. Coetsee[2]

[1]Centre for HRTEM, Nelson Mandela Metropolitan University, Port Elizabeth, [2]Department of Physics, University of the Free State, Bloemfontein, South Africa

Corresponding author e-mail address: michael.lee@nmmu.ac.za

1. Introduction

Strontium fluoride (SrF_2) is one of the most widely used optical materials due to its optical properties (wide bandgap and low phonon energy) as well as physical properties (low refraction index, high radiation resistance, mechanical strength and low hygroscopicity)[1,2]. Europium doped (optimally ~2%) strontium fluoride (Eu:SrF_2) nanophosphors have been shown to possess improved scintillation properties [3]. Previous work on the characterization of the material by X-ray diffraction (XRD) has produced results on the average dimensions for the nanoparticles [4]. However, analysis of exact morphology and orientation for the nanocrystallites will require alternative techniques such as high resolution transmission electron microscopy (HRTEM). In this paper, complimentary results obtained by HRTEM will be compared to results obtained from XRD.

Doped and undoped SrF_2 samples were prepared by a hydrothermal process described in the literature [5]. The reaction product consists of spherical SrF_2 particles having dimensions in the range 0.8-2.0 μm as measured by scanning electron microscopy secondary electron (SEM-SE) imaging. The FIB lamellae produced from the nanophosphor particles were imaged in a TEM. XRD analysis showed the structure of the material to agree with the expected space group Fm3m. The micron-sized particles were assumed to consist of nanocrystallites which are unimodal and single phased. Application of the Scherrer's equation to calculate the crystallite size produced dimensions in the range of 6-8 nm. The accuracy of the Scherrer equation will however depend on a number of factors such as grain size distribution, crystal defects and lattice strain.

2. Results

The high angle annular dark field (HAADF) STEM imaging of the FIB lamella, clearly demonstrate the nanocrystalline composition of the particles shown in figure 1. The selected area diffraction patterns (SAD) clearly shows the presence of numerous, relatively randomly oriented crystallites. The hollow cone technique is used to produce dark field (DF) micrographs obtained by precessing the indicated diffraction ring through the objective aperture by applying hollow cone precession of the incident beam as shown in figure 2. Exposure time was an integer multiple of the precession period. The hollow cone DF TEM images have demonstrated evidence for a bimodal distribution of crystallite sizes. Firstly, a 5-10 nm size distribution which is in reasonable agreement with the XRD Scherrer calculation was measured. A second distribution of crystallite sizes in the range of 50-80 nm was also observed, as shown in figure 2. Data from the hollow cone TEM technique has therefore shown the crystallite size distribution to be bimodal which was not possible to determine by the XRD Scherrer equation.

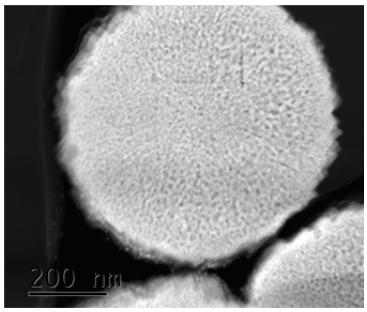

Fig.1: HAADF STEM micrograph revealing the nanocrystalline nature of the phosphor particles

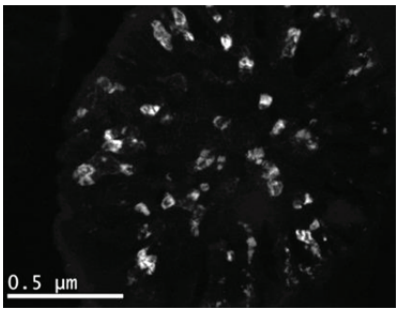

Fig. 2: TEM hollow cone DF TEM image showing a selection of large (50-80 nm) crystallites within the phosphor particle

3. References

[1] K.V. Ivanovskikh, V.A. Pustovarov, M. Kirm, B.V. Shulgin. *J. Appl. Spectrosc.* ***72*** *(2005) 564.*
[2] B.M. Van der Ende, L. Aarts and A. Meijerink. *Adv. Mater.* ***21****(2009) 3073.*
[3] S.Kurosawa, Y. Yokota, T. Yanagida, A. Yoshikawa Phys. *Status Solidi C* ***9*** *(2012) 2275.*
[4] M.Y.A. Yagoub, H.C. Swart, L.L. Noto, J.H. O'Connel, M.E. Lee, E. Coetsee*. J. Lumin.* ***156*** *(2014) 150.*
[5] J. J. Peng, S. Hou, X. Liu, J. Feng, X. Yu, Y. Xing, Z. Su. *Mater. Res. Bull.* ***47*** *(2012) 328.*

Characteristics of amorphous transparent and conductive oxides grown by combinatorial pulsed laser deposition

G. **Socol[1], E. Axente[1], J. Hermann[2], A. C. Galca[3], D. Pantelica[4], P. Ionescu[4], N. Becherescu[5], C. Martin[6], E. Lambers[7], and V. Craciun[1]**

[1]National Institute for Lasers, Plasma and Radiation Physics, Măgurele, Romania

[2] LP3, CNRS - Aix-Marseille University, Marseille, France

[3] National Institute for Materials Physics, Măgurele, Romania

[4]Horia Hulubei National Institute for Physics and Nuclear Engineering, Măgurele, Romania

[5]Appel Laser, Bucharest, Romania

[6]Ramapo College of New Jersey, NJ, USA

[7]MAIC, University of Florida, Gainesville, USA

Amorphous and transparent semiconductor oxides are key components of new thin film transistors (TFTs), solar cells electrodes and displays. By controlling their stoichiometry, they can be used as TFT channel (semiconductive behavior) or as transparent electrode (conductive behavior). Recently, room temperature deposited indium zinc oxide (IZO) and indium gallium zinc oxide (IGZO) thin films were shown to exhibit very good transparency in the visible range, low resistivity, and high mobility. Since the optical and electrical properties of these films depend on the In/(In+Zn) and Ga/(In+Ga+Zn) values, the accurate measurement of these ratios is important for future developments and applications.

In this presentation we focus on the relationship between composition and properties of IZO and IGZO thin films synthesized using the Combinatorial Pulsed Laser Deposition technique. An accurate monitoring of the thin films elemental composition was performed by Laser-Induced Breakdown Spectroscopy (LIBS) based on plasma modeling in view of further *in-situ* and real-time technological developments and process control in case of ASOs fabrication. The cation fractions measured by LIBS were compared to values obtained by complementary measurements using Rutherford backscattering spectrometry, energy dispersive X-ray analysis and X-ray fluorescence.

The optical properties (thickness profile and refractive index determination) of the thin films were inferred from spectroscopic ellipsometry data acquired in the visible range and optical reflectance measured from 30 cm^{-1} (4 meV) to 30 000 cm^{-1} (4 eV). Complementary investigations to obtain the thickness and density of the deposited films as well as their surface and interface roughness have been performed by fitting the measured X-ray reflectivity and X-ray diffuse scattering curves with simulated ones using dedicated models. The room temperature electrical properties were investigated using typical four-point probe geometry and Hall measurements and compared with the values estimated from the optical reflectance data. X-ray photoelectron spectroscopy was used to measure the energy discontinuities in the valence and conduction bands of various dielectric/IGZO and dielectric/IZO heterostructures. All these measurements helped design better transparent and conductive oxides containing lower amounts of In, an element that is rather scarce and therefore expensive.

Chloride-based SiC growth on a-axis 4H-SiC substrates

Ian D. Booker, Ildiko Farkas, Ivan G. Ivanov, Jawad ul Hassan, and Erik Janzén

Semiconductor Materials (IFM), Linköping University, SE-581 83 Linköping, Sweden
Corresponding author e-mail address: erija@ifm.liu.se

1. Introduction

SiC has during the last few years become increasingly important as a power-device material for high voltages. The thick low-doped voltage-supporting epitaxial layer is normally grown by CVD on 4˚ off-cut 4H-SiC substrates at a growth rate of 5-10 µm/h using silane and propane (or ethylene) as precursors. The concentrations of epitaxial defects and dislocations depend to a large extent on the underlying substrate but can also be influenced by the actual epitaxial growth process. Here we will present a study on the properties of the epitaxial layers grown by a Cl-based technique on an a-axis (90˚ off-cut from the c direction) 4H-SiC substrate.

2. Results

We have grown 50 µm thick epitaxial 4H-SiC layers on a-axis 4H-SiC substrates in a hot-wall CVD reactor with a growth rate of 50 µm/h. The precursors were propane and trichlorosilane heavily diluted in a carrier flow of hydrogen. The growth temperature was 1600 ˚C and the C/Si = 1. The growth procedure was very similar to the one optimized for growth on 4˚ off-cut 4H-SiC substrates. We have investigated the epitaxial layers using various techniques. Results from capacitance-voltage (CV), deep level transient spectroscopy (DLTS), minority carrier transient spectroscopy (MCTS), X-ray diffraction (XRD), Time Resolved Photoluminescence (TRPL), Atomic Force Microscopy (AFM), Photoluminescence (PL), and Raman will be presented. Below the results from CV, DLTS and TRPL mapping are shown and discussed.

Schottky contacts of 0.8 mm diameter for DLTS and MCTS were made by thermally evaporating 20 nm Ni onto the sample. Silver paste applied to the highly doped substrate served as ohmic contact. The CV measurement showed a uniform doping density of about $8.5 \cdot 10^{14}$ cm^{-3} in the probed top 4 µm of the epilayer. Deep levels found by DLTS measurements in the range of 77 – 610 K (Fig. 1) were Ti, $Z_{1/2}$, RB1 and $EH_{6/7}$ with densities of $< 2 \cdot 10^{11}$ cm^{-3}, $2 \cdot 10^{12}$ cm^{-3}, $1 \cdot 10^{12}$ cm^{-3} and $1 \cdot 10^{12}$ cm^{-3}, respectively. No new deep levels were found compared to samples grown on 4˚ off-cut wafers in the same reactor and the detected densities were also similar. The $Z_{1/2}$ signal is composed of two strongly overlapping components both known to be related to the carbon vacancy defect created during growth. At high temperatures around 600 K, the carbon vacancy related peak EH_7 overlaps with EH_6. No attempts were made to separate the overlapping signals. RB1 is linked to an iron contamination of the reactor as a result of chlorine corrosion of steel parts.

A TRPL mapping (Fig. 2) with a step size of 100 µm was made in order to detect stacking faults and other structural defects influencing the carrier lifetime. The setup used a 10kHz pulsed 355 nm Nd:YAG laser for excitation and a Hamamatsu PMT with a 390±10 nm bandpass filter to select out the near band-edge luminescence signal. The injection level was in the $1 \cdot 10^{16}$ cm^{-3} range and the decay constant was extracted from the asymptotic part of the decay curve after the signal intensity has been reduced by more than 3 orders of magnitude, corresponding to low injection conditions. The wafer flat is on the upper right side. Structural defects originating mainly from the substrate are visible as low lifetime lines throughout the wafer along the [0001] direction. Further analysis will include mapping with different below band-gap bandpass filters to select out luminescence specifically from stacking faults.

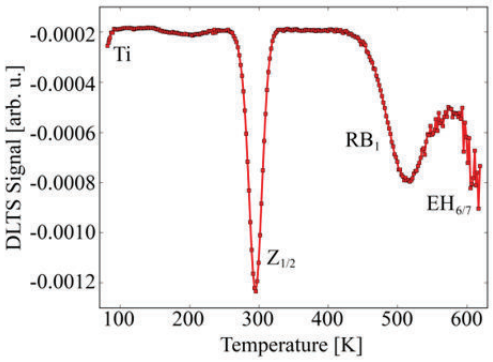

Fig. 1: DLTS spectrum using a cosine correlation function (Hz).

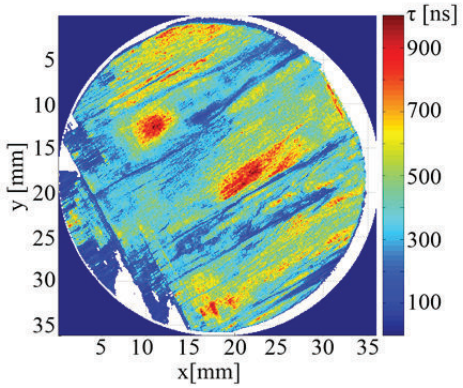

Fig. 2: TRPL decay constant mapping (100µm step size) under low injection condition.

Response of Ni/4H-SiC Schottky barrier diodes to alpha-particle irradiation at different fluences

E. Omotoso[1,2], W.E. Meyer[1], F.D. Auret[1], M. Diale[1], S.M.M. Coelho[1] and P.N.M. Ngoepe[1]

[1] *Department of Physics, University of Pretoria, Private Bag X20, Hatfield 0028, South Africa*
[2] *Departments of Physics, Obafemi Awolowo University, Ile-Ife, 220005, Nigeria*
Corresponding author e-mail address: ezekiel.omotoso@up.ac.za

1. Introduction

Silicon carbide (SiC) is a promising semiconductor with a wide bandgap of 3.26 eV [1], which has drawn the interest of many researchers due to its excellent properties such as high thermal conductivity, high breakdown field and high saturated drift velocity [2]. These characteristics make SiC a very good semiconductor capable of outperforming silicon in electronic devices for high-power, high-frequency and high-temperature applications [3], and is a key material for the next-generation photonic [4]. We have investigated the effect of alpha-particle irradiation on 4H-SiC SBDs. The motivation is mainly to study the behaviour of 4H-SiC SBD after alpha-particle irradiation at different fluences and the signature of the new emanated defect.
Resistive evaporation was employed for the fabrication of nickel for both ohmic and Schottky contacts on 1.9×10^{16} cm^{-3} N-doped 4H-SiC. The SBDs were exposed at room temperature to alpha-particle irradiation from ^{251}Am of energy 5.4 MeV with fluence ranging from 2.56×10^{10} to 9.20×10^{11} particles-cm^{-2}. In this study, current-voltage, capacitance-voltage and deep level transient spectroscopy (DLTS) have been carried out on Schottky barrier diodes (SBDs) to study the change in characteristics of the devices at different fluences.

2. Results

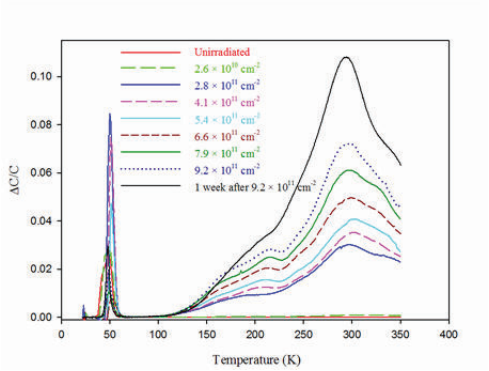

Fig. 1: DLTS spectra of Ni/4H-SiC SBDs unirradiated and irradiated at different fluences. All spectra were recorded using a quiescent reverse bias of 5 V, filling pulse bias of 1 V, rate window of 80 s^{-1} and filling pulse width of 2 ms.

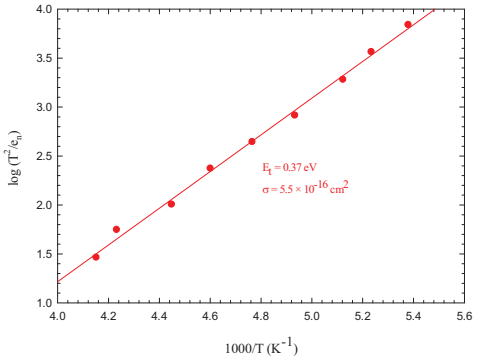

Fig. 2: Arrhenius plot of the $E_{0.37}$ defect after bombarded at fluence 9.2×10^{11} cm^{-2} at 300 K at conditions stated in Fig. 1 at different rate window.

The ideality factor was 1.20 for the as-deposited sample and increased to 1.85 after 9.2×10^{11} alpha-particles-cm^{-2} bombardment. The Schottky barrier height (SBH) for both *I-V* and *C-V* decreased with fluence from 1.37 to 1.12 eV and 2.46 to 1.92 eV, respectively. SBH_{C-V} is greater because an inhomogeneous interface has no effect on the SBH produced from *C-V*. Irradiation at low fluence, did not affect the saturation current, but it began to increase at a fluence of 7.9×10^{11} alpha-particles-cm^{-2}. The free carrier concentration, N_d, measured by *C-V* at approximately 0.70 µm depth, decreased with fluence from 1.7×10^{16} to 1.1×10^{16} cm^{-3}. The reduction in N_d indicates that compensating defects were created during the irradiation. Prior to bombardment, we observed four defects with energies 0.10, 0.12, 0.16 and 0.65 eV below the conduction band. Alpha-particle irradiation introduced one additional defect with a very broad peak after receiving a 2.8×10^{11} cm^{-2} fluence, and the peak became conspicuous after several irradiations as shown in Fig. 1. The signature in term of energy and apparent capture cross section was estimated to be 0.37 eV and 5.5×10^{-16} cm^2, respectively as shown in Fig. 2. The introduction rate of this defect was determined to be 6484±72 cm^{-1}.

3. References

[1] L.M. Tolbert, B. Ozpineci, S.K. Islam, M.S. Chinthavali, Power and Energy Systems, Proceedings, 1 (2003) 317-321.
[2] M. Siad, M. Abdesslam, A.C. Chami, Applied Surface Science, 258 (2012) 6819-6822.
[3] R. Madar, Nature, 430 (2004) 974-975.
[4] S. Yamada, B.-S. Song, T. Asano, S. Noda, Applied Physics Letters, 99 (2011).

Transport characteristics of n-ZnO/p-Si heterojunction as determined from temperature dependent current-voltage measurements

Stive Roussel Tankio Djiokap[1], **Zelalem Nigussa Urgessa**[1], **Crispin Munyelele Mbulanga**[1], **Andre Venter**[1], **Johannes Reinhardt Botha**[1]

[1]*Department of Physics, Nelson Mandela Metropolitan University, P.O. Box 77000, Port Elizabeth 6031, South Africa*

Corresponding author e-mail address: zelalem.urgessa@nmmu.ac.za

1. Introduction

As a wide band gap semiconductor, zinc oxide (ZnO) has attracted a great deal of attention because of the desire to fabricate, for example, efficient ultraviolet light-emitting diodes [1]. ZnO is also of interest because it exhibits a large exciton binding energy of 60 meV, allowing exciton-governed light emission at room temperature. Up to now, light emission from ZnO homojunctions is difficult to achieve due to the lack of p-type doping. This difficulty has prompted researchers to also focus on p-n heterojunctions with different substrates, among them silicon (Si), which is cheaper and readily available. Diode-like rectifying junctions between ZnO/Si have been reported [2]. However, the possible recombination mechanisms are not well understood. In this report the temperature dependence of the current-voltage (I-V) characteristics of the heterojunction between solution-grown ZnO and Si is reported. For the I-V measurements, circular aluminium ohmic contacts were evaporated resistively onto the ZnO surface, while a Ga-In eutectic was used as a back contact.

2. Results

Fig.1 shows typical I-V characteristics of n-ZnO/p-Si measured between 100 K and 295 K. It can be seen from the data that the junction is rectifying at all temperatures. However, the reverse current strongly depends on temperature. As can be seen from the room temperature (RT) forward I-V characteristics of the device (Fig.2) there is at least two recombination channels. At low bias voltages the current is proportional to the applied voltage; this phenomenon is attributed to the tunnelling of thermally generated carriers [3]. As the applied bias voltage increases, $I \sim V^{\alpha}$ (with $\alpha = 2.7$) which is attributed to space charge limited current [4]. The dependence of device parameters like the ideality factor, barrier height and reverse saturation current as function of measurement temperature as well as possible recombination mechanisms are presented in the paper.

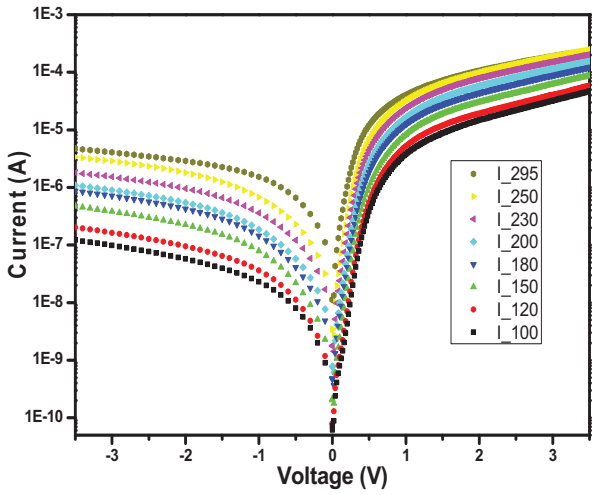

Fig.1: I-V characteristics of ZnO/Si device at different temperatures.

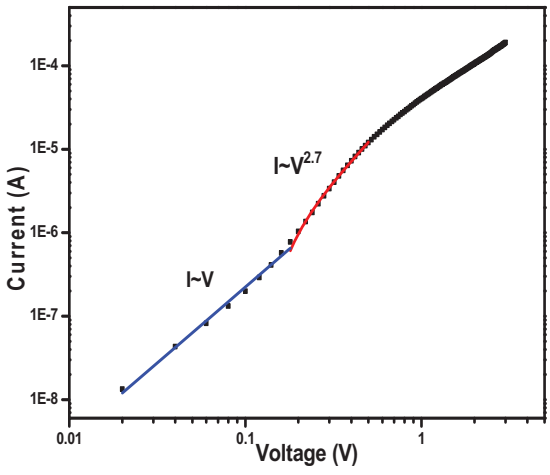

Fig.2: RT log-log plot of a typical ZnO/Si device

3. References

[1] D.M. Bagnall *et al*., Appl. Phys. Lett. **70**, 2230 (1997).
[2] Z.N. Urgessa et al., Physica B **439** (2014) 149–152.
[3] N. K. Reddy et al., Appl. Phys. Lett. **92**, 043127 (2008).
[4] R. Ghosh et al., Appl. Phys. Lett. 90, 243106 (2007).

Scientific Programme
Wednesday 6 May

Time	Activity	Speaker	Abstract Page
Session 4 Chair: Prof Ernest van Dyk			
8:30	**Opening/Notices**		
8:40	The Quantum Design of Photosynthesis	Rienk van Grondelle	15
9:10	Making every photon count - optical nanoscopy and single molecule spectroscopy applied to natural light-harvesting materials	Tjaart Krüger	16
9:40	Proteins as opto-electronic materials?	David Cahen	17
10:10	Discussion		
10:30	TEA		
Session 5 Chair: Prof JR Botha			
10:50	Preparation and measurements of MOVPE multiple InAs/GaAs/GaAsSb quantum dot structures for the telecom wavelength region emitted from 1.3 to 1.8 μm	Eduard Hulicius	18
11:20	VO_2 nanorod as a new candidate for near infrared light harvesting	Amos Akande	19
11:40	Evolution of stress in thin hard films by surface Brillouin scattering	Daniel Wamwangi	20
12:00	The defect passivation effect of hydrogen on the optical properties of solution-grown ZnO nanorods	ZN Urgessa	21
12:20	Discussion		
12:40	Lunch		
13:30	Poster Session 2 (All even numbered posters presented)		
15:00	TEA		
15:15 - 16:00	Poster Session 2 Continue		
16:10	Game Drive/Sundowners		
19:00	Dinner		

The Quantum Design of Photosynthesis

Rienk van Grondelle

VU University, Amsterdam, The Netherlands

Photosynthesis has found an ultrafast and highly efficient way of converting the energy of the sun into electrochemical energy. The solar energy is collected by Light-Harvesting complexes (LHC) and then transferred to the Reaction Center (RC) where the excitation energy is converted into a charge separated state with almost 100% efficiency. That separation of charges creates an electrochemical gradient across the photosynthetic membrane which ultimately powers the photosynthetic organism. The understanding of the molecular mechanisms of light harvesting and charge separation will provide a template for the design of efficient artificial solar energy conversion systems.

Upon excitation of the photosynthetic system the energy is delocalized over several cofactors creating collective excited states (excitons) that provide efficient and ultrafast paths for energy transfer using the principles of quantum mechanics. In the reaction center the excitons become mixed with charge transfer (CT) character (exciton-CT states), which provide ultrafast channels for charge transfer. However, both the LHC and the RC have to cope with a counter effect: disorder. The slow protein motions (static disorder) produce slightly different conformations which, in turn, modulate the energy of the exciton-CT states. In this scenario, in some of the LHC/RC complexes within the sample ensemble the energy could be trapped in some unproductive states leading to unacceptable energy losses.

Here I will show that LHCs and RCs have found a unique solution for overcoming this barrier: they use the principles of quantum mechanics to probe many possible pathways at the same time and to select the most efficient one that fits their realization of the disorder. They use electronic coherence for ultrafast energy and electron transfer and have selected specific vibrations to sustain those coherences. In this way photosynthetic energy transfer and charge separation have achieved their amazing efficiency. At the same time these same interactions are used to photoprotect the system against unwanted byproducts of light harvesting and charge separation at high light intensities.

Making every photon count: Optical nanoscopy and single molecule spectroscopy applied to natural light-harvesting materials

Tjaart Krüger[1], **Rienk van Grondelle**[2]

[1]*University of Pretoria, Private bag X20, Hatfield 0028, South Africa*
[2]*VU University Amsterdam, De Boelelaan 1081, 1081 HV Amsterdam, the Netherlands*
tjaart.kruger@up.ac.za

1. Introduction

Artificial photosynthesis is envisioned by many to be an important component of mankind's long-term energy solution. Bio-inspired photosystems appear most promising, but the first constructs over the past few years have clearly pointed to the infancy of this field [1]. To make progress, a very detailed understanding of natural photosynthesis is required in order to wisely extract the most important design principles. Here, the primary steps of photosynthesis – light harvesting and charge separation – are the most crucial to ensure that the energy of an absorbed photon is stored with a sufficiently high probability, which is commonly 90-100% under conditions of low solar radiation! The latter of the two – charge separation – is understood sufficiently well for the purpose of designing artificial devices. However, the former – light harvesting – has proven to be a very complex process and further experimental and theoretical advances are being awaited. One such promising technique is known as single molecule spectroscopy (SMS), where the averaging effect of an ensemble is overcome by investigating dynamical processes of a single light-harvesting unit.

SMS, in fact, laid the foundation for optical nanoscopy, also known as superresolution microscopy, which has developed tremendously since the first experimental results appeared less than 10 years ago [2]. The new set of techniques enables optical imaging of structures down to the nanometer scale, a two orders of magnitude improvement over the diffraction limit. Application of the technique was found particularly useful in biology, because subcellular structures can now be unraveled using light. Optical nanoscopy is widely regarded as one of the most important developments in biophysical chemistry and chemical physics during the past two decades. It may therefore not be surprising that the founders were awarded the 2014 Nobel Prize in Chemistry.

The first part of the presentation will highlight the principles of optical nanoscopy, point out the limitations in applying the techniques to autofluorescent systems, such as photosynthetic light-harvesting complexes, and encourage application to other areas of materials science research where optical imaging on the mesoscopic scale will be instructive. The second part of the presentation will highlight three design principles of photosynthetic light harvesting that were revealed using SMS.

2. Results

In nature, proteins strongly bind a high density of chromophores to form extended, complex networks of light-harvesting antennae, operating at a remarkable speed and efficiency. Even more intriguing is the level of adaptability to environmental influences at the macromolecular scale to maintain a constant energy throughput at the photochemical reaction centre where charge separation occurs. One important part of this regulation involves very efficient absorption of solar energy and thermal dissipation of any excess excitation energy, leading to a finely tuned feedback self-protection mechanism. This should be done despite (or rather: with the help of) structural fluctuations of the protein on a wide range of timescales. By mimicking the natural conditions that would give rise to the self-protection state under levels of intense sunlight, we have shown that the main light-harvesting complex of plants – LHCII – uses intrinsically available thermal energy dissipation channels by finely controlling its structural disorder on timescales of ms to tens of seconds [3]. Furthermore, using a mutant of LHCII where the terminal emitter chromophore cluster is disrupted, it was demonstrated that the terminal emitter cluster in wild-type LHCII is responsible for energy transfer robustness due to the combination of the particular energy gaps of the lowest exciton states and the strong excitonic coupling of the chromophores in this cluster [4]. Finally, based on the spectral dynamics of light-harvesting complexes from plant photosystem I and II, we can conclude that the particular protein microenvironment of a chlorophyll dimer is responsible for considerable tuning of the extent of shade absorption of plants [5].

3. References

[1] R. E. Blankenship *et al. Science* (2011) 805; J. Barber and P. D. Tran. *J. R. Soc. Interface* (2013) 20120984.
[2] E. Betzig, G. H. Patterson, R. Sougrat, O. W. Lindwasser, S. Olenych, J. S. Bonifacino, M. W. Davidson, J. Lippincott-Schwartz and H. F. Hess. *Science* (2006) 1642; S. T. Hess, T. P. Giriajan and M. D. Mason. *Biophys. J.* (2006) 4258; M. J. Rust, M. Bates and X. Zhuang. *Nature Methods* (2006) 793.
[3] T. P. J Krüger, C. Ilioaia, M. P. Johnson, A. V. Ruban, E. Papagiannakis, P. Horton and R. van Grondelle. *Biophys. J.* (2012) 2669.
[4] C. Ramanan, J. M. Gruber, P. Maly, M. Negretti, V. I. Novoderezhkin, T. P. J. Krüger, T. Mancal, R. Croce and R. van Grondelle. *Biophys. J.* (2015) 1047.
[5] T. P. J Krüger, E. Wientjes, R. Croce and R. van Grondelle. *Proc. Natl. Acad. Sci. USA* (2011) 13516.

Proteins as opto-electronic materials?

David Cahen and Mordechai Sheves*

Weizmann Institute of Science

We have shown that electron transport (ETp), i.e., conduction, through protein monolayers in a solid state–like configuration is remarkably efficient, compared to most molecules, including conjugated ones.[1] Some proteins also have a natural electron transfer (ET) function and ET and ETp are related, but while nature regulates ET via redox chemistry, where control over the process is achieved even at the expense of free energy and low rates (and ubiquity), in ETp no redox process is needed. This allows study of optically active, no-redox proteins, such as the rhodopsins. We studied ETp in the dark and under illumination, esp. in bacteriorohodopsin, but also in halorhodopsin and the light-oxygen-voltage (LOV) sensing domain proteins. The experimental data on ETp via proteins show poor fits with current ET models (pathway or average packing density), such as lack of distance dependence. We will discuss progress towards understanding solid-state ETp charge transport ,which will help to advance bio-opto-electronics.

[1] N. Amdursky et al., *Adv. Mater.* 42,7142-7161 (2014) *Electronic Transport via Proteins* 10.1002/adma.201402304 (progress report).

* Collaboration with I. Pecht; work done with former group members: Drs. N. Amdursky, D. Marchak and L. Sepunaru, with present ones, Drs. C. Guo, S. Mukhopadhyay, and Xi Yu, and with Sheves group members Drs. N. Friedman and S. Dutta. LOV protein work with W. Gaertner and A. Losi (MPI Muelheim).

Preparation and measurements of MOVPE multiple InAs/GaAs/GaAsSb quantum dot structures for the telecom wavelength region emitted from 1.3 to 1.8 μm

Alice Hospodková[1], Jiří Pangrác[1], Markéta Zíková[1] Jiří Oswald[1], Pavel Krčil[1], Philomela Komninou[2], Eduard Hulicius[1]

[1]Institute of Physics ASCR, v.v.i., Cukrovarnická 10, 162 00 Prague 6, Czech Republic
[2]Department of Physics, Aristotle University of Thessaloniki GR-54124 Thessaloniki, Greece

Although the self-assembled InAs/GaAs quantum dots (QDs) are intensively studied during more than the last twenty years, the mass production of QD lasers started only in 2010 and the production of telecommunication QD lasers was announced even last year [1]. The main problem is the complexity of QD preparation process which includes not only the epitaxial layer growth but also Stranski-Krastanow formation, subsequent dissolution of QDs during capping, diversity of QD size and shape or the surfactant behavior of In atoms. The situation is even more complicated when QDs are covered by InGaAs or GaAsSb strain reducing layer (SRL) to shift the QD luminescence toward telecom wavelength. The GaAsSb SRL seems to be more suitable for MOVPE grown QD structures [2]. However, in these structures the surfacting behavior of In and Sb atoms is enhanced which complicates growth of multiple QD (MQD) structures for semiconductor laser application.

In this talk I will present our results obtained on QD and MQD structures with InAs/GaAs QDs covered by GaAsSb SRL. The growth of these structures was studied in situ by reflectance anisotropy spectroscopy (RAS), which offer direct observation of processes during the structure growth such as quantum dot formation, and dissolution or surfacting of In and Sb atoms. The surfacting of In atoms in structures where QDs are covered only by GaAs or by GaAsSb SRL will be compared. Enhanced In surfacting was observed for structures with GaAsSb SRL. Possible ways how to suppress surfacting of both types of atoms and how to prevent their transport on epitaxial surface to subsequent QD layer in MQD structures will be suggested. Different interruption and growth rates of the separation layer growth under varying temperature or composition gradient of GaAsSb SRL will be discussed with respect to the suppression of undesired surfacting of In and Sb atoms. The conclusions derived from RAS measurements will be supported by TEM, AFM and photoluminescence (PL) results.

Properties of InAs/GaAs QDs prepared by the MOVPE technology covered by GaAsSb SRL with extremely long emission wavelength at 1.8 μm will be presented. The prolongation of the emission wavelength was achieved by the introduction of GaAsSb SRL with Sb content of about 30% in the solid phase. The high Sb concentration in the SRL causes the preservation of QD size, which is about 15 nm wide at the base and 5 nm high. Increased QD size prolongs the PL wavelength. Furthermore, high content of antimony leads to a creation of type II heterostructure for which a red shift of the PL wavelength and decrease of the PL intensity is typical. Low PL intensity may complicate light emitting applications; however, fast separation of carriers in the type II structure is an advantage for detector or solar cell application, especially with the long wavelength. With respect to the perspective application of this structure, the photocurrent (PC) measurement was chosen as the complementary characterization method. A depression of PC for quantum well wavelength region (900-1200 nm) was observed for positive bias, while the PC from QDs (over 1200 nm) is not sensitive to the electric field orientation at all. Explanation of this unexpected phenomenon will be suggested.

References

[1] Semiconductor lasers: Fundamentals and Applications, edited by A Baranov, E Tournie, Elsevier 2013, ISBN 0857096400.
[2] A. Hospodková et al, J. Cryst. Growth 370 (2013) 303. doi: 10.1016/j.jcrysgro.2012.08.007

VO_2 nanorod as a new candidate for near infrared light harvesting

Amos Akande[1, 2], Bonex Mwakikunga[1], K. E. Rammutla[2], Funda Mpanza[3], Kittessa Roro[4]

[1]*DST /CSIR South Africa*

National Centre for Nano-Structured Materials Council for Scientific and Industrial Research, P O Box 395, Pretoria 0001,

[2]University of Limpopo Department of Physics, P/Bag X1106, Sovenga, 0727, RSA

[3]*Heriot-Watt University, Scotland, United Kingdom*

[4]*R&D core-Energy, Council for Scientific and IndustrialResearch, P O Box 395, Pretoria 0001, South Africa*

Corresponding author e-mail address: aakande@csir.co.za

1. Introduction

Vanadium dioxide (VO_2) thermocromic properties have been widely applied in many devices in an attempt to solving the world energy crises. One of such devices is thermochromic/switchable/smart window, an energy saving window which is transparent to infrared light with high refractive index above 70 °C (the transition temperature of VO_2) and refracts infrared light with low refractive index below this temperature [1-2]. In this current attempt, we have investigated the potentials of VO_2 nanorod structure for near infrared light harvesting by coating the material on p-type Si wafers using a simple doctor blading method.

2. Results

The n-VO_2|p-Si solar cell was annealed at 70 °C and tested with a SF 150 small beam simulator by SCIENCETECH Inc. from Ontario Canada.
Photon power conversion efficiency (PCE) was calculated form the values of the open-circuit voltage (Voc), fill factor (FF), and short-circuit current density (Jsc), and a decreasing trend of PCE was observed with the photon power.

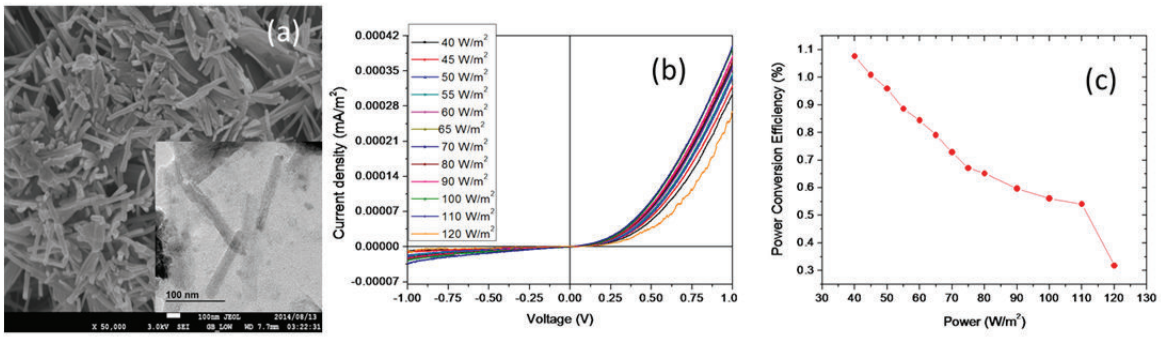

Fig. 1: (a) SEM and TEM images of the VO_2 powder, (b-c) is the forward output current-voltage characteristics of the preliminary single junction p-Si-n-VO_2 solar (a) is the voltage sweep from -1 V to +1V for different photon and (c) is the calculation of the power-conversion efficiency (PCE) of the solar cells showing exponential decay-like trend with the input or photon power.

3. References

[1] A.A. Akande , K. E. Rammutla, T. Moyo, N. S.E. Osman, Steven S. Nkosi, C.J. Jafta, and Bonex W. Mwakikunga, J Magn. Magn. Mater. **375**, (2015) 1-9.
[2] A.A. Akande, E.C Linganiso, B.P Dhonge, K.E. Rammutla, A. Machatine, L. Prinsloo, H. Kunert, B.W. Mwakikunga, *J of Mat. Chem.and Phy.* ***151,*** *(2015) 206–214.*

Evolution of stress in thin hard films by surface Brillouin scattering

Daniel Wamwangi[1], **Clemence Sumanya**[2], **Thomas Wittkowski**[3], **Darrell Comins**[1]

[1] *University of the Witwatersrand 1, School of Physics, Private Bag 3, 2050, WITS Johannesburg*
[2]*Physics Department, Chinhoyi University of Technology, Chinhoyi, Zimbabwe*
[3]*I.E.E. S.A., Luxembourg*

Corresponding author e-mail address: Daniel.wamwangi@wits.ac.za

1. Introduction

Transition metal based thin films continue to attract tremendous research interest due to their excellent properties. As such they are widely used as protective coatings in optics and cutting tools due to their chemical properties, low wear and tear under extreme environments [1]. However delamination and intrinsic stress remain a great challenge especially in multilayer thin films. The mechanisms of thin film growth and intrinsic stress can be understood by investigating stress evolution through modification of elastic constants after insitu Ar^+ incorporation during film growth. In this work, we present an alternative approach to investigate stress evolution of either crystalline or amorphous thin hard films using the components of the elastic constant tensor. Thin films of transitional metal carbide on etched (100) Si substrates have been grown by RF magnetron sputtering at 0 and - 60V bias to observe stress evolution by surface Brillouin scattering. A RF power of 175W and Ar_2 working gas pressure of 1.0 $x10^{-3}$mbar were used for film synthesis. X-ray Reflectometry has been used extract the film growth rate from measurements of film thickness, interfacial roughness and density. The density values were used to extract and simulate velocity dispersion curves obtained from surface Brillouin scattering spectra. A low surface roughness has been determined by X-ray Reflectometry for all films to $\leq$ 1.5 nm. Surface Brillouin studies on the - 60V biased and pristine samples have shown the propagation of Rayleigh surface acoustic wave and higher frequency peaks. The presence of the high frequency shift indicates a high film quality. The velocity dispersion curves show an increase in surface acoustic phonon velocity corresponding to an increase in elastic constants upon biasing. It is observed that Ar^+ incorporation changes the C_{33} elastic constant by 38% with a resulting columnar thin film growth from the C_{11}/C_{33} <1 values.

2. Results

Fig 1 shows the typical surface Brillouin scattering spectra of transitional metal carbide. The true surface acoustic wave and the higher frequency peaks (Sezawa waves). The evidence of stress evolution is presented in Fig 2 which depicts an increase in the surface acoustic phonon velocity of the irradiated samples.

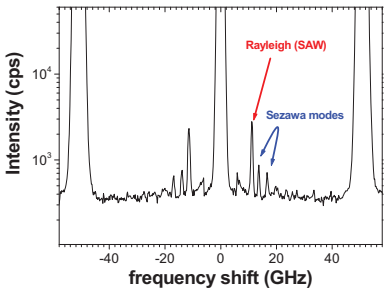

Fig. 1: SBS spectrum of a 442 nm Cr_3C_2 thin film deposited at 175W and $5x10^{-3}$ Ar_2 gas pressure.

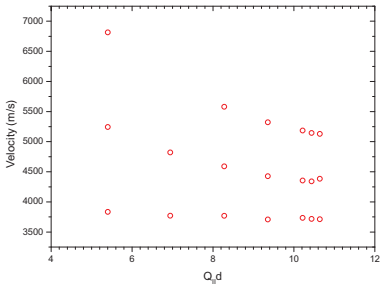

Fig. 2: Velocity dispersion curves for the CrC thin film on Si(100).

3. References

[1] A. Palmero, E.D. van Hattum, W.M. Arnoldbik, F.H.P.M. Habraken, *Surface & Coatings Technology* **188-189**, 392 (2004).

The defect passivation effect of hydrogen on the optical properties of solution-grown ZnO nanorods

ZN Urgessa[1], CM Mbulanga[1], SR Tankio Djiokap[1], JR Botha[1], M.M Duvenhage[2], H.C. Swart[2]

[1]*Department of Physics, Nelson Mandela Metropolitan University, P.O. Box 77000, Port Elizabeth 6031, South Africa*
[2]*Department of Physics, University of the Free State, P.O. Box 339, Bloemfontein ZA9300, South Africa*
Corresponding author e-mail address: zelalem.urgessa@nmmu.ac.za

1. Introduction

Hydrogen incorporates readily into most semiconductors and often behaves as an amphoteric impurity [1-3]. It can be incorporated unintentionally during crystal growth and during many processing steps [2]. In ZnO, it is exclusively a donor [1-3] and can incorporate on two stable sites: interstitially (H_i) and at an oxygen vacancy (H_O) [1-2]. In solution-grown ZnO nanorods, which are investigated in this study, hydrogen is a constituent of the precursors and is the main donor impurity. The knowledge of how hydrogen interacts with itself or other defects is not only of fundamental scientific interest, but also of crucial importance for the understanding of device processing and the performance of devices [2]. In this study, systematic isochronal and isothermal annealing has been conducted and its effect on both the room temperature (RT) and the low temperature photoluminescence (PL) characteristics is presented. Critical attention was given to hydrogen-related lines and the quenching of defect-related luminescence.

2. Results

Fig.1 shows typical behavior of the RT PL intensity measured in the (a) UV and (b) V_O- deep level emission (DLE) [4] regions, as a function of annealing temperature. For annealing temperatures below 300 ^oC an exponential increase in the UV and a concomitant decrease in the DLE intensity can be seen, which is ascribed to the removal of surface adsorbents, the conversion of H_i to H_O and the passivation of oxygen vacancies (V_O) by H. Between 300 ^oC and ~ 500 ^oC the UV emission decreases exponentially, whereas the DLE increases significantly. This behavior may be due to the out-diffusion of H_O and consequently a reduction in defect passivation effects. Between 500 ^oC and 700 ^oC no significant change is observed in the UV intensity, while the DLE now decreases. Above 700 ^oC, both the UV and DLE increase significantly. This overall increase in emission intensity at these high temperatures, is suggested to result from three effects; improvement in bulk crystal quality, the activation of another donor (observed in low temperature PL) and the simultaneous degradation of crystallite surfaces. Unlike the case of PL, a comparison of results from as-grown and annealed samples using X-ray photoelectron spectroscopy (XPS) and Time-of-Flight Secondary Ion Mass Spectrometry (TOF-SIMS) studies shows no significant effect of annealing. From a systematic comparison of PL, XRD, XPS and SIMS results the conversion of H_i to H_O is concluded to be the main cause for the exponential increase in the PL intensity for sample annealed below 300 ^oC. These results help clarify the relationship between hydrogen-related defects in ZnO and hydrogen-related free carrier concentration described in various studies. Details of the growth method, RT and low temperature PL, XPS and SIMS characteristics will be presented in this paper.

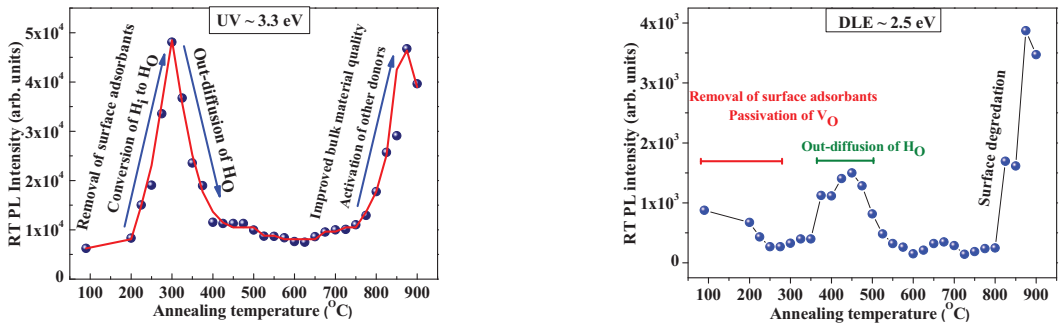

Fig. 1: Effect of annealing on RT PL intensity as a function of annealing temperature in oxygen: (a) UV, (b) DLE. Annealing time was 30 min.

3. References

[1] E. V. Lavrov, F. Herklotz, and J. Weber. *Phys. Rev. B* **79** (2009)165210.
[2] J. Weber, phys. stat. sol. (c) **5** (2008) 535.
[3]C. G. Van de Walle, J. Neugebauer, *Nature* **423** (2003) 626.
[4] T. Moe Børseth *et al*. Appl. Phys. Lett., 89(2006), 262112

Scientific Programme
Thursday 7 May

Time	Activity	Speaker	Abstract Page
Session 6 Chair: Prof Walter Meyer			
9:00	**Opening/Notices**		
9:10	Defects in Zinc Oxide Grown By Pulsed Laser Deposition	Francis Chi-Chung Ling	23
9:40	Inductively coupled plasma induced defects in n-Si using low energy Ar ions	Sergio Coelho	24
10:00	Effect of Substrate temperature on the defect related emission of ZnO thin films prepared by pulsed laser deposition	Vinod Kumar	25
10:20	Discussion		
10:40	TEA		
Session 7 Chair: Prof Ted Kroon			
10:50	Structural and Optical Properties of Group-III Nitride Nanorods Grown by Reactive Magnetron Sputter Epitaxy	Jens Birch	26
11:20	Another method to determine the refractive index of $Al_xGa_{1-x}N$	J.A.A. Engelbrecht	27
11:40	Optoelectronic properties and structural dependence of carbon nanomaterials-based hybrid organic photovoltaic devices	B. Aïssa	28
12:00	Characterisation of Defects in Photovoltaic modules using Electroluminescence and Large-Area Light Beam Induced Current (LA-LBIC) techniques	EE van Dyk	29
12:20	Discussion		
12:40	Lunch		
Session 8 Chair: Prof Japie Engelbrecht			
13:30	Non-Rare Earth Doped Persistent Luminescence Materials	Jorma Hölsä	30
13:50	Effect of Ag doping on the luminescence of ZnO and ZnO:Tb	Abd Ellateef Abbass	31
14:10	Luminescence investigation of dual mode emitting Ho^{3+} doped tellurite glass	Anurag Pandey	32
14:30	Synthesis and Characterization of luminescence magnetic nanocomposite for biomedicine application	Ayabei Kiplagat	33
14:50	Discussion		
15:00	TEA		
Session 9 Chair: Prof Koos Terblans			
15:20	Structure and Spectroscopic Properties of $M(Qn)_3$ complexes (M = Aluminium, Gallium, Indium, Europium; Qn = 8-hydroxyquinoline and derivatives thereof)	Hendrik Visser	34
15:40	XPS investigation of the photon degradation of Znq_2 green organic phosphor	Mart-Mari Duvenhage	35
16:00	Ab-Initio calculation of the electronic states induced by Nb and Cr doping of rutile and anatase TiO_2	Winfred Mulwa	36
16:20	Opto-electrical Properties of poly (3-hexylthiophene-2, 5- diyl) (P3HT), [6, 6] phenyl-C61- butyric acid methyl ester (PCBM) and Squariane Systems	M. O. Munyati	37
16:40	Discussion		
19:00	Dinner		

Defects in Zinc Oxide Grown By Pulsed Laser Deposition

Francis Chi-Chung Ling[1], Zilan Wang[1], W. Anwand[2], A. Wagner[2]

[1]Department of Physics, The University of Hong Kong, Hong Kong, P. R. China
[2]Institute für Strahlenphysik, Helmholtz-Zentrum Dresden-Rossendorf, Postfach 510119, D-01314 Dresden, Germany

Email: ccling@hku.hk

ZnO is a wide band gap semiconductor having excellent properties for fabricating optoelectronic devices operating at the wavelength of ultra-violet (UV). The realization of fabricating UV optoelectronic devices with ZnO based technology is hindered by the asymmetric p-type doping difficulty, which is related to the poor understanding of the defects, defect compensation, and defect control in ZnO materials.

Using pulsed laser deposition (PLD), undoped ZnO films with (002) orientation are grown on c-plane sapphire with the systematic variation of the fabrication parameters including the substrate temperature and oxygen pressure during the growth, as well as the post-growth annealing temperature [1]. Defects in the films were characterized by the positron annihilation spectroscopy (PAS), Raman spectroscopy, secondary ion mass (SIMS) and photoluminescence (PL). The electron concentration ($\sim 10^{18}$ cm^{-3}) is similar to the hydrogen concentration measured by SIMS. SIMS study also reveals thermal induced Zn out-diffusion into the sapphire substrate and leaves out the V_{Zn} related defects at the ZnO film. Oxygen deficient defect related Raman lines 560 cm^{-1} and 584 cm^{-1} are identified and with their origins being discussed. PAS reveals two kinds of V_{Zn} related defects having different microstructures in the PLD grown films, which are different from those identified in the ZnO single crystals.

Green luminescence (GL) with more than one origin is found in the films with annealing temperature lower than 900^{o}C. At the annealing temperature of 900^{o}C, the defect emission spectra (measured at 10 K) of all the films irrespective of the initial growth condition exhibit a GL peaked at 2.47 eV and originated from a single defect, and simultaneously the ~3.23 eV donor-to-acceptor-pair (DAP) emission is introduced. PAS study shows that the GL at 2.47 eV and the DAP are correlated to V_{Zn} defect having the ionization levels at E_V+0.15 eV and E_V+0.97 eV [2]. The result is compatible with the LDA+U calculation [3].

References

[1] Zilan Wang et al, J. Appl. Phys. **116**, 033508 (2014).
[2] ZIlan Wang et al, submitted to Appl. Phys. Lett.
[3] A. Janotti and C. G. Van de Walle, Phys. Rev. B **76**, 165202 (2007).

The work is supported by the Research Grant Council, HKSAR under the GRF project no. of 703612P.

Inductively coupled plasma induced defects in n-Si using low energy Ar ions

S. M. M. Coelho, F. D. Auret, J. M. Nel and W. E. Meyer

Department of Physics, University of Pretoria, Private Bag X20, Hatfield, 0028, South Africa.
Corresponding author e-mail address: sergio@up.ac.za

1. Introduction

After more than forty years at the forefront of the semiconductor revolution, silicon remains the most important material due to its electronic and optoelectronic properties. Recently the demand for silicon has outstripped supply due to the increasing popularity of silicon as a photovoltaic material. Plasma processing, whether for etching or deposition, is perhaps the most important technology used in the manufacture of electronic devices. Inductively coupled plasma etching sources show great promise as a replacement for capacitively coupled plasma sources as they produce high density plasmas with low energy ions. These low energy ions cause less damage to the semiconductor while still maintaining a high etch rate.

2. Results

Epitaxially grown n-silicon exposed to 10 eV Ar inductively coupled plasma (ICP) exhibited two electron traps, both of which have an enthalpy of 0.43 eV below the conduction band (Figure 1). Surface states are evident in the deep level transient spectroscopy spectrum of this 10 eV Ar etched sample whereas raising the energy of plasma ions to approximately 20 eV minimized the introduction of surface states but introduced additional defects with deep levels in the bandgap. Plasma treatment did not improve the rectifying properties at room temperature of Schottky barrier diodes evaporated onto this etched surface.

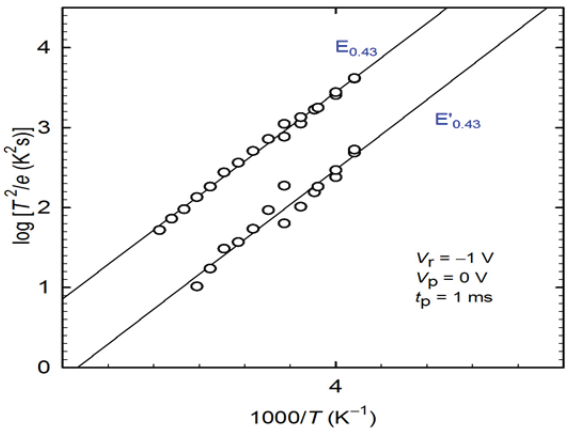

Fig. 1: Arrhenius plots using Laplace-DLTS data of electron-trap defects observed after 10 eV ICP etching. ICP induced defects were measured using resistively evaporated Au diodes. Measurement parameters are noted in the figure.

Effect of Substrate temperature on the defect related emission of ZnO thin films prepared by pulsed laser deposition

Vinod Kumar*, O. M. Ntwaeaborwa, H.C. Swart*

Department of Physics, University of the Free State, Bloemfontein, ZA9300, South Africa
Corresponding author e-mail address: vinod.phy@gmail.com, swarthc@ufs.ac.za

1. Introduction

Zinc Oxide (ZnO) has attracted much attention in research activities with potential applications such as light emitting diode, spintronic device, transparent conductive electrodes, laser and solar cells due to its wide band gap (~3.37 eV) and large exciton binding energy (~60 meV) [1,2]. There are several deposition techniques used to grow ZnO thin films, including chemical vapour deposition (CVD) [3], magnetron sputtering [4], spray pyrolysis [5], the sol-gel method [6] and pulsed laser deposition (PLD) [7]. In the case of PLD prepared films, the degree of orientation is influenced by the deposition conditions such as temperature, background gas composition and pressure, and kinetic energy of the plume particles [7]. The trivalent rare earth (RE^{3+}) doped ZnO belong to one kind of novel optical materials and have drawn an increasing amount of attention [8]. Terbium doped ZnO (ZnO:Tb^{3+}) thin films were prepared by PLD at different substrate temperatures. In the present work, the effects of substrate temperature on the structure, optical and luminescence properties of ZnO:Tb^{3+} thin film were investigated in detail. A correlation was found between the defects (confirmed by X-ray photoelectron spectroscopy) and the Photoluminescence (PL) results.

2. Results

Figure 1 shows the XRD patterns of the ZnO thin films deposited on Si substrates at different substrate temperatures ranging from room temperature (RT) to 400ºC. According to the XRD patterns, all ZnO films were oriented along the (002) plane. This is in line with the characteristics of the hexagonal ZnO wurtzite where the *c*-axis is perpendicular to the substrate plane [9]. The PL spectra of the ZnO films grown at the different substrate temperatures are shown in figure 2. It is worth noting that the films mainly exhibit emission in the UV region. The strong near-band edge emission at room temperature is due to free exciton recombination. Generally in ZnO, the visible light emission is ascribed to the structural defects [10] such as zinc vacancy (V_{Zn}), oxygen vacancy (V_o), interstitial zinc (Zn_i), interstitial oxygen (O_i) and antisite oxygen defects (O_{Zn}) [10]. The PL spectra of the ZnO:Tb^{3+} thin films are characterized by three different types of transitions, the one is due to exciton recombination emission, the second is due to defect level emission and the third is due to the Tb^{3+} f-f transitions. For the emission due to the Tb^{3+} ions, a green emission peak at 543 nm and a few minor peaks at 489 and 622 nm were detected. These peaks represent the $^5D_4$-$^7F_5$, $^5D_4$-$^7F_6$, and $^5D_4$-$^7F_3$ transitions of Tb^{3+}, respectively [10].

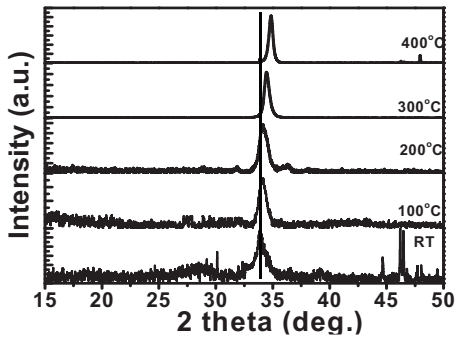

Fig. 1: Effect of substrate temperature on the XRD spectra of ZnO:Tb^{3+} films grown at different substrate temperatures.

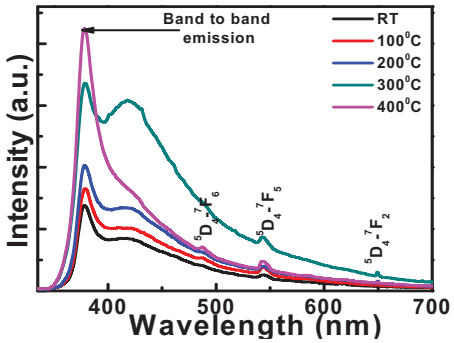

Fig. 2: Photoluminescence graphs of ZnO:Tb^{3+} films obtained at different substrate temperatures.

3. References

[1] U. Ozgur, Y.I. Alivov, C. Liu, A. Teke, M.A. Reshchikov, S. Dogan, V. Avrutin, S.J. Cho, et. al, *J. Appl. Phys.* **98** (2005) 041301.
[2] Vinod Kumar, N. Singh, V. Kumar, A. Kapoor, L.P. Purohit, O.M. Ntwaeaborwa and H.C. Swart, *J. Appl. Phys*. **114** (2013) 134506.
[3] J. Hu and R.G. Gordon, *J. Appl. Phys.* **71** (1992) 880.
[4] Y. Igasaki and H. Saito, *J. Appl. Phys.* **70** (1991) 3613.
[5] A.F. Aktaruzzaman, G.L. Sharma and L.K. Malhotra, *Thin Solid Films* **198** (1991) 67.
[6] Vinod Kumar, R. G. Singh, L. P. Purohit and Fouran Singh, *J. Alloys & Comp.* **544** (2012) 120.
[7] A. Suzuki, T. Matsushita, N. Wada, Y. Sakamoto and M. Okuda, *Jpn. J. Appl. Phys.* **35** (1996) L56.
[8] X. Chen and Wenqin Luo, *J. Nanoscie. Nanotechn*. **10** (2010) 1482.
[9] S. Choopum, R.D. Vispute, W. Zoch, A. Balsamo, R.P. Sharma, T. Venkatesan, et. al, *Appl. Phys. Lett.* **75** (1991) 3947.
[10] Vinod Kumar, S. Som, V. Kumar, V. Kumar, E. Coetsee, O.M. Ntwaeaborwa and H.C. Swart, *Chemical Eng. J.*, **255** (2014) 54.

Structural and Optical Properties of Group-III Nitride Nanorods Grown by Reactive Magnetron Sputter Epitaxy

Jens Birch[1], **Ching-Lien Hsiao**[1], **Muhammad Junaid**[1], **Justinas Palisaitis**[1], **Per Sandström**[1]
Per O. Å. Persson[1], **Lars Hultman, Roger Magnusson**[2], **and Kenneth Järrendahl**[2]

[1] *Thin Film Physics Division, IFM, Linköping University, 582 83 Linköping, Sweden*
[2] *Applied Optics Division, IFM, Linköping University, 582 83 Linköping, Sweden*
Corresponding author e-mail address: jebir@ifm.liu.se

Introduction

One-dimensional group-III Nitride nanorods (NR), have drawn a large interest during the past decade thanks to great prospects for improved optoelectronics by e.g., increased quantum efficiency, higher sensitivity, lower heat generation, etc. as compared to bulk and quantum well-based devices.
Magnetron Sputter Epitaxy (MSE) allows for epitaxial growth of $Al_{1-x}In_xN$ NRs as well as GaN NRs.[1,2] Moreover, low temperature group-III N epilayer growth is possible by MSE[3] and it is easily scalable to large areas, which make it an industrially potent, yet unexploited, technique.

Results

$Al_{1-x}In_xN$ NRs grown on ZrTiN seed layers feature In-rich cores and Al-rich shells, as observed by high resolution electron microscopy (HREM) and quantitative valence electron energy loss spectroscopy using scanning transmission electron microscopy. Such nanorods exhibit near band-edge optical emission at ~5 eV, as observed by cathode luminescence. An internal composition gradient in $Al_{1-x}In_xN$ nanorods leads to a curved-lattice epitaxial growth (CLEG) [4] which is utilized for high precision tailoring of nanorod morphologies, such as spirals and zig-zag shapes which opens the possibility to obtain new unique optical properties. For example, $Al_{1-x}In_xN$ spirals with a pitch of ~200 nm can be designed to produce either fully right-handed or left-handed circularly polarized reflected light at specific wavelengths in the UV-regime (see Fig 1).

High quality GaN NRs were grown by MSE at 1000°C on Si(111), 4-H SiC(0001) and SiO_x substrates, using a liquid Ga-target. NRs can be grown at a thickness ~35 nm and lengths up to several µm without extended defects as seen in HREM. Low-temperature micro photoluminescence (µPL) reveal intense and sharp band-edge emission, characteristic of donor-bound exitons, with a FWHM = 1.7 meV at 3.48 eV. (see Fig. 2)

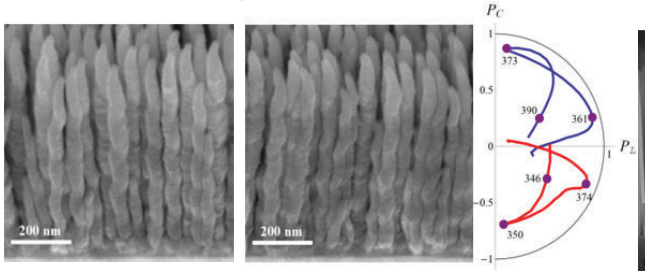

a) b) c)

Figure 1. Scanning electron micrographs showing a) lefthanded and b) right-handed InAlN nanospirals. c) The degree of circular polarization (P_C) and linear polarization (P_L) of reflected light

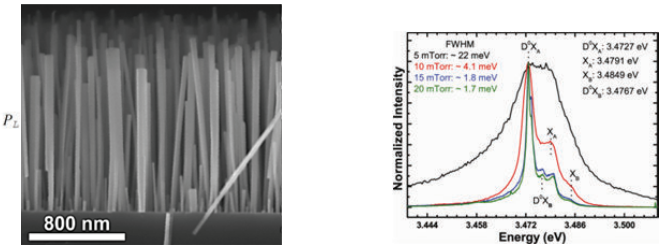

a) b)

Figure 2. a) Scanning electron micrographs of GaN NRs, grown on SiO_x by reactive MSE in a 20 mTorr pure N_2 environment, in side-view and top-view projections. b)Micro PL spectra from GaN NRs on SiO_x, grown at different N_2 pressures.

In conclusion, we show that reactive Magnetron Sputter epitaxy (MSE) can be used to produce high quality group-III Nitride NRs, with optical properties comparable to e.g., MBE grown structures, as well as new tailored NRs by CLEG, featuring unique polarizing properties.

References

[1] C.-L. Hsiao, *et al.* APEX 4, 115002 (2011)
[2] M. Junaid "Magnetron Sputter Epitaxy of GaN Epilayers and Nanorods", Thesis 2012, Linköping Studies in Science and Technology. Dissertation #1482, ISBN 978-91-7519-782-1; http://urn.kb.se/resolve?urn=urn:nbn:se:liu:diva-84655
[3] C.-L. Hsiao, *et al*. Thin Solid Films 524, 113 (2012)
[4] C.-L. Hsiao, *et al.* Nano Letters, *Accepted* (2014) DOI: 10.1021/nl503564k

Another method to determine the refractive index of $Al_xGa_{1-x}N$

J.A.A. Engelbrecht[1], B. Septhon[1], E. Minnaar[2] and M.C. Wagener[1]

[1]Physics Department, NMMU, Port Elizabeth
[2]HRTEM Facility, NMMU, Port Elizabeth
Corresponding author e-mail address: Japie.Engelbrecht@nmmu.ac.za

1. Introduction

AlGaN alloys continue to be of great interest due to the application of these alloys in high-power, high-temperature and high-frequency devices such as field-effect transistors, UV-light emitting LED's and laser diodes[1-3]. A range of different electrical and optical properties can be obtained by varying the alloy composition of $Al_xGa_{1-x}N$ by changing the amount of Al in the alloy. The characterization of these alloys to determine the various physical properties as a function of Al content is therefore necessary. Optical characterization is preferred as this technique has the advantage of being non-contact and non-destructive.

In this work, the use of infrared reflection spectroscopy to evaluate $Al_xGa_{1-x}N$ epilayers grown with varying Al content by metalorganic vapour phase deposition (MOCVD) on sapphire substrates was investigated. The layer thickness was readily determined using interference fringes in the reflectance spectra of the samples[4]. However, this requires knowledge of the refractive index n as function of the wavelength. Determination of the refractive index of $Al_xGa_{1-x}N$ is challenging, since the refractive index is a function of wavelength and the aluminium content of an $Al_xGa_{1-x}N$ sample, as well as the temperature of the sample[5]. A number of techniques have been reported for the determination of the refractive index for $Al_xGa_{1-x}N$, including from the refractive indexes of AlN and GaN, ellipsometry measurements or Sellmeier type equations[6].

The present investigation aims to provide an alternative method to determine the refractive index of $Al_xGa_{1-x}N$ at room temperature. The method is based on the manipulation of earlier published experimental results[6] (Fig.1) and relations from the slope and y-intercept of straight line graphs. The new formulation was then employed to obtain the thickness of the measured $Al_xGa_{1-x}N$ epilayers, using the observed interference fringes (Fig. 2).

2. Results

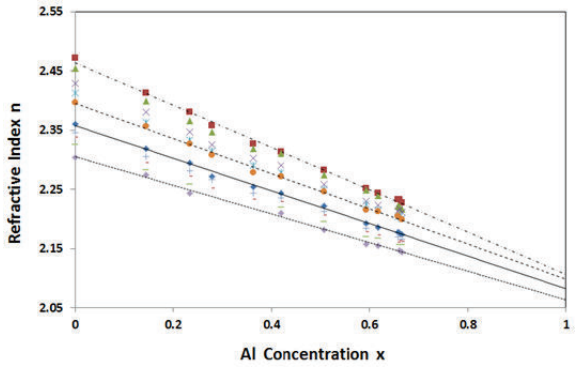

Fig. 1: Examples of straight-line fits of previous results.

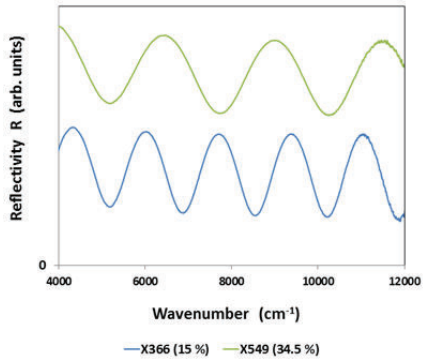

Fig. 2: Interference spectra of two $Al_xGa_{1-x}N$ epilayers.

3. References

1. N. Maeda, T. Saitoh, K. Tsubaki, T. Nishida and N. Kobayashi, Jpn. J. Appl. Physics 38 (1999) L987-L989.
2. T. Takano, Y. Narita, A. Horiuchi and H. Kawanishi, Appl. Phys. Lett. 84 (2004) 3567-3569.
3. J. Han, M.H. Crawford, R.J. Shul, J.J. Figiel, M. Banas, L. Zhang, Y.K. Song, H. Zhou and A.V. Nurmikko, Appl. Phys. Lett. 73 (1998) 1688-1690.
4. F. Reizman, J. Appl. Phys. 36 (1965) 3804
5. U. Tisch, B. Meyler, O. Katz, E. Finkman and J. Salzman, J. Appl. Phys. 89 (2001) 2676-2685.
6. N.A. Sanford, L.H. Robins, A.V. Davydov, A. Shapiro, D.V. Tsvetkov, A.V. Dmitriev, S. Keller, U.K. Mishra and S.P. DenBaars, J. Appl. Phys. 94 (2003) 2980-2991.

Optoelectronic properties and structural dependence of carbon nanomaterials-based hybrid organic photovoltaic devices

B. Aïssa[1], R. Akilimali[2], and F. Rosei[2]

[1] Qatar Environment and Energy Research Institute (QEERI). Qatar Foundation. P.O. Box 5825, Doha, Qatar,
[2] Centre Énergie, Matériaux et Télécommunications, INRS, 1650, boulevard Lionel-Boulet. Varennes, Quebec, J3X 1S2, Canada

Corresponding author e-mail address: baissa@qf.org.qa

1. Introduction

We report on the incorporation of carbon nanomaterials (CNMs) such as single-walled carbon nanotubes (SWCNTs) into organic PV (OPV) cells for efficiency optimization. Although CNMs have been used before in OPVs, the focus is put here to elucidate the effect of the structural properties of the CNMs on OPV performance, which is poorly understood. More specifically, we address the issue of improving the performance of a new hybrid OPV device by combining the physical and chemical characteristics of light-sensitive conjugated polymers (CP), with the high electrical conductivity of SWCNTs by blending the both in a composite photoactive layer. The focus is put on exploring in depth the electronic and optoelectronic properties of the composite material in an OPV scheme and exploring its corresponding photo-conversion capability. The root-mean-square roughness, photoluminescence and optical absorption were found to increase with increasing SWCNTs content and a nonlinear correlation between the nanotubes loads and the open circuit voltage VOC was clearly pointed-out.

Characterisation of Defects in Photovoltaic modules using Electroluminescence and Large-Area Light Beam Induced Current (LA-LBIC) techniques

JL Crozier, M Okullo, EE van Dyk, FJ Vorster

Department of Physics, Nelson Mandela Metropolitan University, Port Elizabeth, 6031,
Corresponding author e-mail address: s207094248@nmmu.ac.za

1. Introduction

The performance and longevity of photovoltaic (PV) modules can be severely limited by poor material, manufacturing defects and physical cracks. Cell mismatch can occur when a solar cell in a series-connected string produces a lower current than the other cells in that string[1]. The current output of the entire string is limited by the weakest cell in the string so damage to a single cell in a module can affect the entire module's current output. These material defects are not always identifiable in visual inspection so additional characterisation techniques are necessary.

In this study Electroluminescence (EL) imaging and Large-Area Light Beam Induced Current (LA-LBIC) measurements were used. EL is an effective, fast and non-destructive characterisation technique for PV modules and is widely used in PV module manufacturing to assess the quality of the finished module[2, 3]. The EL emitted under forward bias is related to the recombination, optical and resistive properties of the cell. LA-LBIC is also a non-destructive spatial characterisation tool capable of measuring the photo-response of PV modules[4]. The PV module is spot-illuminated using a light source mounted above the module on a motorised x-y scanning stage. At each point the current output of the module is measured at a set voltage level. This provides a photo-response map of the PV module related to the wavelength of the light source used.

2. Results

Figure 1 shows an EL image of a mono-crystalline silicon module with striation rings visible as a dark circle in the centre of the cell. In this region of the cell the presence of oxygen precipitates results in the recombination of electron hole pairs. This defect occurs during the wafer growth stage and affects the efficiency of the cell and will lower the module efficiency. However, it is not regarded as a module failure. The corresponding LA-LBIC photo-response map is shown in figure 2. The striation ring is visible in the centre of the cell as an area of decreased photo-response. LA-LBIC and EL measurements have shown good agreement in measurement results and the two techniques have proved complementarity in PV module characterisation.

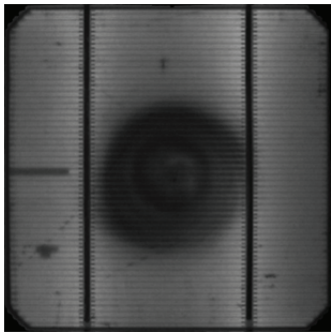

Figure 1: The EL image of a cell in a mono-crystalline module taken at an applied current of 40mA/cm^2.

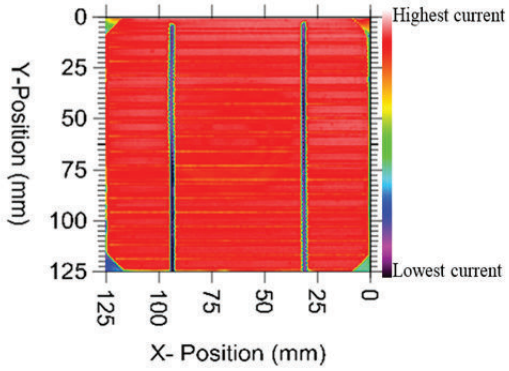

Figure 2: Photo-response map of mono-crystalline cell.

3. References

1. Vorster, F.J. and E.E. Van Dyk, *Current-Voltage characteristics of high-concentration photovoltaic arrays.* Progress in Photovoltaics: Research and Applications, 2005. **13**: p. 55-66.
2. Fuyuki, T. and A. Kitiyanan, *Photographic diagnosis of crystalline silicon solar cells utilizing electroluminescence.* Applied Physics A, 2008. **96**(1): p. 189-196.
3. IEAPVPS, *Performance and Reliability of Photovoltaic Systems Subtask 3.2:Review of Failures of Photovoltaic Modules*, 2014, IEA International Energy Agency.
4. Vorasayan, P., T.R. Betts, and R. Gottschalg, *Spatially distributed model for the analysis of laser beam induced current (LBIC) measurements of thin film silicon solar modules.* Solar Energy Materials and Solar Cells, 2011. **95**(1): p. 111-114.

Non-Rare Earth Doped Persistent Luminescence Materials

Mika Lastusaari[1,2], Lucas C.V. Rodrigues[1,3], José M. Carvalho[3], Maria C.F.C. Felinto[4], Hermi F. Brito[3], Jorma Hölsä[1-3]

[1]University of Turku, Department of Chemistry, FI-20014 Turku, Finland
[2]Turku University Centre for Materials and Surfaces (MatSurf), Turku, Finland
[3]University of São Paulo, Institute of Chemistry, São Paulo-SP, Brazil
[4]Instituto de Pesquisas Energéticas e Nucleares, Centro de Química e Meio Ambiente, São Paulo-SP, Brazil
Corresponding author e-mail address: jholsa@utu.fi

1. Introduction

Both the commercial markets as well as research and development of persistent luminescence phosphors have been dominated by materials doped with Eu^{2+}. The domination of Eu^{2+} over other rare earths (R; *e.g.* Ce^{3+}, Pr^{3+}, Tb^{3+}) is due to *e.g.* the strong and easily tunable emission (Fig. 1) as well as the favourable energy level scheme of Eu^{2+} *vs.* the host band structure [1]. For many reasons this situation may soon change: i) europium is needed for many other phosphor applications as well, ii) the recovery and recycling of europium from persistent luminescence materials is nearly impossible and iii) *e.g.* the biotechnical applications require strongly red emitting biomarkers. The economic pressure due to both aggressive and wildly fluctuating pricing policy of rare earths is probably the most important driving force to the change, nevertheless.

2. Results

The pursuit for cheaper persistent luminescence materials has already resulted in the adoption of such inexpensive host materials as the alkaline earth aluminates, MAl_2O_4 (M: Ca, Sr), $Sr_2MgSi_2O_7$ or $Sr_4Al_{14}O_{25}$ [1]. The replacement of Eu^{2+} (and R^{3+} co-) dopants with non-rare earths is ensuing at a much slower pace despite many outstanding possibilities. For example, the first persistent luminescence material, the famous Bologna Stone from the beginning of the 17th century, uses doping with Cu^{+} in BaS [2]. The 3d elements such as Ti^{3+}, Cr^{3+} and Mn^{2+} have been shown to give strong persistent luminescence, too [1,3]. Many main group metal ions such as Pb^{2+} and Bi^{3+} can also be used as dopants. Further, to improve either the absorption of incident radiation, the efficiency of emission or its tunability, combinations with conventional dopants (*e.g.* Eu^{2+}-Mn^{2+} or Cr^{3+}-Pr^{3+}) or with non-rare earth ones (*e.g.* Cr^{3+}-Bi^{3+} or Mn^{2+}-Bi^{3+}) may be used [3]. As for the mechanism of persistent luminescence, it is necessary to consider first the redox behaviour of the dopants. It is noted at once that each dopant has an oxidized counterpart: $Eu^{2+/3+}$, $Ce^{3+/IV}$, $Pr^{3+/IV}$, $Tb^{3+/IV}$, $Ti^{3+/IV}$, $Cr^{3+/IV}$, $Cu^{+/2+}$, $Pb^{2+/IV}$ and $Bi^{3+/V}$. However, this does not necessarily mean that this counterpart is easily observed experimentally. The mechanism should thus be similar to that for the very efficient Eu^{2+} based persistent luminescence and the electrons act as charge carriers [1].
Eventually, the properties of a Eu^{2+}-Mn^{2+} dopant combination in $BaMg_2Si_2O_7$ [4] is described (Fig. 2). Efficient persistent luminescence and also tuning of emission from red to blue *via e.g.* magenta can be achieved. System's efficiency depends now not only on the individual dopants but also on the persistent energy transfer between them.

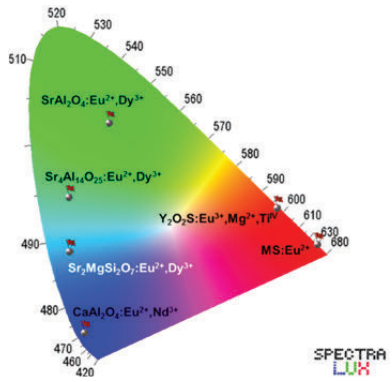

Fig. 1: The CIE color diagram for different commercial persistent luminescence materials [1].

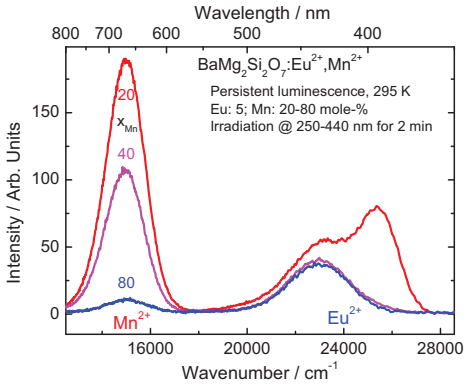

Fig. 2: The persistent energy transfer in the Eu^{2+},Mn^{2+} co-doped $BaMg_2Si_2O_7$ (Eu^{2+}: 5; Mn^{2+}: 20-80 mole-%) at 295 K [4].

3. References

[1] H. F. Brito, J. Hölsä, T. Laamanen, M. Lastusaari, M. Malkamäki and L. C. V. Rodrigues. *Opt. Mater. Express* **2** (2012) 371.
[2] M. Lastusaari, T. Laamanen, M. Malkamäki, K. O. Eskola, A. Kotlov, S. Carlson, E. Welter, H. F. Brito, M. Bettinelli, H. Jungner and J. Hölsä. *Eur. J. Miner.* **24** (2012) 885.
[3] Y. Zhuang, Y. Katayama, J. Ueda and S. Tanabe. *Opt. Mater.* **36** (2014) 1907.
[4] T. Aitasalo, A. Hietikko, J. Hölsä, M. Lastusaari and J. Niittykoski. *Unpublished.*

Effect of Ag doping on the luminescence of ZnO and ZnO:Tb

Abd Ellateef Abbass,[1,2] H.C. Swart,[1] and R.E. Kroon[1,*]

[1]Department of Physics, University of the Free State, Bloemfontein, ZA9300, South Africa
[2]Department of Physics, Sudan University of Science and Technology, Sudan
[*]KroonRE@ufs.ac.za

1. Introduction

ZnO has attracted considerable attention as a low-cost, environmentally-friendly photonic material because of its direct bandgap in the near ultraviolet region and its visible defect emissions. It is often doped to enhance or modify its optical properties. Liu *et al.* reported that metallic Ag nanoparticles (NPs) will precipitate if an excessive amount of Ag is doped into ZnO [1]. Localized surface plasmon resonance (LSPR) effects associated with metallic NPs are of great interest because they have the potential to significantly increase the luminescence intensity of phosphors as a result of enhancement of the electric field of incident electromagnetic radiation. For instance, Cheng *et al.* observed a sixfold enhancement in the near bandgap emission of ZnO nanorods by capping them with Au nanoparticles and attributed this to surface plasmons [2]. In this study we prepared ZnO and ZnO:Tb (a promising material for phosphor converted white light emitting diodes [3]) by the combustion method and investigated the effect of doping such samples with Ag on their luminescence properties.

2. Results

Fig. 1 shows the luminescence of undoped ZnO excited by a He-Cd laser at 325 nm. This spectrum consists of a sharp peak near 390 nm due to near band edge emission (exciton recombination) and a broad emission band centred near 610 nm which is attributed to recombination of electrons trapped at Zn interstitial sites with holes trapped at O interstitial sites. The addition of 1 mol% Ag caused more than a twofold increase in the near band emission while leaving the broad deep level emission band almost unchanged. The X-ray diffraction pattern of the Ag doped sample (not shown) contained a small peak characteristic of metallic Ag and the increase of the near band edge emission has been attributed to LSPR effects [1]. Whereas our measurement showed very little change in the deep level defect emission intensity, it has been reported to be suppressed [4] or enhanced [1].
Fig. 2 shows the luminescence of ZnO doped with 5 mol% Tb, showing that the addition of Tb partially suppresses the broad deep level emission and produces the characteristic luminescence of Tb^{3+} ions, dominated by a green peak near 545 nm corresponding to the $^5D_4$-$^7F_5$ transition. Doping the sample with both 5 mol% Tb and 1 mol% Ag quenches the deep level defect emission and reduces the Tb luminescence as well, although there is still strong near band edge recombination. LSPR enhancement normally requires overlap of the plasmon resonance frequency with the emission centre excitation band, and based on that condition the addition of Ag to Tb doped ZnO might be expected to rather enhance the Tb emission than the near edge ZnO emission. The fact that this is not observed experimentally may suggest the enhancement of the near edge emission is not due to LSPR as suggested in [1], but instead due to other possible factors e.g. Ag enhances the exciton production rate or efficiency of radiative exciton recombination, or decreases the non-radiative exciton recombination rate [4].

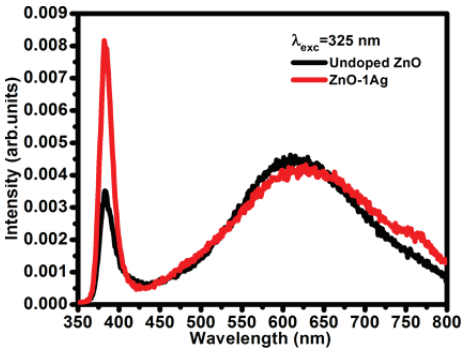

Fig. 1: Emission spectra of undoped ZnO and ZnO doped with 1 mol% Ag.

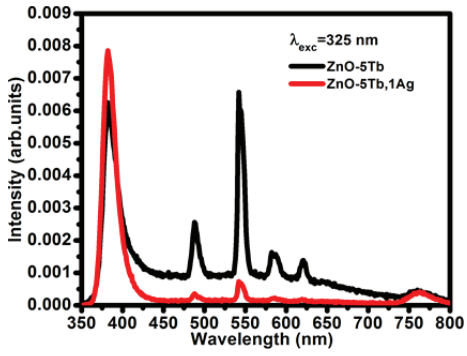

Fig. 2 Emission spectra of ZnO doped with 5 mol% Tb only or with 5 mol% Tb and 1 mol% Ag.

3. References

[1] M. Liu, S.W. Qu, W.W. Yu, S.Y. Bao, C.Y. Ma, Q.Y. Zhang, J. He, J.C. Jiang, C.L. Chen. *Appl. Phys. Lett.* **97** (2010) 231906.
[2] C.W. Cheng, E.J. Sie, B. Liu, C.H.A. Huan, T.C. Sum, H.D. Sun, H.J. Fan. *Appl. Phys. Lett.* **96** (2010) 071107.
[3] V. Kumar, S. Som, V. Kumar, V. Kumar, O.M. Ntwaeaborwa, E. Coetsee, H.C. Swart. *Chem. Eng. J.* **255** (2014) 541-552.
[4] F. Lugo. Ph.D. dissertation, University of Florida (2010). Accessed from http://ufdc.ufl.edu/UFE0041602/00001 (29 Jan 2015).

Luminescence investigation of dual mode emitting Ho^{3+} doped tellurite glass

Anurag Pandey[1], **H. C. Swart**[1]

[1]*Department of Physics, University of the Free State, Box 339, Bloemfontein 9300, South Africa*

Corresponding author e-mail address: anuragpandey439@gmail.com (Anurag Pandey)

swarthc@ufs.ac.za (H C Swart)

1. Introduction

Lanthanides activated luminescent materials having increasing interest among researchers owing to its broad area of applications in photonic, sensing, security and biomedical fields [1]. Rare earth doped glasses are one of the best luminescent solids because of their multifunctional uses from daily live to scientific applications. Tellurite glasses are a better choice for preparing luminescent glasses rather than other oxides due to its low phonon frequency characteristics [2]. Triply ionized holmium is a good candidate for an activator due to its strong emission in the green region and dual mode emitting properties [3]. Several glass synthesis techniques are in used but the melt-quenching technique is the simplest and cheapest method for the preparing of glasses [2].The present work is focused upon luminescence emission from the Ho^{3+} doped TeO_2-ZnO glass prepared by a melting and quenching method.

2. Results

The amorphous nature of the prepared glass was checked by X-ray diffraction patterns of the prepared glass while the thermal behavior was discussed on the basis of thermogravimetric analyses. The luminescence property of the glass was determined via absorption and photoluminescence emission spectra. Fig. 1 shows the photoluminescence emission spectra of the prepared glass upon 980 and 488 nm excitations. The results suggest a tunable two photon upconversion emission and intense green emitting downconversion emission from the sample which is also explained via a suitable energy level structure diagram. Thus dual mode emission (up and down-conversion) observed from the prepared glass is useful in lighting and enhancing the efficiency of solar panels.

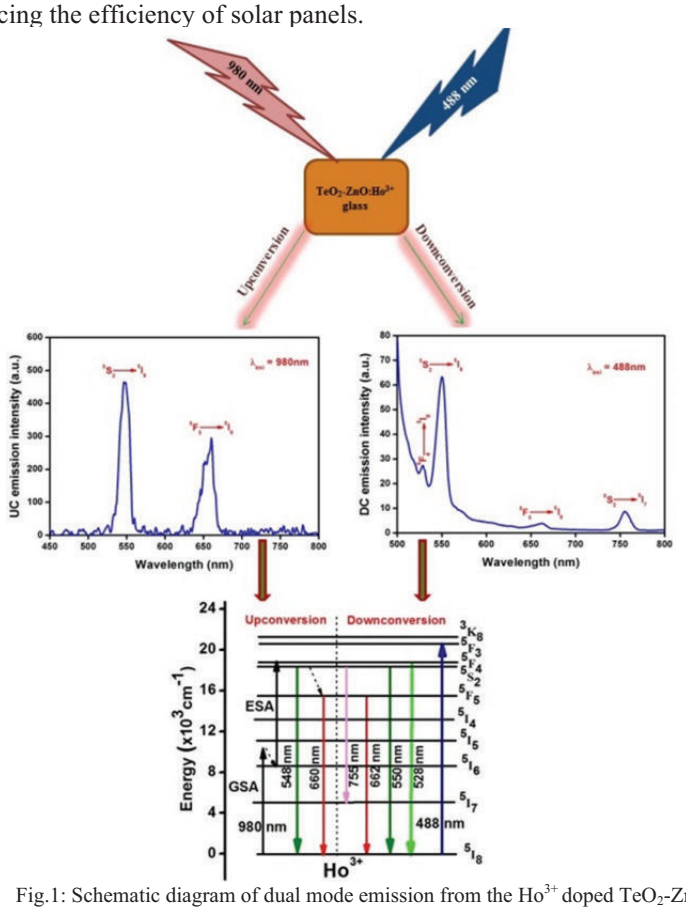

Fig.1: Schematic diagram of dual mode emission from the Ho^{3+} doped TeO_2-ZnO glass.

3. References

[1]A. Pandey, S. Som, V. Kumar, V. Kumar, K. Kumar, V. K. Rai, and H. C. Swart. *Sens. Actuators B* **202** (2014) 1305.
[2] D. K. Mohanty, V. K. Rai, Y. Dwivedi and S. B. Rai. *Appl. Phys. B* **104** (2011) 233.
[3] A. Pandey, V. K. Rai. *Dalton Trans.* **42** (2013) 11005.

Synthesis and Characterization of luminescence magnetic nanocomposite for biomedicine application

Ayabei Kiplagat[1], Martin O. Onani[1]*, Mervin Meyer[2], Teresa A. Akenga[3] and Francis B. Dejene[4]

[1]DST/Mintek Nanotechnology Innovation Centre, Department of Chemistry, University of the Western Cape, Private Bag X17, Bellville, South Africa
[2]DST/Mintek Nanotechnology Innovation Centre, Department of Biotechnology, University of the Western Cape, Private Bag X17, Bellville, South Africa
[3]Department of Chemistry, University of Eldoret, P. O. Box1102, Eldoret, Kenya
[4] Department of physics, University of the Free State, QwaQwa Campus, Private bag X13, Phuthaditha 9866, South Africa

1. Introduction

In the recent past, magnetic materials and semiconductor inorganic materials have been developed and applied (as independent) in fields including biomedicine, especially biotechnological processes imaging, tracking, and separating biological molecules or cells. Processes of biomedical diagnosis and therapy require nanometer scale particles featuring characteristics such as magnetization and fluorescence [1-4]. In the last two decades research has been focused on fabrication of QDs constituting elements of groups II-IV owing to their potential application in lasers, light emitting diodes and biological studies. However, biological applications of the as-prepared QDs were limited by presence of highly toxic Cadmium core. Strategies have been employed to alleviate toxicity of Cd based core coating it with less toxic materials such as a ZnS shell. However, exposure to UV light or oxidation results in the release of cadmium via surface oxidation. In the current study new type of Indium based quantum dot was synthesized and conjugated to the magnetic nanoparticles. The QD were characterized by PL, HRTEM, XRD, SQUID and FTIR.

2. Results and Discussion

The photoluminescence characteristics of the coupled and uncoupled indium based quantum dots were investigated to determine whether the fluorescing property could be retained in the bifunctional system. Generally, the PL intensity of the QDs was observed to remain almost the same with slight blue shift, most probably due to quenching effects of magnetic nanoparticles (MNPs). Equally the quenching effect of the QDs on the magnetic nanomaterials was also investigated. The toxicity of the as prepared nanoparticles was investigated and results will be reported during the conference.

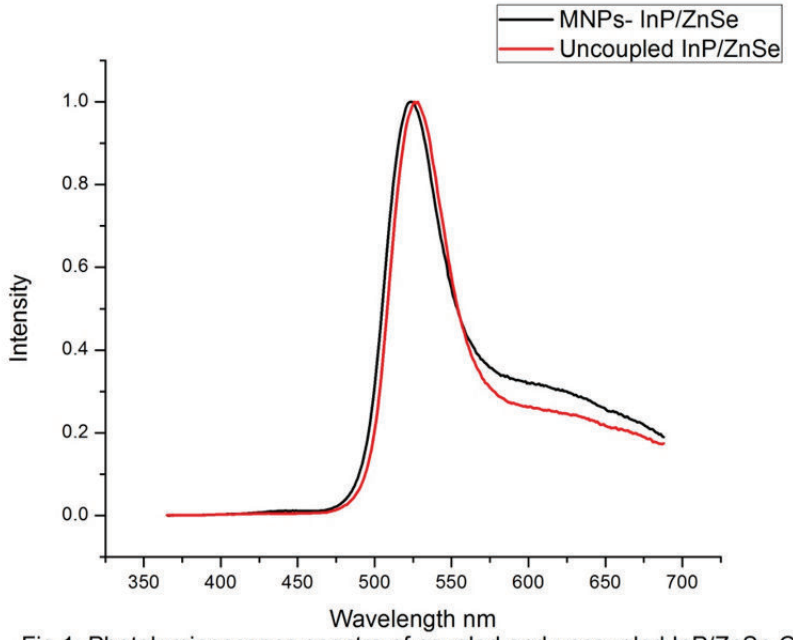

Fig 1: Photoluminescence spectra of coupled and uncoupled InP/ZnSe QDs

3. Reference

[1] Wang, D.; Jibao, H.; Nista, R.; Zeev R. *Nano Letters* **2004**, 4(3), 409-413
[2] Peng, Z.A.; Peng, X.*J. Am. Chem. Soc*. **2001**, *123*, 183-184.
[3] Amala, J. S.; David, M. T; Jayashainy, J.; D. Muthu, G. T. N. D.; Sagayaraj, C, P. *Journal of Alloys and Compounds* **2014,** 606, 254–261
[4] Xiong, Y.; Chunhui, D.; Xiangmin, Z. *Talanta* **2014**, 129, 282–289

Structure and Spectroscopic Properties of $M(Qn)_3$ complexes (M = Aluminium, Gallium, Indium, Europium; Qn = 8-hydroxyquinoline and derivatives thereof)

Hendrik G. Visser[1], Alice Brink[1], Orbett Alexander[1], Hendrik Swart[2], Mart-Mari Duvenhage[2] and Martin Ntwaeaborwa[2]

[1] Department of Chemistry, University of the Free State, PO Box 339, Bloemfontein, South Africa
[2] Department of Chemistry, University of the Free State, PO Box 339, Bloemfontein, South
Corresponding author e-mail address: visserhg@ufs.ac.za

1. Introduction

Metal quinolinates are known as key materials in the design of organic light emission diodes (OLEDs). The aluminium complex, tris-(8-hydroxyquinoline) aluminium(III), is the most well-known molecule of this family, although its gallium analogue has also been considered for use in OLEDs [1,2]. Factors that govern the efficacy these metal complexes for potential use in OLEDs include the type of isomer (*mer* versus *fac*), inter-molecular interactions (like π-π stacking) and solvento species "trapped" in the crystal lattice. Furthermore it was shown that the emission spectra of these complexes can be red or blue shifted by using derivatives of 8-hydroxyquinoline on the 5 and 7 positions of the ligand backbone with electron withdrawing or donating properties (as in 5,7dichloro-8-hydroxyquinoline (5,7-Cl_2Qn) or 5,7 dimethyl-8-hydroxyquinoline (5,7-Me_2Qn)) [3-5].

In this work, various complexes of $M(Qn)_3$ (M = Al(III), Ga(III), In(III) and Eu(III); Qn = 8-hydroxyquinoline / 5,7dichloro-8-hydroxyquinoline / 5,7 dimethyl-8-hydroxyquinoline) have been synthesized and characterized with ^{1}H NMR, single crystal X-ray spectroscopy and other means and their photoluminescence properties evaluated [6, 7]. A systematic evaluation of the structural versus luminescence properties of nine $M(Qn)_3$ complexes plus interesting results of two Europium(III) metal complexes are reported here.

2. References

[1] C.W. Tang and S.A. Vanslyke, *Appl. Phys. Lett*. **51** (1987) 913-915.
[2] P.E. Burrows, L.S. Sapochak, L.S. McCarthy, S.R. Forrest and M.E. Thompson, Appl. Phys. Lett., **64** (1994) 2718.
[3] A. Irfan, R. Cui, J. Zhang and L. Hao, *Chem. Phys*. **364** (2009) 39-45.
[4] Y. Qin, I. Kiburu, S. Shah and F. Jakle, *Org. Lett*. 8 (2006) 5227-5230.
[5] Y.W. Shi, M.M. Shi, J.C. Haung, H.Z. Chen, M. Wang, X.D. Liu, Y.G. Ma, H. Xu and B. Yang, *Chem. Commun*. (2006) 1941-1943.
[6] M. Duvenhage, H.C. Swart, O.M. Ntwaeaborwa and H.G. Visser, *Optical Materials*, **25** (2013) 2366-2371.
[7] M. Duvenhage, H.G. Visser, O.M. Ntwaeaborwa and H.C. Swart, *Physica B*, **439** (2014) 46 - 49.

XPS investigation of the photon degradation of Znq_2 green organic phosphor

Mart-Mari Duvenhage[1], **Martin Ntwaeaborwa**[1] **and Hendrik Swart**[1]

[1] *Department of Physics, University of the Free State, Bloemfontein, South Africa*
Corresponding author e-mail address: swarthc@ufs.ac.za

1. Introduction

Although tris-(8-hydroxyquinoline) aluminium (Alq_3) is used as a green emissive layer in organic light emitting diodes (OLED) [1] it tends to degrade with time leading to a decrease in device performance and efficiency. It has been reported that by substituting Al with Zn to form bis-(8-hydroxyquinoline) zinc (Znq_2), the Znq_2 shows advantages over the Alq_3 in the electron transport and higher quantum yields in device performance which would result in lower operating voltages [2].

The photoluminescence (PL) spectrum of Znq_2 showed a peak at 506 nm, fig. 1, corresponding to the $Znq_2.2H_2O$ crystal form of Znq_2 [3, 4]. There was also a two fold increase in intensity from Alq_3 to Znq_2. Znq_2 powder was irradiated with an UV source for 400 hours and the intensity vs time was monitored. A decrease of 30% in intensity was observed after 400 hours. A rapid decrease in intensity of 10% was observed for the first few hours after exposure, but slowed down for longer exposure times. X-ray photoelectron spectroscopy (XPS) were done on the as prepared and degraded powders. The O1s peak of the as prepared sample consisted of two peaks. The one at 530.9 eV was attributed to the C-O-Zn bond and the one at 532.2 eV to chemisorbed species. After degradation the O1s peak consisted of three peaks. The third peak at 532.8 eV was attributed to the carbonyl and methoxy O1s species that were present in the degraded products [5]. One peak was fitted for the N1s peak for both the as prepared and degraded samples. This peak was attributed to the C-N=N bond. This was an indication that no rupturing of the pyridyl ring took place during UV irradiation. Carbon appeared in Znq_2 in five chemical environments resulting in five identifiable binding energies for the C1s transition, fig. 2. A sixth peak was attributed to chemisorbed species like CO and CO_2. The degraded Znq2 formed four degraded products as was indicated by Rosseli [6]. This concludes that the phenoxide ring ruptured and new bonds like C=O and C-OH had formed.

2. Results

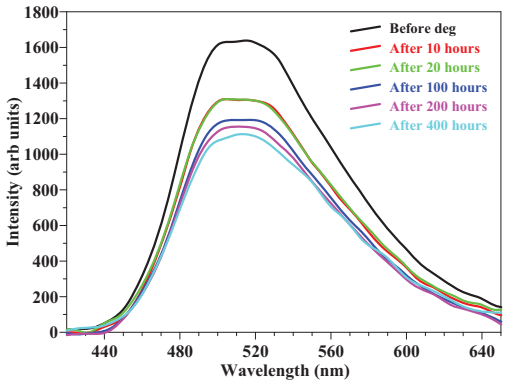

Fig. 1: Evolution of the emission band with time of Znq_2 under UV exposure (λ = 365 nm).

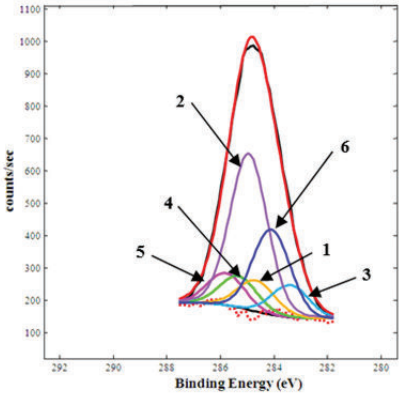

Fig. 2: High resolution C1s XPS peak of as prepared Znq_2.

3. References

[1] C.W. Tang and S.A. Vanslyke, *Appl. Phys. Lett.* **51** (1987) 913-915.
[2] X. Bing-she, H. Yu-ying, W. Hua, Z. He-feng, L. Xu-guang and C. Ming-wei, *Solid State Commun.* **136** (2005) 318-322.
[3] X. Wang, M. Shao and L. Liu, *Synth. Met.* **160** (2010) 718-721.
[4] R. Reisfeld, E. Zigansky and T. Saraidarov, *Opt. Mater.* **30** (2008) 1706-1709.
[5] D. Datta, V. Tripathi, C.K. Suman, V.K. Shukla and S. Kumar, *Proc. of ACID*, (2006) 206-209.
[6] F.P. Rosseli, W.G. Quirino, C. Legnani, V.L. Calil, K.C. Teixeira, A.A. Leitao, R.B. Capaz, M. Cremona and C.A. Achete, *Org. Electron.* **10** (2009) 1417-1423.

Ab-Initio calculation of the electronic states induced by Nb and Cr doping of rutile and anatase TiO_2

Winfred Mulwa[1] , Francis Dejene[1] , Cecil N.M.Ouma[2]

[1]*University of the Free State-Qwaqwa campus, Department of physics, Private Bag x13, Phuthaditjhaba, 9866, SOUTH AFRICA.*
[2] *University of Pretoria, Department of Physics, Private Bag x20, Hatfield, Pretoria, 0028, SOUTH AFRICA.*
Winfred Mulwa, mulwawinfred@gmail.com

1. Introduction

In this study, plane wave self consistent field calculations have been performed on the electronic structure of rutile and anatase phases of titanium dioxide (TiO_2). To this end *ab-initio* calculations have been performed for a 48-atom rutile supercell and 96-atom anatase supercell using the plane wave code – Quantum Espresso [1]. Density functional theory (DFT) with hybrid functionals have been used to obtain a more accurate description of the electronic properties of titanium dioxide in addition to the standard exchange-correlation (XC) functionals namely; the local density approximation (LDA) and the generalized gradient approximation (GGA). In this study, the screened hybrid functional of Heyd-Scuseria-Erzehoff (HSE06) has been used. HSE06 is known to overcome most of the shortcomings of both the LDA and GGA XC functionals [2]. Both the titanium dioxide structures were fully optimized by minimizing the local total energy and atomic forces, after which band structure and density of states were calculated. Band gap energies 1.89 eV (rutile), 2.28 eV (anatase) and 2.25 eV (rutile), 2.65 eV (anatase) were obtained using GGA-PBE and HSE06 functionals respectively. Experimental value for band gap is 3.0 eV for rutile and 3.2 eV for anatase [3]. In order to obtain the bulk equilibrium properties, the energy volume curves for the two structures were fitted to the Murnaghan equation of state [1].

$$P(V) = \frac{K_0}{K_0^1}\left[\left(\frac{V}{V_0}\right)^{-k_0^1} - 1\right] \qquad (1)$$

Substitutional chromium and Niobium at the titanium sites was found to introduced new electronic states within the band gap. These new states are discussed with respect to tuning doped titanium dioxide for the application in photocatalysis [4].

2. Results

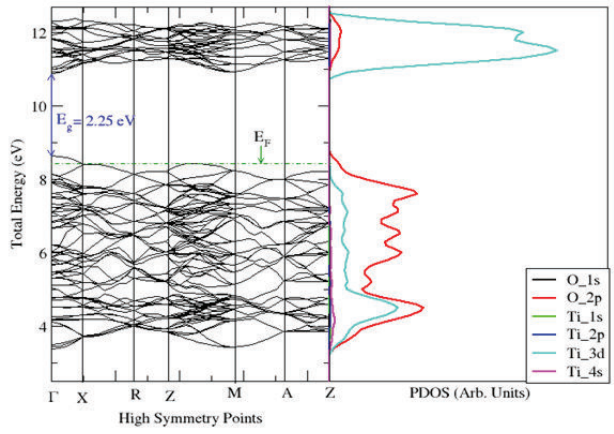

Fig.1: Bands and PDOS of 48-atom rutile using HSE06 functionals.

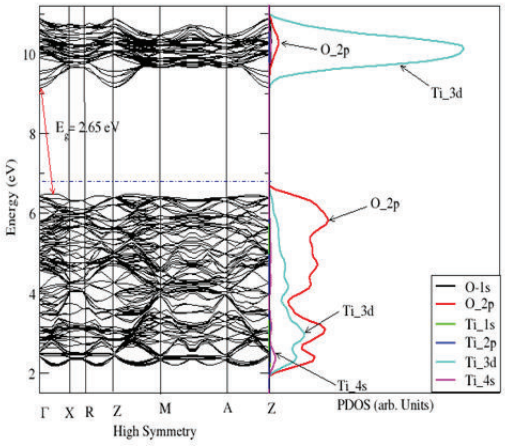

Fig. 2: Bands and PDOS of 96-atom anatase using HSEO6 functionals

3. References

[1] S. Scandolo, P. Gannozzi, C. Cavazzoni, S. de Gironcoli, A. Pasquarello, S. Baroni and Z. Kristallogr. *Phys. Rev. B*. **31** (1985) 805-813.
[2] J. Heyd, E. Gustavo Scuseria, and M. Ernzerhof Erratum. *J. Chem. Phys.* **124** (2006) 219906.
[3] D. Cromer and K. Herrington. *Chem. Phys. Lett.* **513** (2011) 218-223.
[4] C. Cheng pan and C. Jeffrey Wu. *Mater. Chem. Phys.* **100** (2006) 102-107.

Opto-electrical Properties of poly (3- hexylthiophene-2, 5- diyl) (P3HT), [6, 6] phenyl-C61- butyric acid methyl ester (PCBM) and Squariane Systems

[1]M. O. Munyati, [2]M Tembo, [3]S. Hatwaambo1 and [4]M. Maaza

[1]Department of Chemistry, School of Natural Sciences, University of Zambia, P. O. Box 32379, Lusaka, 10101 Zambia.
[2,3]Department of Physics, School of Natural Sciences, University of Zambia, P. O. Box 32379, Lusaka, 10101 Zambia.
[4]Nanosciences Laboratories, Materials Research Department, iThemba LABS, P. O. Box 722, Somerset West 7129, Western Cape, South Africa.

[1]Corresponding author e-mail address: omunyati@unza.zm

1. Introduction

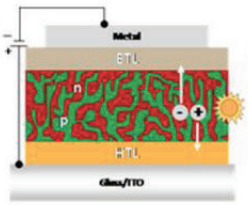

Conjugated polymers have in recent years received active attention following spectacular developments in optical, electronic and photonic research of these materials. Polymer solar cells are favourable candidates for low cost, light weight, large area and mechanically flexible photovoltaic devices. The most promising device is a bulk heterojunction (BHJ) blend based on P3HT:PCBM[1]. The active material consists of P3HT as the donor (D) and fullerene PCBM as the acceptor (A). Excitation in P3HT leads to the formation of excitons that diffuse to the D/A interface where charge separation occurs and the charges eventually collected at the electrodes. However, organic solar cells have generally recorded low photoconversion efficiencies compared to their inorganic counterparts, typically around 5 %. One strategy to increase the photoconversion efficiency is to broaden the absorption range of the BHJ system. This has been done by incorporating small organic molecules such as squarylium III (SQ3) dyes. These molecules generally absorb in the long wavelength range and have good thermal stability under ambient conditions. In addition, SQ molecules are reported to increase photon harvesting via Förster resonance energy transfer (FRET)[2]. In this work, we report the results of optical, morphological and electrical properties of P3HT:SQ:PCBM ternary system used for photovoltaic applications.

2. Experimental

Ternary systems comprising P3HT:PCBM with varying amounts of squarylium III (SQ3) were prepared and deposited by spin coating to obtain nano-size thin films. The films produced were subsequently annealed at 140 °C for 10 min. Absorption spectra and electrical measurements were used to evaluate the effects of thermal annealing and dye loading on the different blends. The films were characterized for their surface morphology and film thickness using atomic force microscopy. Photo-conversion efficiencies were determined following current – voltage measurements under dark and illumination conditions.

3. Results

A significant increase in the maximum peak absorbance, from 0.31 to 0.36 a.u. was observed by incorporating SQ3 molecules at 13 % w/w loading. The absorption range was also observed to broaden (400 – 700 nm) extending to the near infra-red. The V_{oc}, I_{sc} and FF in the control P3HT:PCBM were 0.53 V, 0.78 mA and 0.35 which change to 0.64 V, 9.68 mA and 0.4 in P3HT:SQ3:PCBM blends. The inclusion of SQ3 dye molecules resulted in enhanced light harvesting capacity due to widening of the absorption range. This consequentially resulted in an increase in photogenerated excitons and I_{sc}. Increase in V_{oc} is ascribed to the elevation of HOMO of P3HT due to increase in disorder arising from inclusion SQ3[3]. The rise is HOMO is attributed to increased interchain orbital delocalization. The HOMO of SQ3 is reported to be located between the HOMO and LUMO of levels of P3HT and PCBM. It has been further suggested that incorporation of SQ molecules introduce a second exciton generation system and charge transfer mechanism. Photoinduced charge transfer is not only favourable between P3HT and PCBM but also between SQ3 and PCBM. Thus, the synergistic effect of improved light harvesting characteristics with additional exciton generation and charge transfer mechanism resulted in an increase in photoconversion efficiency. The photoconversion efficiency increased from 1.3 % to 3.9 %.

4. References

[1] Mayer A C., Scully S R, Hardin B E., Rowell M W and McGehee M D, Mater. Today, 10(11), 28–33 (2007).
[2] Huang J S, Goh T, Li X, Sfeir M Y, Bielinsk E A, Z. H. Kafafi (Ed.), Organic Photovoltaics XIV, 8830 (2013).
[3] Peet J, Tamayo A B, Dang X-D, Seo J H and Nguyen T-Q, Appl. Phys. Lett. 93, 163306 (2008)

Poster Abstracts

Poster No	Authors	Title
1	Moges Tsega, Dong-Hau Kuo, Walelign Wubet, F.B. Dejene	Effects of the copper content on the structural and electrical properties of $Cu_2ZnSnSe_4$ bulks used in thin-film solar cells
2	Funda Mpanza, Kittessa Roro, H. Upadhyaya, Bonex Mwakikunga	n-WO_3|p-Si tandem layer solar cells as new candidates on the Shockley-Queisser chart of photovoltaic efficiency
3	R.D Schultz, E.E van Dyk, F.J Vorster	The effect of the Optical System on the Electrical Performance of III-V Concentrator Triple Junction Solar Cells
4	Kelebogile Maabong, Mmantsae Diale, Augusto Machatine, Yelin Hu, Artur Braun	Surface morphology of Iron oxide thin films prepared by dip coating: applications to solar cells
5	Leandré Brandt, Martin Onani, Francis Dejene, Paul Mushonga	Synthesis and characterisation of copper sulphide quantum dots for photovoltaic cell applications
6	Fred Joe Nambala, Mmantsae Diale, Jackie M. Nel, Arran Das, Augusto J. Machatine	AZO as a transparent conductive oxide for inversion-layer silicon solar cells
7	N. H. Mandanirina, J. R. Botha, and M. C. Wagener	Wavelength-modulated photocurrent spectroscopy of GaSb/GaAs quantum ring solar cells
8	G. Webb, E. Igumbore, W.E. Meyer	An Ab-initio Study into possible metastability of the Antimony-vacancy (Sb - V) complex in Germanium.
9	E. Igumbor, C. N. M. Ouma, W. Geoff and W. E. Meyer	Ab initio studies of Split<110> and Tetrahedral Di-interstitials of Germanium (Ge) using Hybrid functional HSE06
10	D. Mustafa, I.G.N. Silva, S.P. Sree, E. Bladt, H.F. Brito, S. Bals, G. Van Tendeloo, J.A. Martens, C.E.A. Kirschhock and E. Breynaert	Self-Assembled Nanotubular Mesoporous Layered Double Hydroxides with Tunable Photoluminescence
11	S.R Dobson, Z.N Urgessa, J.M Nel and J.R Botha	A comprehensive study of the parameters affecting cylindrical phase separation in PS-b-PMMA copolymer thin films
12	Zuraan Paulsen, Martin O. Onani, Joseph O Okil Francis B. Dejene Geoffrey M Mahanga	The Synthesis and Characterization of Magnetic/ Luminescent Fe_3O_4-InP/ZnSe Core-Shell Nanocomposite
13	Sharon Kiprotich, Francis B Dejene, Martin O. Onani, O Thekisoe, R Ngara	The influence of reaction times on structural, optical and luminescence properties of CdTe nanoparticles prepared by wet-chemical process.
14	Zamaswazi P. Tshabalala, David E. Motaung, Gugu H. Mhlongo and Odireleng M. Ntwaeaborwa	Characterization of TiO_2 nanostructures prepared by microwave method for gas sensing
15	Francis B. Dejene	Synthesis and characterization of structural and luminescence properties of TiO_2 nanoparticles for water treatment application

Poster No	Authors	Title
16	F.B. Dejene, L.F. Koao, R.D. Wario	Structure and optical properties of undoped and Mn-doped $ZnO_{(1-x)}S_x$ nano powders prepared by precipitation method
17	Vijay Kumar, M. Gohain, S. Som, Vinod Kumar, B. C. B. Bezuindenhoudt, Hendrik C Swart	Microwave assisted synthesis of ZnO nanoparticles for lighting and dye removal application
18	Katekani Shingange, Gugu H. Mhlongo , David E. Motaung, Odireleng M. Ntwaeaborwa	Preparation of ZnO nanorods and their gas sensing properties
19	J. Ungula, F.B Dejene	Effect of solvent medium on the material properties of ZnO nanoparticles synthesized by sol-gel method.
20	Meehleketo Advice Mayimele, Mmantsae Diale, F. Danie Auret	Analysis of temperature-dependent current-voltage characteristics and extraction of series resistance in Pd/ZnO Schottky diode
21	Helga T. Danga, Mmantsae Diale, Francois D. Auret, Sergio M.M. Coelho	Electrical Characterisation of Electron Beam Exposure Induced Defects in Silicon
22	Trilok Kumar Pathak, Vinod Kumar, H.C. Swart and L.P. Purohit	Effect of doping concentration on the conductivity and optical properties of p-type ZnO thin films
23	Matshisa J. Legodi, Francois D. Auret, Walter E. Meyer and Mmantsae W. Diale	Electrical characteristics of a nearly ideal Ni/4H-SiC interface studied by I–V–T and Admittance techniques
24	Shandirai M. Tunhuma, Mmantsae Diale, Francois D. Auret and Matshisa J. Legodi	The effect of high temperatures on the electrical characteristics of Au/n-GaAs Schottky diodes
25	PNM Ngoepe, W Meyer, M Diale, FD Auret, E Omotoso, HC Swart, MM Duvenage, E Coetsee	Chemical and electrical characteristics of annealed Ni/Ir/Au and Ni/Au contacts on AlGaN
26	E. Omotoso, M. Schmidt, W.E. Meyer, P.J. Janse van Rensburg and F.D. Auret	Low-Temperature Alpha-Particle Irradiation of Pd 4H-SiC Schottky barrier diodes
27	Crispin Munyelele Mbulanga, Zelalem Nigussa Urgessa, Stive Roussel Tankio Djiokap, Johannes Reinhardt Botha, M.M Duvenhage, H.C. Swart	Analysis of deep level emission bands in solution grown ZnO nanorods
28	Setumo V. Motloung, Francis B. Dejene, Hendrik C. Swart, Odirileng M. Ntwaeaborwa	Influence of varying Cr^{3+} mol % in $MgAl_2O_4$:0.1% Eu^{3+}, *x*% Cr^{3+} nanophosphor synthesized by sol-gel process
29	Simon N. Ogugua, Samy K.K. Shaat, Hendrik C. Swart, Odireleng M. Ntwaeaborwa	Synthesis and Characterization of a Novel Rare-Earth Oxyorthosilicates (R_2SiO_5) (R = La, Gd, Y) Doped Dy^{3+} Nanophosphors
30	Kashma Sharma, Vijay Kumar, Vinod Kumar, Hendrik C. Swart	Advances in phosphors based on purely organic materials for solid state lighting applications
31	D.V. Mlotswa, Roz M Madihlaba, M.O. Onani, B.F. Dejene, L.F. Koao	Rare earth doped lanthanum strontium borate ($La_2Sr_3(BO_3)_4$: xTb^{3+}) polycrystalline green phosphors

Poster No	Authors	Title
32	Ali Wako, Francis Dejene and Hendrik C. Swart	Structural and luminescence properties of $SrAl_2O_4:Eu^{2+}$, Dy^{3+}/Nd^{3+} phosphor thin films grown by pulsed laser deposition
33	A Yousif, OM Ntwaeaborwa and HC Swart	Luminescence properties of $CaO:Bi^{3+}$ phosphor
34	K.E Foka, B.F Dejene and H.C Swart	The effect of urea ratio on structural and luminescence properties of YVO_4:Dy phosphor
35	H.A.A. Seed Ahmed,, W.S. Chae, O.M. Ntwaeaborwa and R.E. Kroon	Interaction mechanism for energy transfer from Ce to Tb ions in silica
36	D. D. Ramteke, H. C. Swart, R. S. Gedam	Spectroscopic properties of Pr^{3+} ions embedded in lithium borate glasses
37	Pontsho Mbule, Martin Ntwaeaborwa, Bakang Mothudi and Mokhotjwa Dhlamini	$Zn_2SiO_4:Mn^{2+}$ co-doped with Tm^{3+} and other Re ions (Re = Rare-earth): Synthesis, Structure and Optical Properties
38	Raphael Nyenge, Samy Shaat, Luyanda Noto, Puseletso Mokoena, Hendrik Swart, Martin Ntwaeaborwa	TOF SIMS Analysis, Structure and Photoluminescence Properties of Pulsed Laser Deposited $CaS:Eu^{2+}$ thin films
39	Tero Laihinen, Mika Lastusaari, Laura Pihlgren, Lucas C.V. Rodrigues, Jorma Hölsä	Systematic Study of Up-Conversion Luminescence in $NaYF_4:Yb^{3+},R^{3+}$
40	Abdub G. Alia, Francis B. Dejenea and Hendrik C. Swart	The influence of oxygen partial pressure on material properties of Eu^{3+}- doped Y_2O_2S thin films deposited by Pulsed Laser Deposition method
41	Mika Lastusaari, Lucas C.V. Rodrigues,, Manu Lahtinen, Hermi F. Brito, Hendrik C. Swart, Jorma Hölsä	Interplay between phase transitions and thermoluminescence in $BaAl_2O_4$
42	Mika Lastusaari,, Lucas C.V. Rodrigues,Cássio C.S. Pedroso, Rodrigo V. Rodrigues, Hermi F. Brito, Miroslav Maryško, Petriina Paturi, Jivaldo R. Matos, Jorma Hölsä	Magneto-optical investigation of the cyclic redox $R_2O_2S \leftrightarrow R_2O_2SO_4$ (R: Eu, Tb) reactions
43	Gugu H. Mhlongo, David E. Motaung	Pd doped ZnO nanostructures: Structural, luminescence and gas sensing properties

[P01]

Effects of the copper content on the structural and electrical properties of $Cu_2ZnSnSe_4$ bulks used in thin-film solar cells

Moges Tsega[1,*] Dong-Hau Kuo,[2] Walelign Wubet[3], F.B. Dejene[4]

[1,4] *Department of Physics, University of the Free State (Qwaqwa Campus), Private Bag X13, Phuthaditjhaba, 9866, South Africa*
[2,3] *Department of Materials Science and Engineering, National Taiwan University of Science and Technology, Taipei 10607, Taiwan*

[*] *Corresponding author: mogestsega@yahoo.com (Moges Tsega)*

1. Abstract

We have investigated the concept of defect in $Cu_xZnSnSe_4$ (x= 1.6–2.0) and $Cu_y(Zn_{0.9}Sn_{1.1})Se_4$ (y= 1.6-2.0) bulks prepared by liquid-phase sintering at 600 ^oC for 2 h with soluble sintering aids of Sb_2S_3 and Te. All $Cu_xZnSnSe_4$ pellets exhibited *p*-type conductivity regardless of Cu contents but $Cu_y(Zn_{0.9}Sn_{1.1})Se_4$ pellets show *p*-type at y=1.6 and *n*-type at y= 1.8-2.0. SEM surface images showed the sintered CZTSe bulk exhibited a smooth, densely packed and homogeneous surface at the nearly stoichiometric composition. Increasing the copper excess also yields a rougher CZTSe morphology. The non-stoichiometric composition of CZTSe under various Cu contents caused the intrinsic defects, and the structural and electrical properties of the bulks can be explained based on the point defect properties. The deficiency of Cu content in CZTSe bulks easily leads to smaller unit cells.

2. Introduction

The *p*-type and Cu-deficient CZTSe film with a Zn/Sn ratio of 1.15 – 1.25 has been frequently used as an absorber layer [1,2]. However, some reports mentioned the Cu excess. Dharmadasa et al. and Chaure et al. reported the *p*-type $CuInSe_2$ (CISe) thin films prepared by an electrodeposition technique under a Cu-rich condition [3,4]. The increase of open circuit voltage also has been reported for the Cu-rich CISe thin-film absorber [5]. Recently, thin-film solar cell devices with the Zn-rich (Zn/Sn > 1) and Cu-rich (not Cu/(Zn+Sn) but Cn/Zn > 2) CZTSe absorbers show the device efficiency > 9%. So far, several groups have reported the advantages of Cu-poor and Cu-rich compositions in CIGSe and CZTSe thin-film solar cells to increase the conversion efficiency. However, there are no systematic studies for the effects of Cu content on defects and the structural and electrical properties. In this regard, the present paper investigates the effect of Cu content on the microstructural and electrical properties of CZTSe bulks prepared by a liquid-phase sintering method with sintering aids of Sb_2S_3 and Te.

3. Results

Hall effect measurements were carried out for CZTSe-a-x (x= 1.6–2.0) and CZTSe-b-y (y= 1.6-2.0) pellets after sintering at 600 ^oC for 2 h. The specimens were symbolized in terms of CZTSe-a-x for $Cu_x[(Zn_1Sn_1)_{0.9}Sb_{0.2}](Se_{3.3}S_{0.3}Te_{0.4})$ and CZTSe-b-y for $Cu_y[(Zn_{0.8}Sn)Sb_{0.2}](Se_{3.3}S_{0.3}Te_{0.4})$. For CZTSe-a-$x$ formula, all CZTSe pellets exhibited *p*-type conductivity regardless of the Cu content. For CZTSe-b-y formula, the pellets at y= 1.6 exhibited *p*-type conductivity whereas CZTSe pellets at y= 1.8 and y= 2.0 exhibited *n*-type conductivity. The hole concentration (n_p) of 1.5×10^{17}– $2.03\times10^{18}cm^{-3}$ for *p*-type CZTSe-a-x pellets increased with the increase Cu content from x= 1.6 to 2.0. The hole concentration (n_p) of $4.43\times10^{17}cm^{-3}$ was observed for *p*-type CZTSe-b-y pellet whereas the hole concentration (n_p) of 6.35×10^{17}– $4.88\times10^{17}cm^{-3}$ for *n*-type CZTSe-b-y pellets decreased with the increase in Cu content from y= 1.8 to 2.0. Electrical mobility (μ) of CZTSe-a-x pellets consistently increased from 1.23, 27.2 to 36.7 $cm^2/V{\cdot}s$ as the x value increased from 1.6, 1.8 to 2.0, respectively. Electrical mobility (μ) of CZTSe-b-y pellets consistently increased from 17.72, 21.29 to 58.40 $cm^2/V{\cdot}s$ as the y value increased from 1.6, 1.8 to 2.0, respectively.

References

[1] T. K. Todorov, K. B. Reuter, and D. B. Mitzi, Adv. Mater. 22 (2010) E156–E159.
[2] H. Katagiri, K. Jimbo, S. Yamada, T. Kamimura, W. S. Maw, T. Fukano, T. Ito and T. Motohiro, Appl. Phys. Express 1 (2008) 041201.
[3] N.B. Chaure, J. Young, A.P. Samantilleke and I.M. Dharmadasa, Sol. Energy Mater. Sol. Cells 81 (2004) 125–133.
[4] I.M. Dharmadasa, R.P. Burton and M. Simmonds, Sol. Energy Mater. Sol. Cells 90 (2006) 2191–2200.
[5] L. Gutay, D. Regesch, J.K. Larsen, Y. Aida, V. Depredur and S. Siebentritt, Appl. Phys.Lett. 99 (2011) 151912.

[P02]

n-WO_3|p-Si tandem layer solar cells as new candidates on the Shockley-Queisser chart of photovoltaic efficiency

Funda Mpanza[1,2,*], **Kittessa Roro**[3], **H. Upadhyaya**[2], **Bonex Mwakikunga**[2]

[1]*Heriot-Watt University, Scotland, United Kingdom*
[2]*DST /CSIR National Centre for Nano-Structured Materials Council for Scientific and Industrial Research, P O Box 395, Pretoria 0001, South Africa*
[3]*R&D core-Energy Initiatives, Council for Scientific and Industrial Research, P O Box 395, Pretoria 0001, South Africa*

[*]*Corresponding author e-mail address: Fsm5@hw.ac.uk*

1. Introduction

Significant debate has been ensuing among photovoltaics community since 1962 when Shockley and Queisser (S-Q) [1] developed a model for estimating the efficiency of a solar cell by matching the materials band gap energy to the sun's emission spectrum. The S-Q equation has been written as

$$\eta(x_g) = \left[x_g \int_{x_g}^{\infty} x^2 dx / (e^x - 1) \right] / \int_0^{\infty} x^3 dx / (e^x - 1) \qquad (1)$$

where x_g is E_g/kT_s where E_g is the material's band gap energy and T_s is the temperature of the sun. This equation arrives at the maximum efficiency of 33% for materials with band gap between 1.1 to 1.4 eV. For Si with band of 1.1 eV, the theoretical maximum efficiency works out to be 29%. The other materials with band gaps in this range are GaAs, AlGaN, InP and the like [2]. Most of these materials are scarce. Although Si ores are abundant, the cost of producing pure Si substantial such that the golden triangle, consisting of cost-efficiency- and - durability, is compromised. In order to reduce the cost while keeping the durability high, we have turned to tandem metal oxide coatings on Si wafers.

2. Results

WO_3 films were coated on p-Si by doctor-blading method and were tested for solar cell parameters in a solar simulator. Figure 1(a) shows the I-V curves with I_{sc} and V_{oc} clearly visible in (b). In (c) the efficiency of such a solar cell improves with increase in light intensity. This can be explained from blue-shift in the light source as the light intensity increases and this moves the impinging light spectrum closer to the optical band gap of the WO_3 and hence the S-Q effect of Equation 1 applies. Currently, metal oxides which are cheap as well as having a bang gap close to 1.1 – 1.4 eV are being tested as part of on-going work and preliminarily show a $\eta > 1.2$ showing that there is potential in this class of solar cells to grow to higher efficiency values.

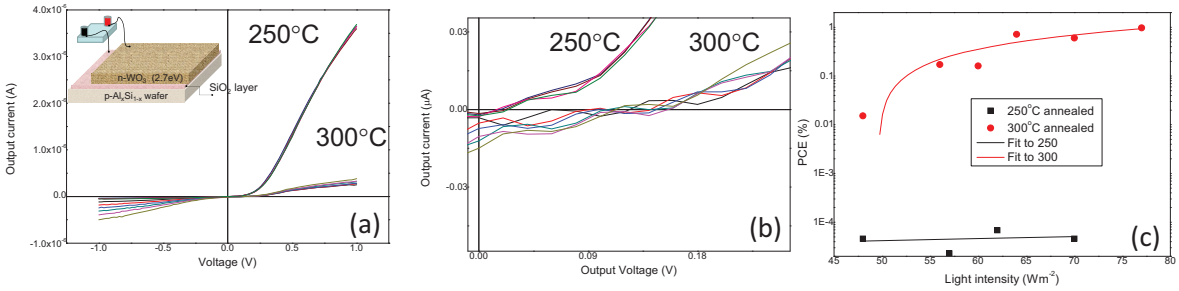

Fig. 1: Forward output current-voltage characteristics of the preliminary single junction p-Si-n-WO_3 solar cell annealed at 250°C and 300°C respectively (a) is the voltage sweep from -1 V to +1V (b) zoom-in picture of the same characteristic exposing V_{OC} and I_{SC} values around the origin of the graph and (c) the calculation of the photon-conversion efficiency (PCE) of the solar cells showing that annealing at high temperature improves the PCE.

3. References

[1] W. Shockley, H.J. Queisser, Detailed balance limit of efficiency of p-n junction solar cells, J Appl. Phys 32 (1961) 510-519
[2] Reported timeline of solar cell energy conversion efficiencies (from National Renewable Energy Laboratory (USA) (http://en.wikipedia.org/wiki/File: PVeff (rev110707)d.png)

[P03]

The effect of the Optical System on the Electrical Performance of III-V Concentrator Triple Junction Solar Cells

R.D Schultz[1], **E.E van Dyk, F.J Vorster**

[1] *Nelson Mandela University, Physics Department, Port Elizabeth, South Africa, P.O. BOX 77000, 6031*

S206029578@nmmu.ac.za

1. Introduction

The progression of the development of High Concentrated Photovoltaic (H-CPV) technology promises lower costs and higher cell and module efficiencies. However, development is limited by various materials and device aspects. One of these, the power production limiting effects of the optical system on a Concentrator Triple Junction (CTJ) cell in an H-CPV module, is the focus of this paper. With carefully designed experiments, which included spectral measurements, topographic intensity profiles in the cell plane and the analysis of I-V curves of the CTJ cell/H-CPV module, one can fully characterise loss mechanisms associated with the optical system and their effect on the electrical performance of the CTJ cell.

2. Results

Figures 1 and 2 show the effect of optical absorption and chromatic aberration on the subcells within a CTJ cell, respectively.

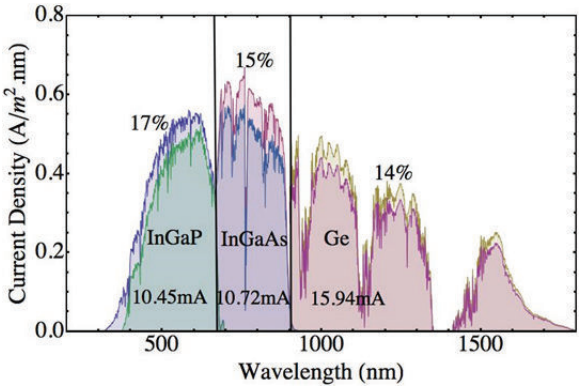

Fig.1: The reduction in the current density spectrum for each individual subcell in a CTJ cell due to absorption by the optical system at 1-sun (AM1.5D).

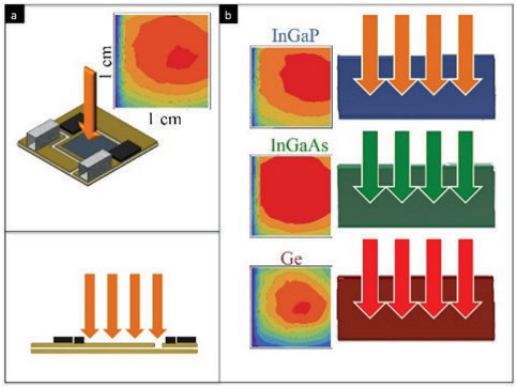

Fig. 2: Illustration and spectral distributional measurements showing the chromatic aberration created by the refractive optics for each individual subcell in a CTJ cell.

In Figure 1 the spectrum represents the current density, at 1-sun AM 1.5, without any optical components, while the lower spectrum is that with the optical elements in place. Due to the interactions of photons with the optical system, an average reduction in the current density of 14.6 % across the wavelength range is shown. As a result, the Ge subcell is mismatched by about 150% with respect to the limiting InGaP subcell junction.

In Figure 2(a) the intensity profile across the cell is shown, while Figure 2(b) illustrates the individual intensity profiles for each subcell. As the InGaP subcell utilizes energies with shorter wavelengths, the focal lengths are much shorter. At this Fresnel lens set distance from the cell, the incident concentrated sunlight wavelengths (400-700 nm) that correspond to the InGaP absorption region, will illuminate the whole cell. As the InGaAs subcell utilizes energies with mid- to long-range wavelengths, the combined spectral intensity profile lies beyond the focal plane of the H-CPV module. This leads to the spectral intensity being “defocused” which causes a wider, lower intensity profile beyond the focal point of the InGaP subcell. At this set position of the cell from the lens, the spectral profile results in a decrease in the potential current generation from the InGaAs subcell due to the concentration factor difference between subcells.

3. Conclusion

To conclude, good characterization of the optical system would allow for the identification of factors that will influence the performance of CTJ cells. Taking these factors into consideration, together with careful and informed CTJ cell design, more efficient and reliable H-CPV systems can be realized.

[P04]

Surface morphology and structural properties of iron oxide thin film photoanode prepared by dip coating: effect of electrochemical oxidation

Kelebogile Maabong[1], Mmantsae Diale[1], Augusto Machatine[1], Yelin Hu[2], Artur Braun[2]

[1]Department of Physics, University of Pretoria, Pretoria, 0002, South Africa
[2]Laboratory of High Ceramics, Empa, Swiss Federal Laboratories for Materials Science and Technology, CH-8600, Dubendorf, Switzerland
Corresponding author e-mail address: kelemaabong@gmail.com

1. Introduction

Metal oxides have attracted a considerable attention as transparent electrodes, active layers and charge collectors in optical applications due to their interesting properties [1]. Due to its a nearly ideal band gap (~ 2.1 eV) for solar energy conversions, low cost, chemical stability, natural abundance, n-type conductivity, "rust"- iron oxide (α-Fe_2O_3) - is regarded as a promising semiconductor in photovoltaic (PV) solar cells and photoelectrochemical (PEC) cells [2]. However, despite the good characteristics α-Fe_2O_3 absorbs weakly and conducts poorly due to poor carrier transport and rapid recombination of photo-generated electrons and holes. Surface morphology and structural properties strongly influences photoactivity efficiency of nanostructured electrodes [3]. α-Fe_2O_3 thin films were prepared by dip-coating method on fluorinated tin oxide (FTO) conductive glass substrates from Fe $(NO_3)_3 \bullet 9H_2O$ (28.0 g) and oleic acid (17.0 g) precursor. Four layers of hematite films were obtained after repeated dip coating and annealing at 500 ^{o} C for 2 hours. The photoanodes were electrochemically oxidized (anodized) in 1M KOH at a constant potential of 500 mV for 1 min in dark and light conditions. The structural properties of α-Fe_2O_3 nanoparticles were investigated.

2. Results

Fig 1 shows top view images of high resolution FE-SEM of pristine and anodized α-fe_2O_3 thin film photoanodes. The nanoparticles were spherical in shape. The micrographs depict a denser surface after electrochemical oxidation of photoanodes in light. Fig 2 shows XRD diffractograms of the films. The results show decrease in linewidth of the peaks in anodized samples which indicates increase in crystallite sizes upon the treatment.

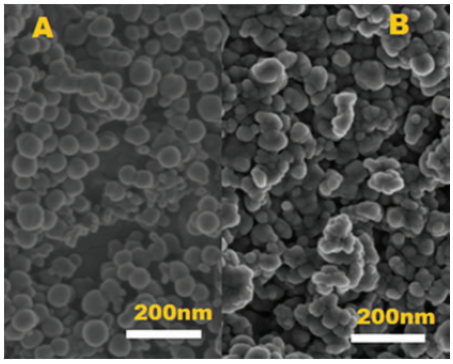

Fig 1. SEM micrographs of dip-coated α-Fe_2O_3 before (A) and after (B) electrochemical oxidation

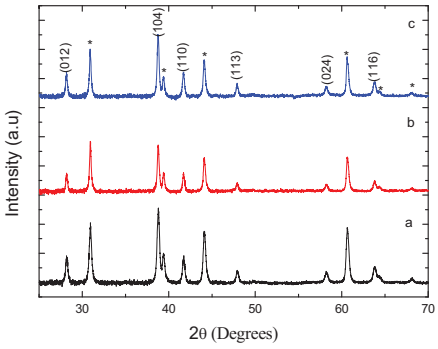

Fig 2. XRD diffractograms of dip-coated α-Fe_2O_3 before (a) and after (b,c) electrochemical oxidation

3. References

1. Yuan, L., et al., *Morphological transformation of hematite nanostructures during oxidation of iron.* Nanoscale, 2013. **5**(16): p. 7581-8.
2. Braun, A., et al., *Direct Observation of Two Electron Holes in a Hematite Photoanode during Photoelectrochemical Water Splitting.* The Journal of Physical Chemistry C, 2012. **116**(32): p. 16870-16875.
3. Hausmann D. M, and Gordon R. G, *Surface Morphology and crystallinity control in the atomic layer deposition (ALD) of hafnium and zirconium oxide thin films* Journal of Crystal Growth,(2003) **249** p.251–261.

[P05]

Synthesis and characterisation copper sulphide quantum dots for photovoltaic applications

Leandré Brandt[1], Martin Onani[1], Francis Dejene[2], Paul Mushonga[2]

[1]*Department of Chemistry, University of the Western Cape, Private Bag X17, Bellville 7535, South-Africa*
2Department of Physics, University of the Free State (QwaQwa Campus), Private Bag X13, Phuthaditjhaba,9866 , South-Africa
[2]*University of Zimbabwe Campus, Harare, 00263, Zimbabwe*
Corresponding author e-mail address:monani@uwc.ac.za

1. Introduction

The development of nanometer-sized materials plays an important role in next generation electronic and optoelectronic devices due to their to unique chemical and physical properties differing from their bulk counterpart such as their small size, size dependent properties and large surface to- volume ratio [1]. Semiconductor nanostructures are promising building blocks for the development of photovoltaic devices, for example in all-inorganic nanoparticle solar cells [2–3], dye sensitized solar cells, [4–5], and hybrid nanocrystal-polymer composite solar cells [6-7]. Challenges of such developments arise in the aptitude to find a semiconductor nanocrystal with a suitable bandgap, near 1 eV for a conventional, single-gap device having unique characteristics such as being an earth-abundant element and of environmentally benign composition. Copper(I) sulphide supersedes these challenging requirements making it a suitable candidate for applications in such devices. The major reason for the investigation of copper sulphide is their ease to form mixed phases, accordingly there are several solid phases such as Cu_2S (β, γ-chalcocite), $Cu_{1.96}S$ (djurleite), and CuS (covellite). Due to the copper vacancies within the lattice of these phases, they are identified as p-type semiconductor materials making them suitable for applications in photovoltaic cells [8]. Among these, Cu_2S is known to be an indirect and direct semiconductor bandgap material with a characteristic bulk bandgap of 1.21 eV and 1.8 eV, respectively [9]. Copper sulphide has the ability to form sub-stoichiometric compounds Cu_xS ($2 \geq x \geq 1$) due to its fairly complex crystal chemistry [10]. In a recent report, Han *et. al.* synthesized copper sulphide nanoparticles by directly heating a dodecanethiol solution with dispersed $Cu(acac)_2$ powder under the protection of nitrogen gas to 200 ℃, resulting in the formation of monodispersed $Cu_{1.94}S$ nanocrystals over a fairly large size distribution range upon the pyrolysis of $Cu(acac)_2$ in dodecanethiol via a facile one-pot heating up synthesis method[11]. Although significant promises in thin film studies of Cu_2S/CdS have been reported on, few literature reports on the synthesis and characterisation of copper (I) sulphide nanoparticles exist making it an attractive field for further research.

2. Objective

In this project we report an attempt on developing a facile, environmentally benign and low-cost synthesis method to obtain highly uniform and monodispersed Cu_2S nanocrystals with controllable size and shape. Secondly, we aim to characterize these nanocrystals and demonstrate their potential use in photovoltaic devices, in hopes to stimulate the development and competency of low cost and high performance semiconductor nanostructured material solar cells compared to conventional solar cells in the near future. Various synthesis methods including wet chemical and hot injection organometallic routes are employed in the synthesis of copper(I) sulphide quantum dots. Morphological characterisations of the quantum dots are done using high resolution transmission electron microscopy (HRTEM), scanning electron microscopy (SEM). The elemental characterisations are done using energy dispersive X-ray spectroscopy (EDX) and inductively coupled plasma optical emission spectroscope (ICP-OES). The surfactants on the nanoparticles are characterised using fourier transform infrared spectroscopy (FTIR).

3. References

[1] M. Nirmal and L. E. Brus, *Acc. Chem. Res.* **32** (1999), 407.
[2] K. S. Leschkies, R. Divakar, J. Basu, E. Enache-Pommer, J. E. Boercker, C. B. Carter, U. R. Kortshagen, D. J. Norris and E. S. Aydil, *Nano Lett.* **7** (2007), 1793.
[3] B. Tian, X. Zheng, T. J. Kempa, Y. Fang, N. Yu, G. Yu, J. Huang and C. M. Lieber, *Nature*., **449 (**2007) , 885.
[4] M. Law, L. E. Greene, J. C. Johnson, R. Saykally, P. D. Yang; *Nat. Mater.* **4** (2005), 455.
[5] J. B. Baxter and E. S. Aydil, *Appl. Phys. Lett.* **86** (2005**)**, 053114.
[6] I. Gur, N. A. Fromer, C. Chen, A. G. Kanaras and A. P. Alivisato, *Nano Lett.* **7** (2007), 409.
[7] D. H. Cui, J. Xu, T. Zhu, G. Paradee, S. Ashok and M. Gerhold, *Appl. Phys. Lett.* **88** (2006**)**, 183111.
[8] G. Liu, T. Schulmeyer, J. Bro¨tz, A. Klein, W. Jaegermann; "Thin Solid Films", **477** (2003**)**, 431-432.
[9] L. Sen, H. Wang, W. Xu, H. Si, X. Tao, S. Lou, Z. Du and L.S. Li, *J. Colloid Interface Sci.* **330** (2009**)**, 483–487.
[10] U. K. Gautam and B. Mukherjee, *Bull. Mater. Sci.* **29(1**) (2006**)**, 1-5.
[11] W. Han, L. Yi, N. Zhao, A. Tang, M. Gao and Z. Tang, *J. Am. Chem. Soc*, **39** (2008), 130.

[P06]

AZO as a transparent conductive oxide for inversion-layer silicon solar cells

Fred Joe Nambala[1,2], **Mmantsae Diale**[1], **Jackie M. Nel**[1], **Arran Das**[3], **Augusto J. Machatine**[1]

[1] *Department of Physics, University of Pretoria, Private bag X20, Hatfield, 0028. South Africa.*
[2] *Department of Physics, University of Zambia, Box 32379, Great East Road Campus, Lusaka. Zambia.*
[3] *Monash University, Private Bag X60, Roodepoort 1725, South Africa.*
Corresponding author e-mail address: fredjoe.nambala@up.ac.za

1. Introduction

Zinc Oxide (ZnO) has been attracting much attention in research activities for applications in light emitting diodes, spintronic devices, solar cells, etc. [1]. Doping the ZnO changes its properties especially in increasing its electrical conductivity [2]. This work focuses on the development of Aluminium doped Zinc Oxide (AZO) which has property-integrity to allow a research-in-progress hybrid inversion layer silicon solar cell to give maximum efficiency. The effects of thermal post-annealing in controlled air (N and O mixtures) on the electrical, structural and optical properties of undoped and aluminium-doped (i.e., 0%, 2% and 5%) AZO thin films deposited on glass and silicon substrates by the sol-gel method are investigated.

2. Results

AZO was prepared using the sol-gel method with 0%, 2% and 5% Al. Thin films were then deposited on glass as well as crystalline silicon (c-Si) immediately after preparation, after 1 day, after 2 days, and after 3 days, pre-heating at 200˚C between layers. After a number of days, they were post-annealed at 400˚C, 450˚C, 500˚C, 550˚C, 600˚C and 650˚C. Various characterization techniques including four-point probe, PL, UV-Vis, Raman spectroscopy, AFM, SEM and XRD measurements were conducted on the prepared samples. The energy bandgaps for 0%, 2% and 5% of Al in ZnO were determined as 3.48 eV, 3.37 eV and 2.95 eV respectively for samples deposited on microscope glass slides after 1 day ('Day 1', see Fig. 1) from the time of the sol-gel preparation. The determined E_g results for AZO depositions on Day 0, Day 2 and Day 3 after the preparation of the sol-gel are consistent with the trend of reducing bandgap as the concentration of Al increases from 0% through 2% to 5% in the $Al_xZn_{1-x}O$ polycrystalline material configuration. XRD measurements indicate that (002) is the most preferred orientation of the material. Peaks for (010), (011) and (110) orientations were also observed in the XRD pattern. Fig. 2 shows the de-convolution of peaks for AZO on glass Raman spectra, resulting in significant attribution of measured peaks. The results are being analyzed to understand the structural characterization of the AZO. The measurements from the other techniques will also be discussed.

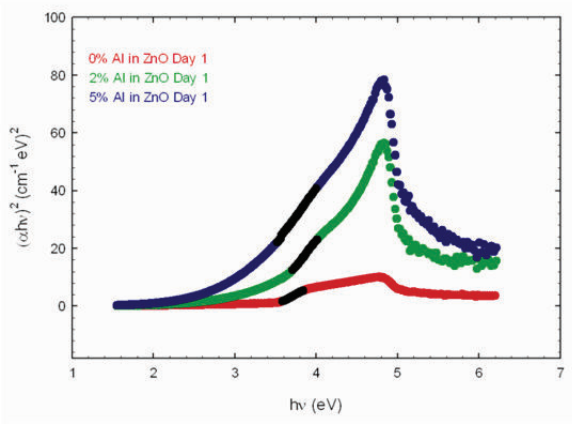

Fig.1: UV-Vis plots with the linear region from which the energy bandgaps were determined in black.

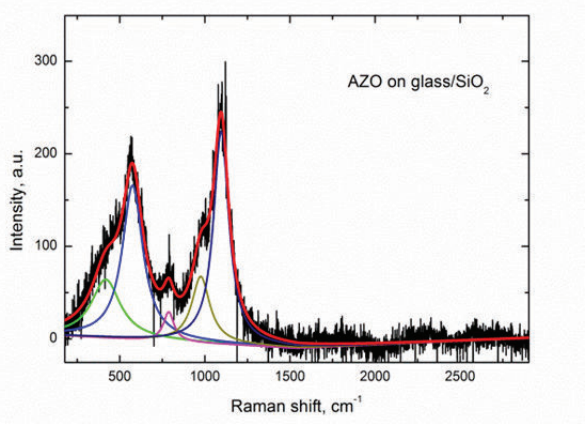

Fig. 2: De-convoluted Raman spectra of AZO/glass.

3. References

[1] U. Ozgur, Y.I. Alivov, C. Liu, A Teke, M.A. Reshchikov, S. Dogan, V. Avrutin, S.J. Cho, et. Al., *J. Appl. Phys.* **98** (2005) 041301.
[2] A. El Manouni, F.J. Manjon, M. Perales, M. Mollar, B. Mari, M.C. Lopez, J.R. Ramos Barrado, *Science Direct* **42** (2007) 134-139.

[P07]

Wavelength-modulated photocurrent spectroscopy of GaSb/GaAs quantum ring solar cells

N. H. Mandanirina, J. R. Botha, and M. C. Wagener

Department of Physics, Nelson Mandela Metropolitan University, Port Elizabeth 6031, South Africa
Corresponding author e-mail address: s213514095@nmmu.ac.za

1. Introduction

In recent years, many studies have been reported on the optical response characterization of type-II GaSb/GaAs quantum dot solar cells [1-2]. It has been shown that incorporating quantum structures into the junction can considerably extend the near band-edge response of the solar cell [2]. Unlike with conventional response measurements, where the intensity of the light source is typically modulated, differential spectroscopy is performed by modulating the wavelength of the pseudo-monochromatic excitation source [3-4]. However, due to the spectral dependence of most excitation sources, the optical intensity is inherently also modulated. As an example, in order to obtain the correct differential quantum efficiency (QE) spectrum of the solar cell, the photon flux of the excitation source would need to be measured separately and subtracted, *i.e.*

$$\frac{dQE\,(\lambda)}{d\lambda} = \frac{dI_{ph}}{d\lambda}\frac{1}{\phi(\lambda)} - \frac{d\phi(\lambda)}{d\lambda}\frac{I_{ph}}{\phi^2(\lambda)} \tag{1}$$

where I_{ph} is the measured photocurrent and $\phi(\lambda)$ the spectral flux density. In this study we report an alternative approach, in which the differential measurement is performed under constant flux (thereby eliminating the second term in eq. 1) by incorporating an *in situ* flux control module.

2. Results and discussion

Figure 1 depicts the differential photo-response setup, in which the flux control module has been incorporated. This module maintains the photon flux density of the incident light source at a constant intensity, thereby ensuring that the measured signal is purely related to the modulation of the excitation wavelength. Figure 2 compares the differential quantum efficiency of the solar cell obtained using the *in situ* (solid red line) and conventional (dashed line) approaches. With the addition of the flux regulator, the second term on the right hand side of eq.1 becomes negligible, and the differential quantum efficiency is measured directly. The large discrepancy observed between the two approaches below 1000 nm could be attributed to a phase shift between the wavelength and flux responses of the solar cell, which in turn would produce a sharp drop in measured photocurrent. By insuring a constant flux, the analysis is therefore greatly simplified and potential anomalies prevented.

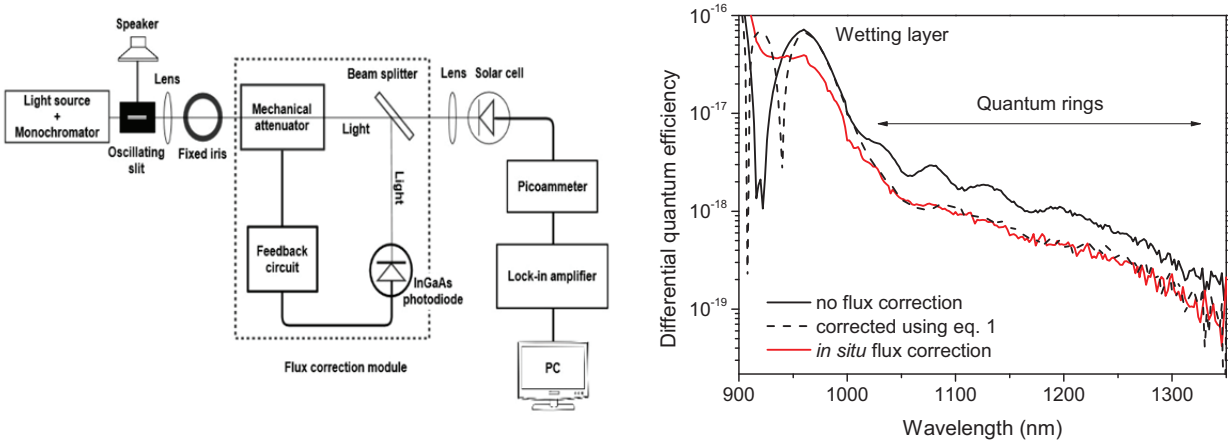

3. References

[1] M. C. Wagener, P. J. Carrington, J. R. Botha, and A. Krier. *J. Appl. Phys.* **116** (2014) 044304.
[2] P. J. Carrington, M. C. Wagener, J. R. Botha, A. M. Sanchez, and A. Krier. *Appl. Phys. Lett.* **101** (2012) 231101.
[3] J. S. Liang, S. D. Wang, Y. S. Huang, L. Malikova, F. H. Pollak, J. P. Debray, R. Hoffman, A. Amtout, and R. A. Stall. *J. Appl. Phys.* **93** (2003) 1874.
[4] J. G. Swanson and V. Montfomery. *J. Elec. Mat.***19** (1990) 13.

[P08]

An Ab-initio Study into possible metastability of the Antimony-vacancy (Sb - V) complex in Germanium

G. Webb, E. Igumbore, W.E. Meyer

University of Pretoria

Corresponding author e-mail address: geoffwebb@mweb.co.za

1. Introduction

We are investigating the possibility of the Antimony-Vacancy complex (E-center) using the Heyd-Scuseria-Ernzerhof (HSE06) hybrid functional within density functional theory (DFT). The results are then compared the predictions we obtained to experimental observations. We have in the past observed interesting results for the similar case of metastability in the Boron – Vacancy complex in silicon and wish to extend this research further to the Antimony-Vacancy complex in Germanium. We investigate the dependencies of the formation energy of the complex to the position of the Germanium vacancy to respect to the substitutional Antimony within the supercell. We examine the ability of the HSE06 functional to accurately predict the thermodynamic charge transition levels and whether or not charge-state controlled metastability exists in that of the Sb-V complex. The nearest neighbor and next nearest neighbor configurations of the Sb-V complex were also examined to give a greater understanding of the nature of this defect.

2. References

[1]C. Ouma, W.E. Meyer. “Metastability of the boron-vacancy (B-V) complex in silicon: Ahybrid functional study” currently under review in Physica Status Solidi (b)

[P09]

Ab initio studies of split<110> and tetrahedral di-interstitials of Germanium using Hybrid functional HSE06

E. Igumbor[1,2], C. N. M. Ouma, W. Geoff[1] and W. E. Meyer[1]

[1]*Department of Physics, University of Pretoria, Pretoria 0002, South Africa*
[2]*Department of Mathematical and Physical Sciences, Samuel Adebgoyega University, Ogwa Edo State Nigeria*
E-mail: Elgumuk@gmail.com

1. Introduction

As a result of its narrow band gap and high carrier mobility, the application of Germanium (Ge) as a promising material for complementary metal-oxide semiconductors (CMOS) technology is attracting attention recently [1]. Studies on Several defects including self-interstitials, interstitials, vacancies and vacancy complexes [2-3] have been carried out. For Silicon, various interstitials and vacancies including self-, di- and tri- has been studied [2] but none have been done on di-interstitials of Ge. In this work we present ab-initio calculation results of Ge Tetrahedral (T) split<110> (SP10) and split<110>/Tetrahedral (SPT) di-interstitial configurations in the frame work of density functional theory(DFT) using hybrid functional (HSE06)[4] exchange correlation functional. The formation and transition level energies of defected configurations charges of -2, -1, 0, +1 and +2 were obtained. Depending on the Fermi level, the formation energies shows that the SP10 is less favorable than T while the combination of SPT forms the most stable di-interstitial defect. We find (+1/+2) transition charge state level of T to be 0.74 eV above VBM and (+1/+2) for (SPT) configurations to be 0.06 eV below the CBM. These di-interstitials exhibited the properties of shallow donor at (+1/+2) above the Fermi level depending on the configurations. We compare this result with calculations of di-interstitial in silicon and available experimental data.

2. Results

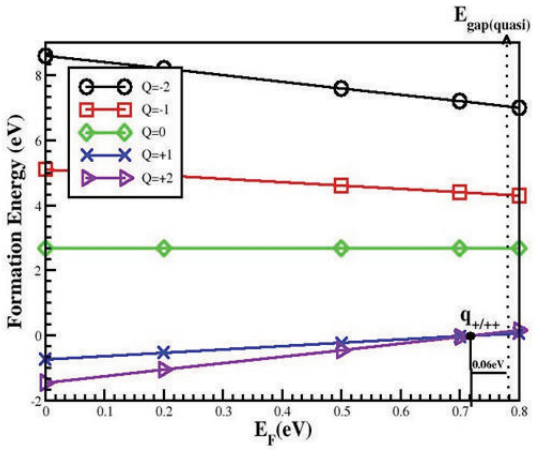

Fig 1: Formation and Fermi energies of SPT configuration

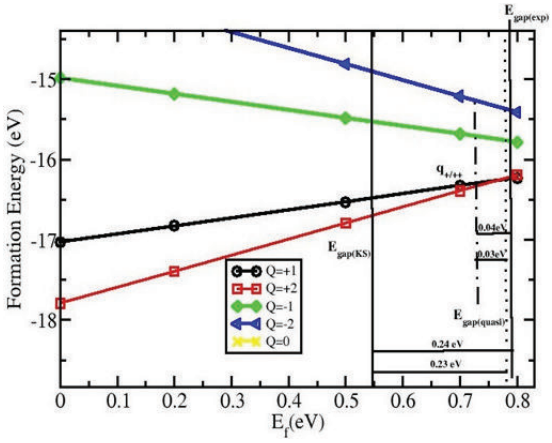

Fig 2: Formation and Fermi energies of T configuration

Using HSE06, the Kohn-Sham and quasi band gap of Ge interstitials are 0.54 and 0.78eV respectively see Fig 1. Formation energies of all the configurations considered are within the range 2.68-7.34 eV at $E_F = 0$. The formation energies decreases from doubly negative charge state to doubly positive charges states in all the configurations except for the T configuration. The introduced charges created states within the Fermi region closed to the Valence Band Maximum (VBM) and Conduction Band Minimum (CBM) for SPT and T configuration respectively.

3. References

[1] M. I. Lee, E. A. Fitzgerald, M. T. Bulsara, M. T. Curie and A Lochtefeld. *J. Appl. Phys.* **97** (2005) 011101.
[2] G S. Edmund AND C. K Meredith. Mat Sci. Eng. **55** (2006) 57-149.
[3] J. R Weber, A. Janotti and C. G Van de Walle Phys Rev B **87** (2013) 035203.
[4] J. Heyd and E. G. Scuseria. *J. Chem Phys* **121** (2004) 3.

[P10]

Self-Assembled Nanotubular Mesoporous Layered Double Hydroxides with Tunable Photoluminescence

D. Mustafa,[1,2] I.G.N. Silva,[2] S.P. Sree,[1] E. Bladt,[3] H.F. Brito,[2] S. Bals,[3] G. Van Tendeloo,[3] J.A. Martens,[2] C.E.A. Kirschhock[2] and E. Breynaert[2]

[1] KULeuven – Center for Surface Chemistry and Catalysis. Kasteelpark Arenberg 23 – box 2461, B-3001 Heverlee, Belgium. eric.breynaert@biw.kuleuven.be
[2] Department of Fundamental Chemistry, University of São Paulo – USP, São Paulo, SP, Brazil. dmustafa@iq.usp.br
[3] Electron Microscopy for Materials Science, University of Antwerp, Belgium.

1. Introduction

Self-assembled luminescent LDH nanotubes (Ø 20nm) combine the potential of RE^{3+} containing LDH with a high surface area and easily accessible mesopores (±175 m^2/g; 0.75 cm^3/g) suitable for hosting large sensitizing dyes and other interesting photonic species such as luminescent nanodots. While standard Layered Double Hydroxides (LDH) represent a unique family of layered inorganic anion exchangers [with composition $[M^{2+}_{1-x}M^{3+}_{x}(OH)_2]^{x+}A^{y-}_{x/y}\bullet nH_2O$; A: anion; M^{2+}/M^{3+} divalent/trivalent metal cation], they exhibit a limited specific surface area and no mesopore volume.[1] The relatively weak interlayer bonding however results in excellent expanding properties and high uptake of bulky organic and inorganic anions. Partial isomorphic substitution with RE^{3+} ions results in a luminescent layered where anionic sensitizing dyes directly adsorb to the positive charge located on the RE^{3+} ions.[2] As such they can serve as antenna molecules efficiently transferring additional photon energy to the RE and offering a route for improving the quantum yield. This explains the huge potential for applying RE^{3+} containing LDH as luminescent material.

2. Results

Nanotubular mesoporous LDHs were synthesized by controlled hydrolysis of metal cation mixtures containing highly coordinating cations in presence of the mesostructure directing agent.

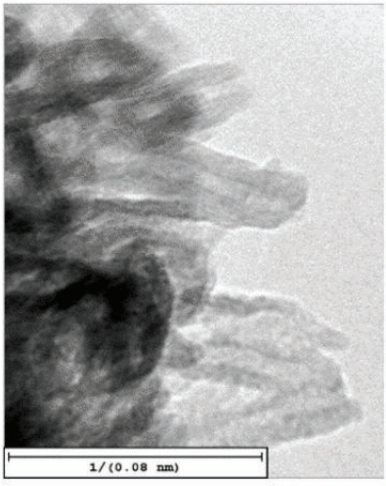

Fig. 1: Bright Field-TEM image of LDH nanotubes

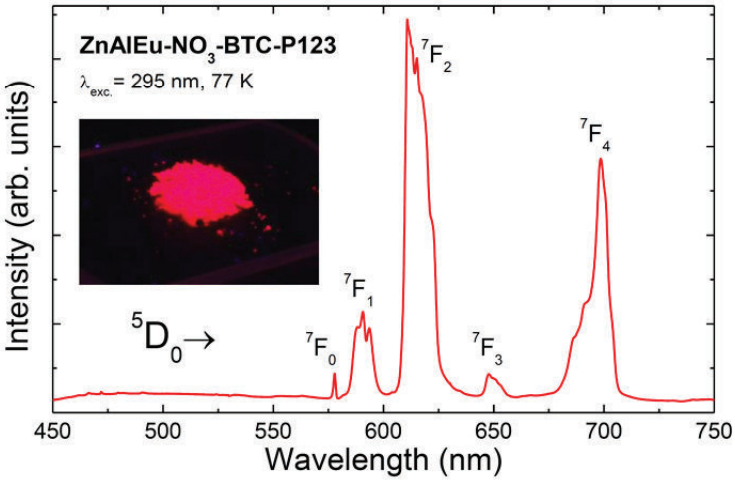

Fig. 2: Emission spectrum for the nanotubular mesoporous LDH recorded at 77 K and excited at 295 nm (BTC band). The inset shows the red emission of

3. References

[1] R. Ma and T. Sasaki *Adv. Mater.* 22 (2010) 5082.
[2] P. Gunawan and R. Xu, *J. Phys. Chem. C* 113 (2009) 17206.

[P11]

A study of the interface kinetics affecting cylindrical phase separation in PS-b-PMMA copolymer thin films

S.R Dobson*[1], Z.N Urgessa[1], J.M Nel[2] and J.R Botha[1]

[1] *Department of Physics, P.O Box 77000, Nelson Mandela Metropolitan University, Port Elizabeth, 6031, South Africa*
[2] *Department of Physics, University of Pretoria, Private bag X20, Hatfield, Pretoria 0028, South Africa*
* *Corresponding author e-mail address: stephen.dobson@nmmu.ac.za*

Abstract

In this study a controlled examination was undertaken in order to confirm and compare the parameters affecting PS-b-PMMA copolymer thin film nano-masks. A PS-b-PMMA copolymer with a molecular weight of 67 100 g.mol-1 (70:30) was used to produce thin film nano-masks on treated and untreated Si substrates. By simultaneously annealing samples of differing thin film thicknesses on the two types of treated silicon substrate in the same ambient (vacuum of 6×10^{-2} mbar) a direct comparison is made between the samples. It is shown that the average domain spacing's for perpendicular-to substrate morphology is approximately 40 nm. Additionally, the effect of thin film thickness on the formation of a perpendicular morphology is clearly demonstrated, with a thickness repeat period of approximately 32 nm. Importantly, interface effects are seen between the thin film and both the substrate and vacuum interfaces, and a minimum vacuum quality is shown to be a necessary requirement for producing uniform perpendicular morphologies across the thin film.

[P12]

The Synthesis and Characterization of Magnetic/ Luminescent Fe_3O_4-InP/ZnSe Core-Shell Nanocomposite

Zuraan Paulsen[1], Martin O. Onani[1]*, Joseph O Okil[2] Francis B. Dejene[3] Geoffrey M Mahanga[4]

[1]Department of Chemistry, University of the Western Cape, Private Bag X17, Bellville, South Africa
[2] 532 Winchester Avenue, Union, New Jersey, 07083, USA
[3]Department of physics, University of the Free State, QwaQwa Campus, Private bag X13, Phuthaditjhaba, 9866, South Africa
[4]Department of physical Sciences, Jaramogi Oginga Odinga University of Science and Technology, P.O. Box 210 - 40601 Bondo – Kenya
Corresponding Author: monani@uwc.ac.za

1. Introduction

Magnetic luminescent nanoparticles have shown great promise in various biomedical applications namely: contrast agents for magnetic resonance imaging, multifunctional drug carrier system, magnetic separation of cells, cell tracking, immunoassay, and magnetic bioseparation. However most of these nanoparticles are cadmium- based. Indium-phosphide is known to be less toxic than cadmium- based products. This experiment describes the synthesis of a core-shell nanocomposite material, which is composed of an iron oxide superparamagnetic core and an InP/ZnSe quantum dot shell. The magnetic nanoparticles (MNP's) and quantum dots (QD's) were synthesized separately before conjugation could occur. The MNP's were functionalized with a thiol-group allowing the QD shell to bind to the surface of the MNP by the formation of a thiol-metal bond.

2. Results

The synthesized nanocomposite was characterized with high- resolution transmission electron microscopy (HR-TEM), energy-dispersive X-ray spectroscopy (EDS), selective electron area diffraction (SAED), scanning electron microscopy (SEM), UV- visible spectroscopy, XRD and photoluminescence. These techniques yielded particle size, morphology, dispersion, and chemical composition including luminescence and florescence properties of the as prepared nanoparticles. The TEM micrograph showed crystalline nanoparticles which are monodispersed. These particles would be more useful in the *in vivo* applications after their solubility is tuned to a desired property. This experiment will continue further by investigating how various capping agents' affects the particles solubility. All the peaks of XRD patterns were analyzed and indexed using ICDD data base, comparing with magnetite standards. The lattice constant *a* was found to be 8.330 Å, which was compared with the lattice parameter for the magnetite of 8.39 Å. Further results will be reported including their applications.

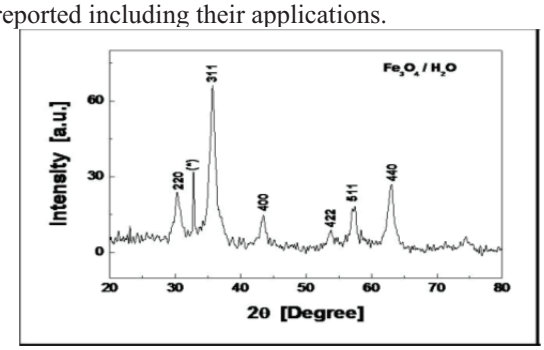

Fig.1: XRD for Fe3O4 magnetic nanocrystals

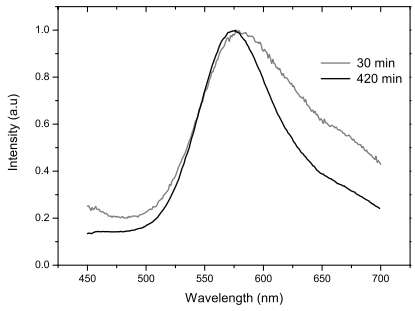

Fig. 2: PL of the aliquot for the synthesis of InP/ZnSe

3. References

[1] Pedro Tartaj1, Mar´ıa del Puerto Morales1, Sabino Veintemillas-Verdaguer, Teresita Gonz´alez-Carre ˜no and Carlos J Serna. 2003.
[2] Shen Wu, Aizhi Sun, Fuqiang Zhai, Jin Wang, Wenhuan Xu, Qian Zhang, Alex A. Volinsky
[3] Shouheng Sun, Hao Zeng, David B. Robinson, Simone Raoux, Philip M. Rice, Shan X. Wang, and Guanxiong Li

[P13]

The influence of reaction times on structural, optical and luminescence properties of CdTe nanoparticles prepared by wet-chemical process

Sharon Kiprotich[1], Francis B Dejene[1], Martin O. Onani[2], O Thekisoe[3], R Ngara[4]

[1]Department of Physics, University of the Free State, (Qwa-Qwa campus), Private Bag X-13, Phuthaditjhaba, 9866, South Africa
[2]Departments of Chemistry, University of the Western Cape, Private Bag X17, Bellville 7535, South Africa
[3]Department of Dept. Zoology and Entomology, University of the Free State, (Qwa-Qwa campus), Private Bag X-13, Phuthaditjhaba, 9866, South Africa
[4] Department of Plant Sciences, University of the Free State, (Qwa-Qwa campus), Private Bag X-13, Phuthaditjhaba, 9866, South Africa
Corresponding author e-mail address: KiprotichS@qwa.ufs.ac.za

1. Introduction

There is a growing interest in using semiconductor quantum dots (QDs) as optical diagnostics in biological applications such as sensors, cancer diagnosis and imaging. The size-controlled fluorescence properties of the nanoparticles, their high fluorescence quantum yields of QDs and stability against photobleaching makes the QDs superior optical labels for multiplex analysis. The QDs show other good properties over classical organic dyes such as broad absorption spectra, very narrow emission spectra and long fluorescence lifetime [1, 2]. The synthesis parameters for these nanoparticles include the reaction temperature and time, the pH of the reaction solution and the molar ratio of the stabilizer to Cd^{2+}. They have considerable influence on particle sizes and photoluminescence quantum yield of the CdTe nanopartciles. In this study CdTe nanparticles were made by a simple green synthesis using L-cystein as a capping agent, potassium tellurite and sodium selenosulphate as a stable tellurium and selenium sources respectively. The dimension of the core determines the band gap and hence the colour of emission. It is known, that an increase in particle sizes produces a redshift in the emission spectrum [3]. In principle, the emission of nanopartciles can be coarse-tuned by the choice of the material and later fine-tuned by playing with the size of the core.

2. Results

Fig. 1 shows the TEM micrographs of the representative CdTe nanoparticles. The micrographs exhibit lattice fringes indicating the good crystallinity of the nanocrystals. The particle sizes as determined by TEM were between 4 and 50 nm depending on reaction time. The XRD pattern for different reaction times corresponded to the hexagonal structure of the pure CdTe nanocrystals without any change in phase. It was observed that the crystallite sizes calculated using the Scherrer equation obtained from each set of synthesis conditions confirmed the obtained TEM measurements with variation of reaction time. The photoluminescence property of the CdTe QDs was found to be reaction time dependent. The emission spectrum was fine tuned from blue (498) nm to red (560 nm) of the visible spectrum (Fig. 2). The nanoparticles emission spectrum showed quite symmetric and narrow shape with a spectral width (the full width at half maximum) of approximately 80 nm (Fig. 2). The UV excitonic peaks illustrate that as the reaction time is increasing from 15 mins to 7hrs; the as synthesized materials were red shifted to a longer wavelength showing an increase in particle size. The band gap of CdTe from the absorption measurement increases to 2.5 eV (498 nm) for samples prepared at reaction time of 15 minutes which are blue shifted to higher energy from the band gap of bulk CdTe (1.5 eV), representing the quantum size effect of the nanoparticles.

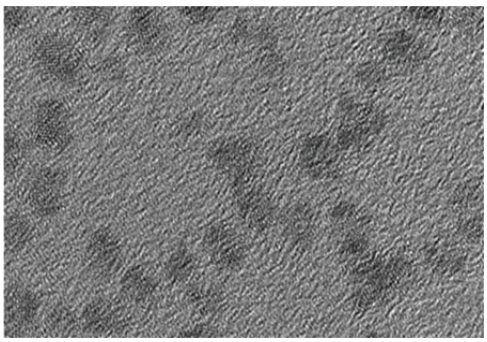

Fig.1: Representative TEM micrographs of CdTe nanoparticles

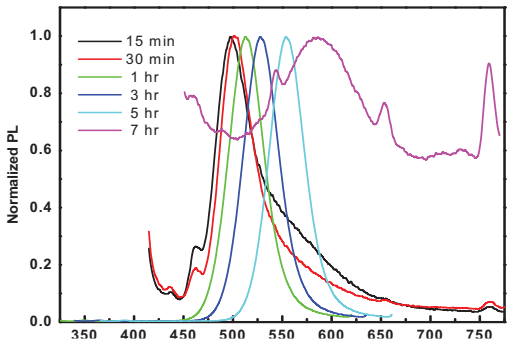

Fig. 2: PL emission spectra of CdTe QDs prepared at various reaction times, emitting at different wavelength when excited by a single excitation wavelength.

3. References

[1] R.E. Galian , G.M. Dela, The use of quantum dots in organic chemistry, *Trac-Trends in Analytical Chemistry*, 2009, **28**, 3, 279-291.
[2] H.C. LI, et al., Progress in the toxicological researches for quantum dots, *Science in China Series B-Chemistry*, 2008, **51**, 5, 393-400.
[3] M.J. Murcia, C.A. Naumann, (2005), *Biofunctionalization of Fluorescent Nanoparticles*, Wiley-VCH, Weinheim, Germany.

[P14]

Characterization of TiO_2 nanostructures prepared by microwave method for gas sensing

Zamaswazi P. Tshabalala[1, 2], **David E. Motaung**[2], **Gugu H. Mhlongo**[2] **and Odireleng M. Ntwaeaborwa**[1]

[1]Department of Physics, University of the Free State, P. O. Box 339, Bloemfontein ZA9300, South Africa
[2]DST/CSIR National Centre for Nano-Structured Materials, Council for Scientific and Industrial Research, Pretoria, 0001, South Africa
Corresponding author e-mail address: DMotaung@csir.co.za

1. Introduction

The need for gas sensors to monitor and detect toxic, explosive and combustible gases in mines and in the environment has stimulated researchers to develop portable gas sensing devices that can detect at low concentration and at room temperature. Monitoring such gases can help to prevent occurrences of fatal accidents such as fire and explosions [1].

Amongst the metal-oxides (MOXs) semiconductors, TiO_2 appears to be the most attractive material because of its diverse applications in various fields such as spintronics, solar cells, photocatalysis and gas sensors [2]. In addition, it has a good thermal stability and can operate in harsh environment. The structure and morphology of MOXs can be controlled by varying the synthesis procedure.

In this study we report the synthesis of TiO_2 nanostructures using a simple hydrothermal method in NaOH solution at 220 °C for 15 minutes. The influence of hydrochloric acid (HCl) aqueous solution as a washing agent on the surface morphology, structure and gas sensing properties of the TiO_2 nanoparticles was investigated. Additionally, the effect of calcination temperature on the properties of TiO_2 nanoparticles was also studied in detail.

2. Results

Fig. 1 shows the XRD patterns of the as-prepared TiO_2 nanoparticles washed with distilled water and different concentrations of HCl. Based on the results in Fig 1, the structure of the starting material, P25 Degussa shows a mixture of both anatase and rutile phases. The material washed with H_2O and HCl aqueous solution after synthesis reveals only the anatase phase. Previous studies reported that pure anatase TiO_2 phase has comparatively good sensing properties. The SEM images of P25 Degussa compared with that washed with H_2O and various concentrations of HCl aqueous solution are shown in Fig. 2. The particle sizes of the as-prepared samples increased as the concentration of the HCl as washing agent was increased as depicted in Fig. 2(c-d). The insets of figure 2 show the particle size distribution. The results revealed that when the grain size increases, grain boundaries decrease providing a large surface area thus increasing the sensing capabilities.

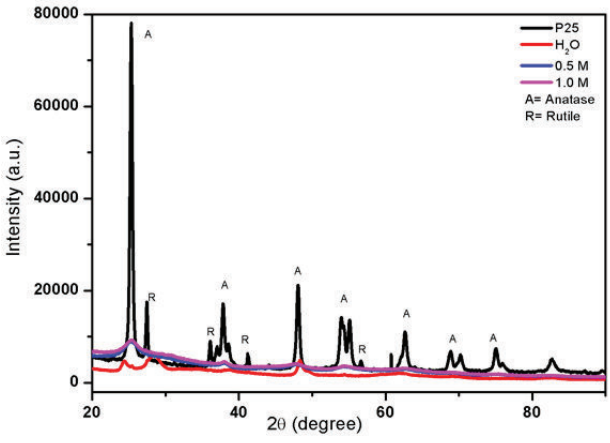

Fig.1: XRD patterns of as-prepared TiO_2 nanoparticles washed with different concentration of HCl.

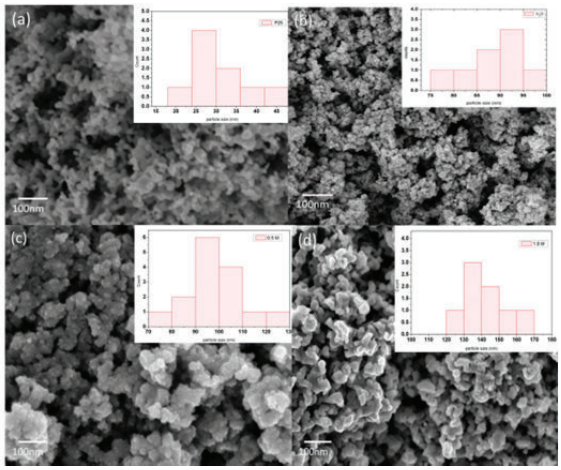

Fig. 2: SEM micrographs of (a) P25, washed with (b) H_2O, (c) 0.5 and (d) 1.0M HCL TiO_2 nanoparticles.

3. References

[1] D. Calestani, M. Zha, R. Mosca, A. Zappettini, M.C. Carotta, V.D. Natale, L. Zanotti, Sens. Actuators B 144 (2010) 472-478.
[2] W. Zhou, H. Liu, R. I. Boughton, G. Du, J. Lin, J. Wang and D. Liu, Journal of Materials Chemistry 20 (2010) 5993-6008.

[P15]

Synthesis and characterization of structural and luminescence properties of TiO_2 nanoparticles for water treatment application

Francis B. Dejene

Department of Physics, University of the Free State, (Qwa-Qwa campus), Private Bag X-13, Phuthaditjhaba, 9866, South Africa
Corresponding author email address: dejenebf@qwa.uovs.ac.za

Introduction

Solar water treatment is a low-technology solution that works to capture the heat and energy from the sun to make water cleaner and healthier for human use and consumption. The oxide nanoparticles synthesized by several methods appears more and more useful because these nanoparticles have good electrical, optical and magnetic properties that are different from their bulk counterparts [1]. Titania nanoparticles have received much interest for applications such as optical devices, sensors, and photocatalysis [2]. There are several factors in determining important properties in the performance of TiO_2 such as particles, crystallinity and the morphology. TiO_2 nanoparticles were synthesized by a simple sol-gel method. The structure and morphology of the synthesised nanocrystalline TiO_2 were characterized by XRD, SEM, UV and PL. The effect of some parameters such as hydrolysis rate, concentration amount of the precursor constituents, and annealing temperature were investigated.

Results

A representative scanning electron microscopy image of the TiO_2 nanoparticles synthesized presented in Fig. 1, indicates that the sample is composed of roughly spherical surface aspects. The anatase to rutile structural phase change occurs when annealed at a temperature greater than 500 °C when evaluated from X-ray diffraction pattern intensities of (101) and (110) peaks, respectively. Annealing samples at high temperature improves crystallinity as confirmed by both SEM and XRD measurements. It was observed that the band gap of TiO_2 varied from 2.49 and 3.26 eV while the crystallite sizes calculated using the Scherrer equation obtained from each set of synthesis conditions changed from 8 to 10 nm with variation of hydrolysis rate. The emmissions spectra (λ_{exc}= 325 nm) of TiO_2 nanoparticles for different hydrolysis rate display peaks at 336, 381 and 486 nm and the broad emission peak at about 381 nm is attributed to band gap transition.

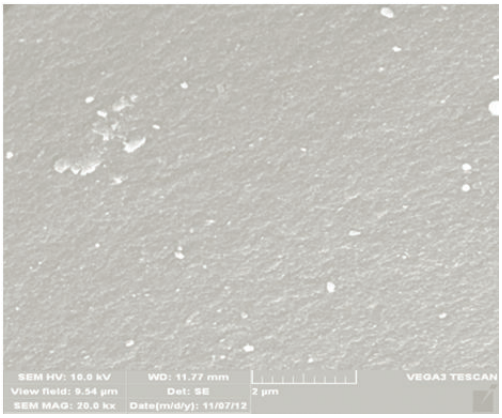

Fig. 1 SEM Micrographs of as prepared TiO_2samples revealed spherical-like morphology

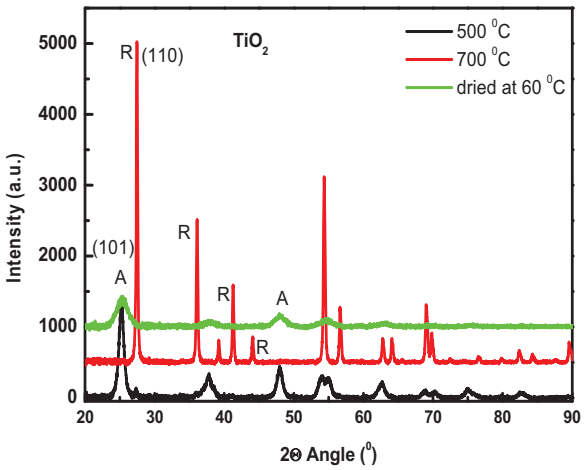

Fig. 2 Powder dried at ≤ 500 °C confirms anatase TiO_2. Peaks sharpen as the calcinations temperature increases. At 700 °C rutile structure appears.

References

1. H. Xu, X. Wang and L. Zhang, *powder Technol.* 185 (2008) 176.
2. O. Harizanov and A. Harizanova, *Sol. Energy Mater. Sol. Cells*, 63 (2000) 185.

[P16]

Structure and optical properties of undoped and Mn-doped $ZnO_{(1-x)}S_x$ nano powders prepared by precipitation method

F.B. Dejene[1], L.F. Koao[1], R.D. Wario[2]

[1]Department of Physics, University of the Free State, (Qwa-Qwa campus), Private Bag X-13, Phuthaditjhaba, 9866, South Africa

[2]Department of Computer Science, University of the Free State, (Qwa-Qwa campus), Private Bag X-13, Phuthaditjhaba, 9866, South Africa

Corresponding author e-mail address: dejenebf@qwa.ufs.ac.za

1. Introduction

With a wide band gap of 3.4 eV and a large exciton binding energy of 60 meV at room temperature, ZnO is attractive for blue and ultra-violet optoelectronic devices, and transparent conducting oxide films for photovoltaic applications. The large excitonic binding energies of ZnO and ZnS could enable efficient excitonic emission at temperatures well above room temperature and therefore lower threshold intensities for optoelectronic devices based on these semiconductors can be expected. Alloying ZnO by incorporating equivalent anions has not been extensively studied. Anion doping in ZnO, i.e., replacing oxygen by sulphur e.g. $ZnO_{(1-x)}S_x$ (ZnOS), has been reported recently [1, 2]. Due to the large electronegativity differences between O and S it would be expected that the bowing parameters of ZnOS are large. The change of anions in ZnO by isoelectronic impurities is important from the viewpoint of band gap engineering. In this work, high-quality undoped and Mn-doped ZnOS nano powders were prepared by the precipitation method.

2. Results

Figure 1 shows the typical XRD pattern of the obtained product. All the strong peaks in this pattern can be readily indexed to hexagonal wurtzite ZnOS structures. ZnOS alloys with a wurtzite structure were achieved for small content of sulphur and no evident phase separation was observed in the investigated composition range as determined by X-ray diffraction. Scanning electron microscopy observations showed the presence of nano-crystallites that decrease in size with Mn-doping. The optical absorption measurements show strong excitonic peak emission without any defect emission in the visible spectrum. The absorption edges of the nano powders shift towards low-energy side with increasing the Mn-dopant content. The presence of the Mn dopant diminishes the excitonic emission. The bandgap energies of the ZnOS nano particles were calculated and found to change from 4.0 to 4.2 eV, showing a nonlinear variation with a bowing behavior that was previously reported. The photoluminescence emission spectra of ZnOS nanoparticles gives four bands centering at about 548 nm, 614 nm, 649 nm and 670 nm, wavelengths. Similar to observations, It has been reported that the dopants of S, Mn can shift the luminescence position of ZnOS nanocrystals.

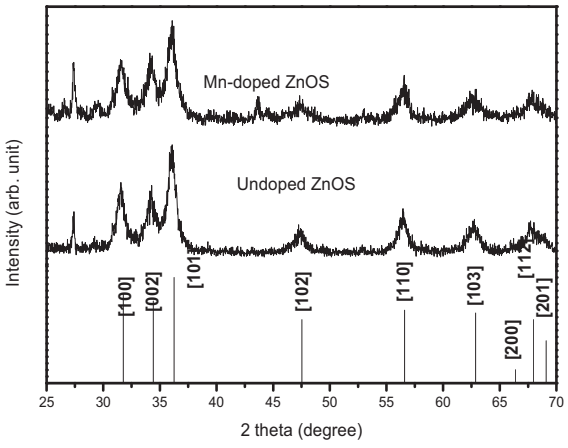

Fig. 1: The XRD pattern of the as-prepared ZnOS nanocrystalline powders.

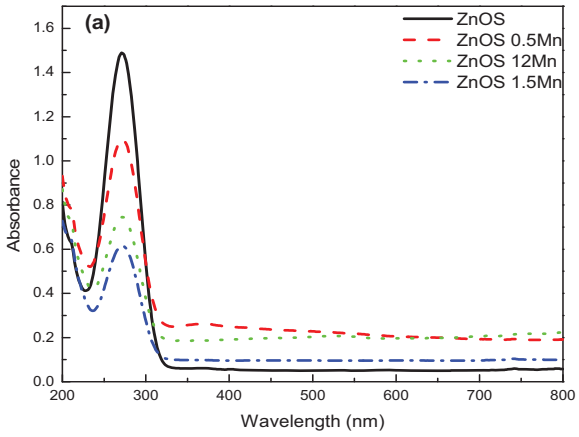

Fig. 2: UV–vis absorption spectra of undoped and Mn-doped ZnOS nanopowders.

3. References

G. Shen, J. H. Cho, S. J. K. Yoo , G-C. Yi, C. J. Lee, J. of Physical Chemistry B, 109(12) (2005) 5491-6.

B. K. Meyer, A. Polity, B. Farangis, Y. He, D. Hasselkamp, Th. Krämer, and C. Wang, Applied Physics Letters 85, (2004) 4929.

[P17]

Microwave assisted synthesis of ZnO nanoparticles for lighting and dye removal application

Vijay Kumar[1*], **M. Gohain**[2], **S. Som**[1], **Vinod Kumar**[1], **B. C. B. Bezuindenhoudt**[2], **Hendrik C Swart**[1*]

[1]Department of Physics, University of Free State, P.O. Box 339, Bloemfontein, ZA 9300, South Africa
[2]Department of Chemistry, University of Free State, P.O. Box 339, Bloemfontein, ZA 9300, South Africa
Corresponding author's e-mail:vj.physics@gmail.com, swarthc@ufs.ac.za

1. Introduction

Organic effluents discharged from the industries contain toxic dyes which contaminate the food chain through the water system. These dye materials show high solubility in the aquatic environment and is easily taken up by aquatic lives. The toxic dye molecules cause serious health hazards when ingested beyond the permitted concentration [1]. A number of technologies and processed have been urbanized to remove dye molecules from water resources [2]. Various adsorbents have been studied for the removal dyes from the waste water. ZnO is a gifted semiconductor material due to its wide band gap with a large exciton binding energy at ambient temperature which makes it a suitable candidate for a wide range of applications [3-4]. ZnO is an efficient material also for dye adsorptions due to its high surface to volume ratio, chemical affinity for the dye molecules as well as its suitable energy band potential alignment for charge transfer [3-4]. Till now, a series of methods have been adopted for the synthesis of ZnO nano structures [3-4]. Among them, the microwave assisted synthesis of ZnO nano particles (NPs) is a less studied area in this sector. The microwave-induced synthesis is an economical and green method for preparing metal oxide nano structures. The objectives of this study were (1) to prepare ZnO NPs and to characterize them with different techniques. (2) to study the effect of annealing on the optical and luminescence properties; and (3) to study the effects of time on the adsorption of methyl orange dye in waste water.

2. Results

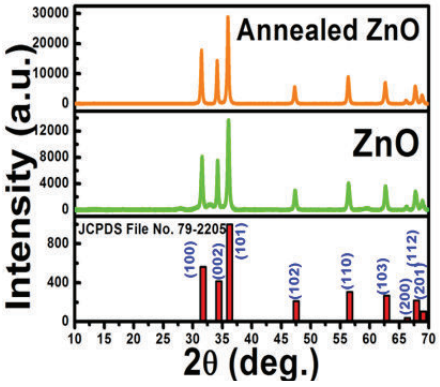

Fig.1: XRD pattern of as-synthesized and annealed sample.

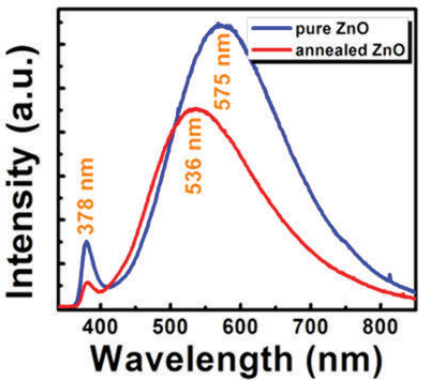

Fig. 2: PL emission of ZnO NPs.

The powder X-ray diffraction (XRD) patterns of the pure and annealed ZnO nano particles are shown in Fig. 1. The XRD peaks were identified and indexed according to the JCPDS file No. 79-2205. The crystallite size calculated from a Debye Scherrer formula was 24 and 26 nm for as-prepared and annealed ZnO, respectively. This is in good agreement with the crystallite size calculated by the Hall- Williamsons in which crystallite sizes were obtained as 33 and 34 nm, respectively. The photoluminescence (PL) spectra of the ZnO nanoparticles have been measured with an excitation wavelength of 325 nm (Fig. 2). It has been found that ZnO nanoparticles exhibited near white emission after annealing at 500 ^{o}C. Two broad and asymmetric emission bands in the visible region centred at 378 and 575 nm were observed in the pure ZnO attributed to band to band and defect transitions in ZnO [5]. After annealing at 500 ^{o}C both the bands intensity decreased, but the peak position for the 575 nm band shifted towards the lower wavelength region whereas the position of the 378 nm peak was fixed. De-convolution of the broad PL peak of pure ZnO revealed seven PL peaks at 378, 390, 410, 515, 595, 700 and 750 nm. The peaks were attributed to different defects: ~ the 700 and 750 nm emissions are due to $V_o^{\bullet\bullet}$ vacancies whereas the 515 emission is due to the $V_o^{\bullet}$ vacancy and the 600 nm emission is due to O_i, where V_o and O_i are oxygen vacancies and interstitials. After annealing the 600, 700 and 750 nm emissions disappeared and at the same time the area under the curve of the 515 and 560 nm peaks increased which were due to the $V_o^{\bullet}$ vacancies. The adsorption capacity of the as synthesized ZnO for methyl orange as a function of contact time has also been compared with that of annealed ZnO NPs.

3. References

[1] P. V. Dadhaniya, A. M. Patel, M. P. Patel and R.G. Patel, *J. Macromol Sci., Part A Pure Appl. Chem*. **46** (2009) 447-454.
[2] D. Solpan and M. Torun, *J. Macromol. Sci., Part A: Pure Appl. Chem*. **42** (2005) 1435–1449.
[3] S. Kuriakose, V. Choudhary,B. Satpati and S. Mohapatra, Phys. Chem. Chem. Phys. 16 (2014) 17560.
[4] V. Kumar, N. Singh, V. Kumar, A. Kapoor, L. P. Purohit, O.M. Ntwaeaborwa and H.C. Swart, J. Appl. Phys. 114 (2013) 134506.
[5] V. Kumar, V. Kumar, S. Som, M. M. Duvenhage, O. M. Ntwaeaborwa, H. C. Swart, Appl. Surf. Sci. 308 (2014) 419-430.

[P18]

Preparation of ZnO nanorods and their gas sensing properties

Katekani Shingange[1,2], **Gugu H. Mhlongo**[2], **David E. Motaung**[2], **Odireleng M. Ntwaeaborwa**[1]

[1] *Department of Physics, University of the Free State, Bloemfontein ZA9300*
[2] *CSIR-National Centre for Nano-structured Materials, PO Box 395, 0001*
Corresponding author e-mail address: gmhlongo@csir.co.za

1. Introduction

Usually, the properties of nanomaterials depend on their size, morphology, and dimensionality. One dimensional ZnO nanomaterials have taken the science world in a gigantic gesture due to their unique properties such as their luminescence characteristics and absorption of UV light. ZnO has many advantages, such as ease of production with various nanostructures via inexpensive and simple methods [1]. These nanostructures have various morphologies and amongst them, the ZnO nanorods have been reported to have great potential for gas sensors [1]. In this work, we report the successful preparation of low dimensional ZnO nanorods with different sizes using a microwave-assisted hydrothermal method by controlling the reaction-time. The influence of variation of microwave reaction time on the structure, optical and sensing properties was studied.

2. Results

To study the effect of microwave reaction time on the structure of the ZnO nanostructures, SEM and XRD analysis were conducted. The XRD patterns in Fig.1 confirm that the hexagonal wurtzite ZnO nanorods were crystallized. As observed in Fig.2, the morphology of the ZnO nanostructures is shown to be highly dependent upon the microwave reaction time. At 10 min, very small particles closely packed to each other to form rod-like structures were observed. However, with a slight increase of reaction time to 15 minutes, these small particles completely evolved to rod-like structures with a smooth surface. Further increase of the reaction time from 20 to 30 min resulted in thicker rods with different sizes. The structure, morphology, photoluminescent, absorption, and sensing properties of these nanostructures will be discussed.

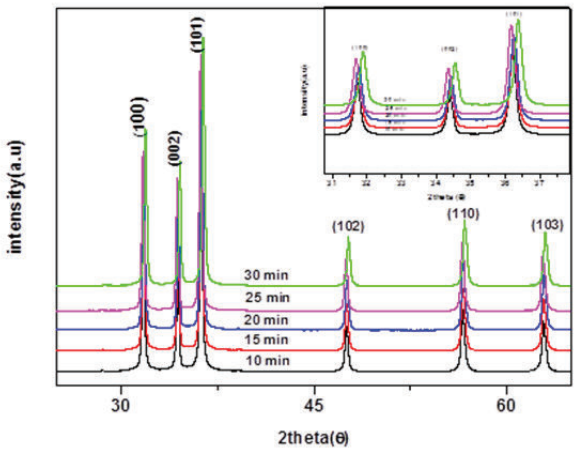

Fig. 1 XRD patterns of the ZnO nanorods obtained at different reaction times

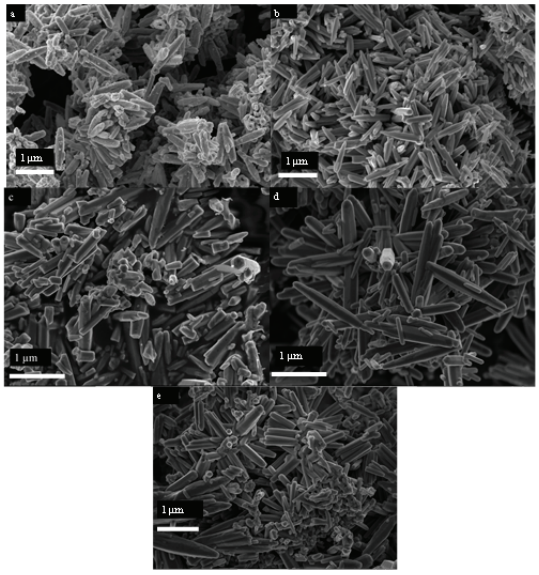

Fig. 2 SEM image of the ZnO nanorods obtained at different reaction times: a-10 min, b-15 min, c-20 min, d-25 min, e-30 min

3. References

1. L. Schmidt-Mende, J. L. MacManus-Driscoll, ZnO-nanostructures,defects and devices.materialstoday,2007,10:40-48

[P19]

Effect of solvent medium on the material properties of ZnO nanoparticles synthesized by sol-gel method.

J. Ungula and F.B Dejene

Department of Physics, University of Free State (Qwaqwa Campus), Private Bag X13, Phuthaditjaba, 9866, South Africa
Corresponding author e-mail:ungulaj@qwa.ufs.ac.za; Tel: +27(0) 844 167 274

1. Introduction

Zinc oxide (ZnO) nanostructure materials have wide range of applications based on unusual and remarkable physical properties such as high conductance, chemical and thermal stability, wide and direct band gap of 3.37 eV and a high excitation binding energy of 60 MeV. Its diverse applications include use in sensors, data storage, solid state lighting, solar cells and transparent conducting oxide. Good optical and luminescence properties of ZnO are very important for its application in different optoelectronic devices [1]. High crystallinity of zinc oxide nanoparticles is one of the most important factors in achieving a high UV emission efficiency. In this research high-quality ZnO nanoparticles have been synthesized by sol-gel method using zinc acetate and sodium hydroxide precursors and characterized using various techniques. The effect of varying volume ratios of water to ethanol solvent on ZnO nanoparticles prepared at constant temperature of 35 ^{o}C was studied. The influence of the solvent provides a means to achieve control over the ZnO nanoparticle size and size distribution, which is essential for tailoring optical, electrical, chemical, and magnetic properties of nanoparticles for specific applications [2].

2. Results

The x-ray diffraction pattern (Fig.1) shows single phase hexagonal structure. The crystallite size, obtained from XRD analysis, of as prepared ZnO nanostructures was found to decrease from 24 to 12 nm with the increase in volume ratio of ethanol in the solvent as peak intensities and sharpness increase with corresponding increase in volume ratio of water. Scanning electron microscopy shows samples prepared in water medium are nanoflakes which are turned to spheres and rods with increasing volume ratios of ethanol. Photoluminescence (PL) measurement for as prepared ZnO nanoparticles shown in Fig.2, indicate the green band emission that is associated with surface defects. However, spectra showed a strong ultra-violet emission, for annealed ZnO nanoparticles, which was centered on 385 nm and weak green emission at 550 nm confirming that the samples possess good optical properties with less structural defects and impurities. The band gap decreased from 3.308 to 3.168eV with an increase in the ethanol composition in the solvent, implying that the optical properties of these materials are clearly affected by the synthesis medium.

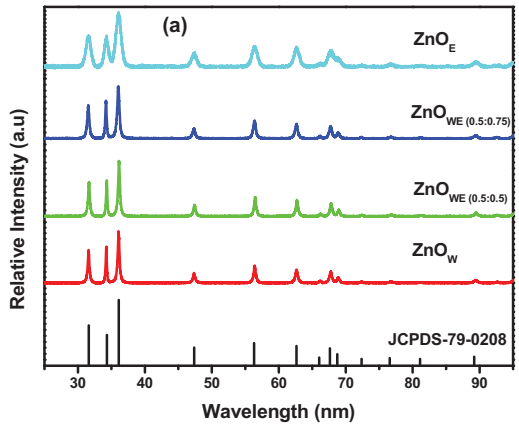

Fig. 1: XRD spectra of ZnO prepared with varying ratios of water and ethanol as solvents.

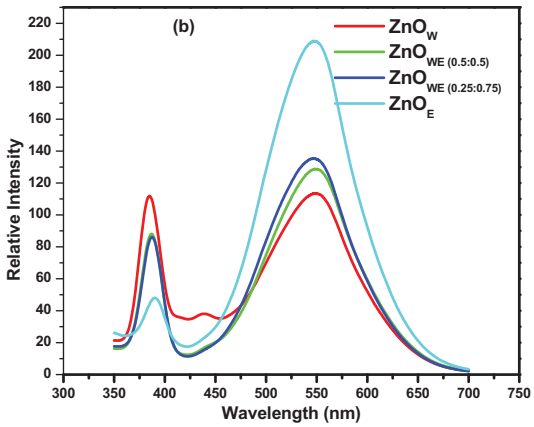

Fig. 2: PL emission spectra of ZnO prepared with varying ratios of water and ethanol.

3. References

[1] X, Daun, Y.Huang, Y.Cui, J.F.Wang, C.M Lieber, *Nature* **409** 66 (2001)
[2] Z. Hu, G. Oskam and P.C. Searson, *Journ. of Colloid and Interface Science* **263** 454 (2003)

[P20]

Analysis of temperature-dependent current-voltage characteristics and extraction of series resistance in Pd/ZnO Schottky diode

Meehleketo Advice Mayimele, Mmantsae Diale, F. Danie Auret

Department of physics, University of Pretoria, Pretoria 0002, South Africa
Corresponding author e-mail address: meehleketo@gmail.com

1. Introduction

In realizing semiconductor-based devices, there are various parameters such as the surface preparation process, the formation of barrier height between the metal and semiconductor and its homogeneity, density of interface states and dislocations, temperature, applied voltage and series resistance (Rs). Amongst all these, the series resistance is an important parameter, which causes the electrical characteristics of devices to be non-ideal [1]. There are various techniques to evaluate the main electrical parameters from the forward bias I-V measurements such as Cheung and Cheung's method and the Ohm's law [2]. Cheung and Cheung's method brings an alternative approach from Ohm's law to determine the barrier height, ideality factor and Rs from the forward I-V measurements, which are the main electrical parameters in the characterization of a Schottky diode and provide useful information concerning the nature of the diodes.
In this work, we analyse temperature dependent forward biased *I-V* measurements on Pd/ZnO Schottky barrier diode in the 30-350 K temperature range. The aim of this study is to compare extracted parameters that control the device performance such as the ideality factor, barrier height and R_s from the *I-V* characteristics by using different methods at the same temperature range. The TE theory with the Gaussian distribution of the barrier potential is used to determine Richardson constant [3].

2. Results

The analysis of current-voltage measurements performed on Pd/ZnO Schottky barrier diodes in the 30-350 K temperature range. Assuming thermionic emission (TE) theory, the forward bias *I-V* characteristics were analysed to extract Pd/ZnO Schottky diode parameters. Comparing Cheung's method in the extraction of the series resistance with Ohm's law, it was observed that at lower temperatures (T<180 K) the series resistance decreased with increasing temperature, the absolute minimum was reached near 180 K and increases linearly with temperature at high temperatures (T>200 K). The barrier height and the ideality factor decreased and increased, respectively, with decrease in temperature, attributed to the existence of barrier height inhomogeneity. Such inhomogeneity was explained based on TE with the assumption of Gaussian distribution of barrier heights with a mean barrier height of 0.986 eV and a standard deviation of 0.015 eV. A mean barrier height of 0.994 eV and Richardson constant value of 37.48 A cm^{-2} K^{-2} were determined from the modified Richardson plot that considers the Gaussian distribution of barrier heights.

3. Reference

[1] Z. Ahmad, M.H. Sayyad, Phys E, 41 (2009) 631-634.
[2] S.K. Cheung, N.W. Cheung, Applied Physics Letters, 49 (1986) 85-87.
[3] J.H. Werner, H.H. Güttler, Journal of Applied Physics, 69 (1991) 1522-1533.

[P21]

Electrical Characterisation of Electron Beam Exposure Induced Defects in Silicon

Helga T. Danga, Mmantsae Diale, Francois D. Auret, Sergio M.M. Coelho

Department of Physics, University of Pretoria, Pretoria 0002
Corresponding author e-mail address: mmantsae.diale@up.ac.za

1. Introduction

Silicon(Si) is one of the most important semiconductor materials and it has been studied extensively [1]. This is mainly due to its low cost, thermal stability, and good durability [2]. It is because of these properties that Si is a suitable candidate for exploring the electron beam exposure (EBE) technique. The main aim of developing the EBE technique was to see if electron beam deposition (EBD) induced defects could be introduced in a controlled manner. Excessive exposure would reduce the functionality of diodes for further study thus putting a limit on how much damage could be introduced. Energetic particles that cause EBD damage are present during EBE but interact directly with the semiconductor whereas during EBD this interaction mostly occurs via the metal used as a contact [3]. Deep level transient spectroscopy (DLTS) and high resolution Laplace-DLTS were used to characterise the defects introduced in epitaxially grown p-type Si during electron beam exposure. In this process, Si samples were first exposed to the conditions of EBD without metal deposition (EBE). The samples were exposed for 50 minutes. After EBE, Aluminium and Nickel Schottky contacts were fabricated using the resistive deposition method.

2. Results

For the aluminium contacts, the defect level H(0.33) was been identified as the interstitial carbon (C_i) related defect. It was a result of induced damage and could only be explained by the presence of donor-like traps [4].The capture cross-section was calculated to be $1.6 \times 10^{-19} cm^{-2}$ from the Arrhenius plot shown in figure 1**.**The defect level observed using the nickel contacts had an activation energy of H(0.55) with a capture cross-section of $6.6 \times 10^{-14} cm^{2}$. This defect has an activation energy similar to the I-defect. Pintilie *et al* observed a similar energy 0.545eV with a capture cross-section $1.7 \times 10^{-15} cm^{2}$ and $9.0 \times 10^{-14} cm^{2}$ after exposing their samples to high irradiation fluences. The defect level was detected using thermally stimulated current (TSC) [5].

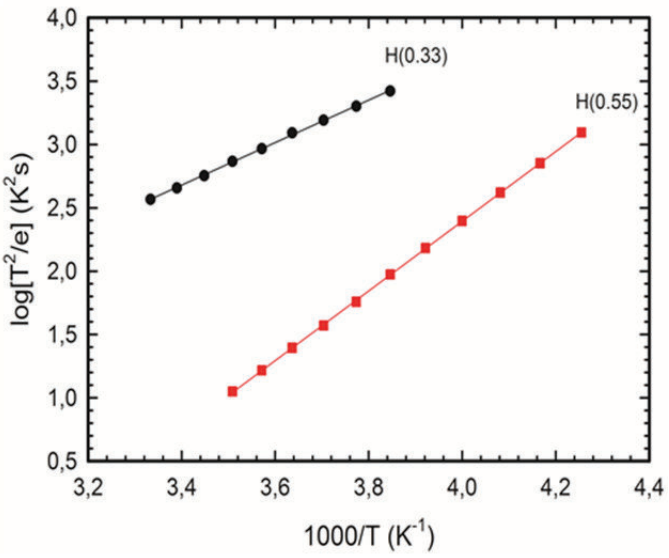

Fig. 1: Arrhenius plots of aluminiun and nickel contacts fabricated on p-type Si after EBE.

3. References

[1] Sze, S.M. 1981: John Wiley and Sons (WIE).
[2] http://www.americanphotonics.com/si.php. 2009.
[3] Coelho, S.M.M., *Thesis* 2014
[4] Paz, O. and F.D. Auret,Mat. Res. Soc. Symp., 1984. **25**.
[5] Pintilie, I., et al., Nuclear Instruments and Methods in Physics Research, 2006. **A 556** p. 197-208.

[P22]

Effect of doping concentration on the conductivity and optical properties of p-type ZnO thin films

Trilok Kumar Pathak[1], Vinod Kumar[2], H.C. Swart[2] and L.P. Purohit[1]

[1]*Semiconductor Research Lab, Department of Physics, Gurukula Kangri University, Haridwar, India*
[2]*Department of Physics, University of the Free State, Bloemfontein, South Africa*
(Corresponding author e-mail address: tpathak01@gmail.com)

1. Introduction

Zinc oxide (ZnO) is a multifunctional material with unique physical and chemical properties as well as good photo stability. ZnO naturally shows n-type conductivity due to a large number of native defects, such as oxygen vacancies and zinc interstitials. Therefore, it is difficult to obtain p-type ZnO thin films. The p-type ZnO contains a self-compensation effect, a deep accepter level and a low solubility of accepter dopants [1]. Theoretical studies demonstrated that the group-V elements might be good p-type dopants for introducing shallowness of the acceptor levels, which always tend to occupy the interstitial sites instead of substitution sites and act mainly as donors. It has been believed that N is one of the better candidates for shallow p-type dopants in ZnO. It has the smallest ionization energy [2]. AC conductivity is an important parameter to investigate the nature of the defect centres. AC conductivity also provides the information about the interior of the materials in the low conductivity region [3]. There are various techniques which were used to synthesize N doped ZnO thin film such as chemical vapor deposition (CVD), pulsed laser deposition (PLD), RF magnetron sputtering and sol-gel technique. Among these sol-gel is a good technique to obtain p-type conductivity with a high carrier concentration and mobility [4]. In the present work, ZnO:N thin films were deposited on glass substrates by the sol-gel technique. The effect of doping on the structural, morphological, optical and electrical properties of ZnO:N thin films was also investigated.

2. Results

The crystalline structure and surface morphology of the films were systematically investigated using X-ray diffraction and Scanning electron microscopy. All the ZnO thin films have a preferential (002) crystalline orientation and showed a wurtzite structure. The band gap of the ZnO:N was calculated using transmittance data obtained with a UV-vis spectrophotometer. The effect of N doping on the resistivity, carrier concentration and Hall mobility is shown in Fig.1. The minimum resistivity (ρ) of the ZnO:N thin films was 0.473 Ω-cm for a 4 at % N doping with a Hall mobility (μ) of 1.995 cm^2/Vs. ZnO:N thin films showed p-type conductivity at a 2 and 3 at% N doping. The AC conductivity measurements were carried out in the frequency range 10 KHz to 0.1MHz as shown in Fig.2. This type of variation is indicative of a localized conduction because the AC conductivity increased with an increase in the frequency. These highly transparent, highly conducting p-type ZnO thin films can be used as a window layer in solar cells and other optoelectronic devices.

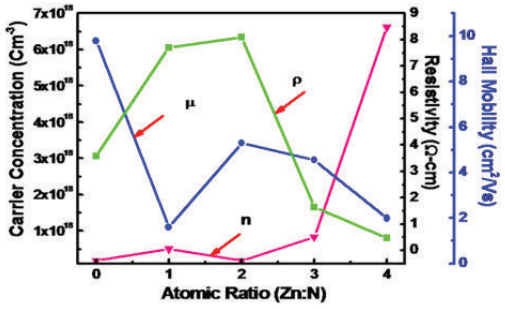

Fig.1: Effect of doping concentration on the resistivity, carrier concentration and Hall mobility of ZnO:N thin

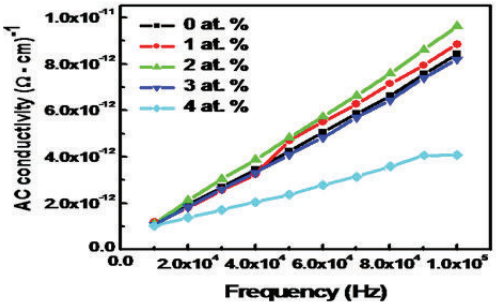

Fig. 2: AC conductivity vs frequency for the ZnO:N thin films at different doping concentrations

3. References

[1] D. Li-ping, W.Shu-ya, Z. Zhi-quin, Z.Guo-jun, *Optoelectronics Letters* **10 (2)** (2014) 0111.
[2] J. Huang, S. Chu, J. Kong, G. Wang, *Adv. Optical Mater* **1** (2013) 179.
[3] *S. Tewari, A. Bhattacharjee, P.P. Sahay, J. Mater. Sci.* **44(2)** (2009) 534.
[4] *M. Zaharescu, S. Mihaiu, A. Toader, I. Atkinson, J. Calderon-Moreno, M. Anastasescu, M. Nicolescu,M. Duta, M. Gartner, K. Vojisavljevic, B.Malic, V.A. Ivanov, E.P. Zaretskaya,Thin solid film* **571(3)** (2014) 727.

[P23]

Electrical characteristics of a nearly ideal Ni/4H-SiC interface studied by I–V–T and Admittance techniques

Matshisa J. Legodi, **Francois D. Auret, Walter E. Meyer and Mmantsae W. Diale**

Department of Physics, University of Pretoria, Private Bag X20, Hatfield, 0028
Corresponding author e-mail address: matshisa.legodi@up.ac.za

1. Introduction

SiC photodiodes are uniquely suitable for extreme radiation environments, have near-perfect visible blindness, low dark current, high speed, and low noise at high temperature operation. Also, low defect density SiC are critical for high power MOSFET applications. The presence of defects in the devices leads to sub-optimal operation, reliability issues and ultimately, premature device failure. W and Ti are metals of choice in n-4H-SiC owing to their good adhesion, speedy processing (sputtering or e-beam) and high temperature stability. However, W and Ti Schottky contacts on 4H-SiC are non-ideal and introduce metallization-induced damage. From both the physics and engineering perspectives, it is critical to understand the origins and nature of these defect-induced non-idealities in order to avoid or use them to our advantage in devices.

2. Results

To this end, we manufactured nearly ideal Ni contacts on 4H-SiC, doping 3.7×10^{14} cm^{-3}. The electrical characteristics are ideal down to 150 K, as shown in Fig. 1, whereupon they exhibit anomalous temperature-dependent Φ_{B0} and n, accompanied by the onset of thermionic-field emission, which we found to increase with doping density. However, we did not observe any "T_0 anomaly" [1] for doping < 7.1×10^{15} cm^{-3}.

The observed temperature-anomaly was traced to interface states of density, $D_{it} = 10^{13}$ eV^{-1} cm^{-2} peaked at ($E_C - E_{it}$) = 0.6 eV which increase towards the Ni/4H-SiC interface, as shown in Fig. 2. The D_{it} is consistent with a Gaussian distribution with parameters: mean_Φ_{B0} = 1.55 eV, σ_0 = 0.02 eV, ρ_2 = 0.065 eV, and $\rho_3 = -3.98\times10^{-3}$ eV, the mean barrier height, standard deviation, voltage deformation coefficients of the Gaussian distribution. These results, taken together with analysis of W/4H-SiC and Ti/4H-SiC systems, suggest that the D_{it} is made up of contributions from dopant-effects or dopant-related defects and surface defects introduced during metallization distributed in the semiconductor interface.

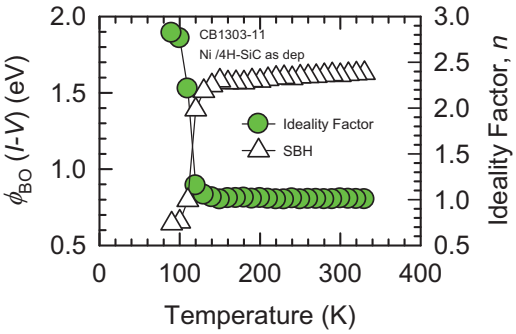

Fig. 1: Ni/4H-SiC showing temperature dependent Schottky barrier height, Φ_{B0}, and ideality factor, n, for the 3.7×10^{14} cm^{-3} sample CB1303-11.

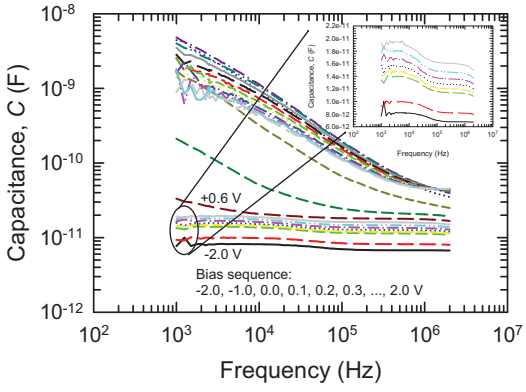

Fig. 2: Insert shows capacitance steps of the G/ω peaks (not shown) and increasing capacitance towards the surface particularly at low frequencies. This indicates inclusion of "excess" interface capacitance to the space charge region (scr) capacitance. The interface capacitance decouples from the scr capacitance at high frequencies.

3. References

[1] A. N. Saxena. *Surface Science*. **13**. (1969) 151.
[2] R. T. Tung. *Physical Review B*. **45**. (1992) 13509.

[P24]

The effect of high temperatures on the electrical characteristics of Au/n-GaAs Schottky diodes

Shandirai M. Tunhuma, Mmantsae Diale, Francois D. Auret and Matshisa J. Legodi

Department of Physics, University of Pretoria, Private Bag X20, Hatfield, 0028
Corresponding author e-mail address: mmantsae.diale@up.ac.za

1. Introduction

Gallium Arsenide is an important material for integrated photonic applications. This is mainly because it readily lends itself to large scale production of single photon sources.[1][2] These photons are excellent carriers of quantum information in communication systems. Significant amounts of waste heat are generated in these computing systems, exposing the GaAs devices to elevated temperature for extended periods. As a result, comprehensive studies of the effects of temperature on the operation of the metal-semiconductor (M-S) structures and on the material itself have become vital.

We investigated the properties of Gold Schottky contacts fabricated on epitaxial n-type GaAs of doping density 1E15 and their thermal stability in the 80 – 480 K temperature range. Current-voltage *(I–V)* and capacitance-voltage (C–V) characteristics were used to study the rectification properties of the M-S contacts. Our *C–V* investigations were carried out in two modes: (1) dynamic annealing, conducted at some elevated temperature in the 300 – 480 K range, and (2) post thermal-exposure measurements, conducted at 300 K. These 300 K measurements were designed to gain insights into any modification to the Au/GaAs system accompanying the annealing in the dynamic mode. We also considered and monitored using Laplace deep level transient spectroscopy (L-DLTS), the effects of the EL2 defect on the capacitance and rectification properties of the Au/GaAs.

2. Results

I–V measurements below 300 K exhibit a temperature dependence that is known to be caused by Schottky barrier inhomogeneities: the ideality factor decreases while the Schottky barrier height increases (both with increasing temperature, below 300 K). We observe a plateau between 300 K and 400 K consistent with high quality, nearly ideal metal-semiconductor contacts. Above 400 K, our results show a decreasing Schottky barrier height and an increasing ideality factor, suggesting a physical modification to the M-S system.

In the dynamic mode, the *C–V* barrier height increases with decreasing temperature. Two distinct and fairly monotonic regions either side of 400 K are observable, although the slope (rate of increase) is less-steep below 400 K. The *C–V* barrier height figures above 400 K in both modes show similar trends. A decreasing trend is evident below 400 K in the post thermal-exposure mode. We noted a sharply increasing free carrier density starting around 300 K and attribute it to the "extra" charges thermally-emitted by the EL2 defect. This is observable up to about 400 K, beyond which both measurement modes yield nominally the same *C–V* barrier height figures. In this region, both the *I–V* and *C–V* barrier heights and the free carrier density show a decrease, consistent with a M-S structure that is being physically modified or changed. Our results suggest that exposure of the Au/GaAs M-S junction to elevated temperatures – even modest exposures – may lead to its physical modification.

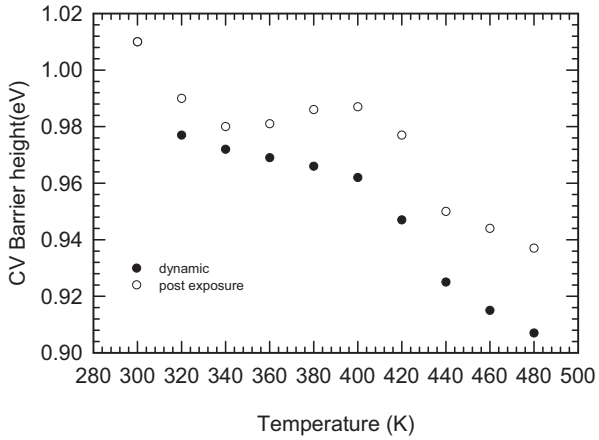

Fig 1.The C-V barrier height as a function of temperature measured first during exposure to high temperatures then at room temperature afterwards

3. References

[1] A.Gaggero,S.J.Nejad,F.Marsili,FMattioli,R.Leoni,D.Bitauld,D.Sahin,G.J.Hamhuis,R Notzel, RSanjines and A.Fiore.*Applied.Physics . Letters* **97**(2010) 151108

[2] A.J Shields *Nat Photonics*1,(2007)215

[P25]

Chemical and electrical characteristics of annealed Ni/Ir/Au and Ni/Au contacts on AlGaN

PNM Ngoepe[1], W Meyer[1], M Diale[1], FD Auret[1], E Omotoso[1]
HC Swart[2], MM Duvenage[2], E Coetsee[2]

[1]Department of Physics, University of Pretoria, Private bag X20, Hatfield, 0028
[2]Department of Physics, University of the Free State, P.O. Box 339, Bloemfontein, 9300
Corresponding author e-mail address: phuti.ngoepe@up.ac.za

1. Introduction

Aluminum gallium nitride (Al_xGa_xN) is a ternary wide direct bandgap semiconductor. The Al to Ga ratio can be varied to achieve various bandgap ranging from 3.4 eV for pure GaN to 6.2 eV for pure AlN. This property makes AlGaN based devices suitable for light emitting and light detecting devices such as LED's and photodiodes. In fabricating a device such as a Schottky diode the metals deposited on the semiconductor play an important role in the operation of the device. This is because the metal-semiconductor contact of a Schottky diode influences the transport mechanisms of the device. It therefore becomes significant to understand the interaction of metals with the semiconductor substrate. Annealing has been used as a method of studying the evolution of the optical and electrical properties of semiconductor based devices [1,2]. In particular a study was performed on AlGaN Ni (20 Å)/ Au (50 Å) and Ni (20 Å)/ Ir (30 Å)/ Au (50 Å) Schottky photodiodes [3]. The samples were subjected to isochronous annealing for 5 min. under an Ar. ambient. The evolution of the chemical properties of these contacts with temperature is studied by using two surface characterization methods namely Time of Flight Secondary Ion Mass Spectroscopy (TOF-SIMS) and X-ray photo electron spectroscopy (XPS).

2. Results

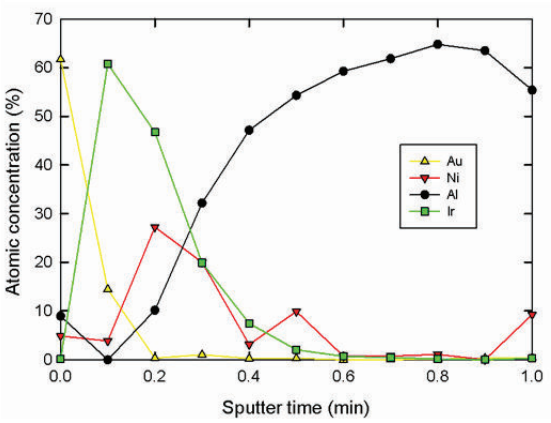

Fig. 1 (a): XPS depth profile of a Ni/Ir/Au metal layer deposited on AlGaN and measured without annealing.

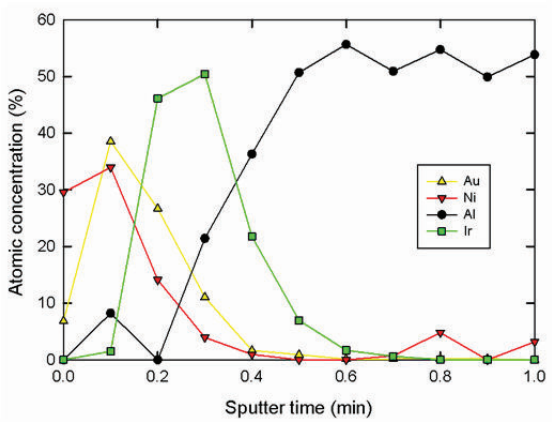

Fig. 2 (b): XPS depth profile of a Ni/Ir/Au metal layer deposited on AlGaN and measured after 600 °C annealing.

The XPS depth profiles of the as deposited and 600 °C annealed AlGaN samples are shown in Fig. 1 (a) and (b). Annealing the sample made the Ni to out-diffuse through the Ir and the Au. The Ir made contact with the AlGaN substrate and thus seemed to have an influence on the transport mechanisms of the photodiode. The inserted Ir layer prevented the Au from making contact with the AlGaN substrate. These profiles are only used to indicate the diffusion process. Due to the overlapping of the Ga and N peaks the atomic concentration thereof are not shown. The atomic concentration of the Al in the substrate is also an over estimation due to this overlapping. More detail about these results and the SIMS profiles will be discussed in detail in the presentation.

3. References

[1] Chang P.C., Chen C.H., Chang S.J., Su Y.K., Yu C.L., Chen P.C. and Wang C.H., *Semicond. Sci. Tecnol.* **19** (2004) 1354.
[2] Sheu J.K., Su Y.K., Chi G.C., Chen W.C., Chen C.Y., Huang C.N., Hong J.M., Yu Y.C., Wang C.W. and Lin E.K. *J. Appl. Phys.* **83** (6) (1998) 3172.
[3] Ngoepe P.N.M., Meyer W.E., Diale M., Auret F.D., and van Schalkwyk L., *Physica B* **439** (2014) 119.

[P26]

Low-Temperature Alpha-Particle Irradiation of Pd/4H-SiC Schottky barrier diodes

E. Omotoso[1,2], M. Schmidt[1], W.E. Meyer[1], P.J. Janse van Rensburg[1] and F.D. Auret[1]

[1] *Department of Physics, University of Pretoria, Private Bag X20, Hatfield 0028, South Africa*
[2] *Departments of Physics, Obafemi Awolowo University, Ile-Ife, 220005, Nigeria*
Corresponding author e-mail address: ezekiel.omotoso@up.ac.za

1. Introduction

Silicon carbide (SiC) is a promising semiconductor with a wide bandgap of 3.26 eV [1], which has drawn the interest of many researchers due to its excellent properties such as high thermal conductivity, high breakdown field and high saturated drift velocity [2]. These characteristics make SiC a semiconductor capable of outperforming silicon in electronic devices for high-power, high-frequency and high-temperature applications [3], and is a key material for the next-generation photonics [4]. We have investigated the effect of low-temperature alpha (α)-particle irradiation on Pd/4H-SiC Schottky barrier diodes (SBDs). The motivation is to study the radiation damage of the sample after bombarded with 1.6 MeV α-particles (He^{2+}) at 20 K and the annealing of the radiation-induced defects taking place with increasing temperature. The fluence of α-particles amounted to 3×10^{13} cm^{-2}.
Thermal admittance and photo-capacitance spectroscopy have been carried out on 10 nm semi-transparent Pd SBDs on 7.1×10^{15} cm^{-3} N-doped 4H-SiC. The admittance data was recorded with the sample reversed biased at –4 V and the AC oscillator voltage amounted to 100 mV. The photo-capacitance spectra were measured such that the sample was forward-biased at 1 V for one minute. With the monochromator shutter closed the monochromator was set to the lowest photon-energy. Then the reverse bias, −4 V, was applied and the dark capacitance was measured. Afterwards the shutter was opened and the capacitance was measured at approximately 10 s at this photon energy. Then the photon energy was increased and the capacitance was measured again. The oscillator frequency of the capacitance bridge during these measurements was 100 kHz and the AC voltage amounted to 100 mV.

2. Results

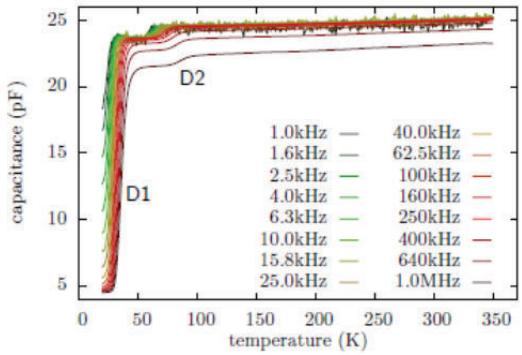

Fig. 1: Admittance spectra of the Pd/4H-SiC SBD before 1.6 MeV alpha-particle bombardment (He^{2+}) at 20 K.

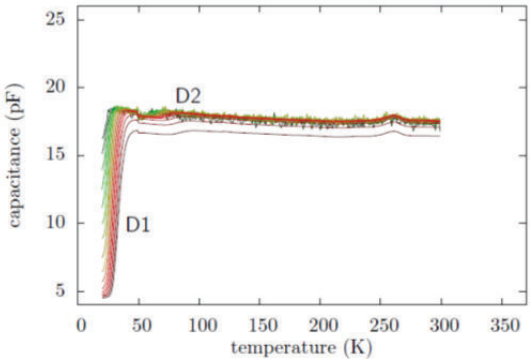

Fig. 2: Admittance spectra of the Pd/4H-SiC SBD after 1.6 MeV alpha-particle bombardment (He^{2+}) at 20 K.

The shallow donors D_1 (the dopant) and D_2 were detected in the as-grown as well as in the α-bombarded samples. Within the error margins of the experiment their concentrations were not affected by the bombardment and annealing. Also for D_2 it is highly probable that it is the electronic defect state of an impurity in 4H-SiC.

After the α-bombardment the temperature was slowly increased and the admittance was measured. The resulting capacitance-temperature characteristics before and after irradiation are shown in Figs 1 and 2. From the optical capacitance-voltage measurements conducted on this sample, it can be deduced that T_αAnn defect can be ionised using 800nm light. The concentration of the T_αAnn is ten times higher than the concentration of the dopant and was stable to both irradiation and annealing at room temperature.

3. References

[1] L.M. Tolbert, B. Ozpineci, S.K. Islam, M.S. Chinthavali, Power and Energy Systems, Proceedings, 1 (2003) 317-321.
[2] M. Siad, M. Abdesslam, A.C. Chami, Applied Surface Science, 258 (2012) 6819-6822.
[3] R. Madar, Nature, 430 (2004) 974-975.
[4] S. Yamada, B.-S. Song, T. Asano, S. Noda, Applied Physics Letters, 99 (2011).

[P27]

Analysis of deep level emission bands in solution grown ZnO nanorods

Crispin Munyelele Mbulanga[1], Zelalem Nigussa Urgessa[1], Stive Roussel Tankio Djiokap[1], Johannes Reinhardt Botha[1] M.M Duvenhage[2], H.C. Swart[2]

[1]*Department of Physics, Nelson Mandela Metropolitan University, P.O. Box 77000, Port Elizabeth 6031, South Africa*
[2]*Department of Physics, University of the Free State, P.O. Box 339, Bloemfontein ZA9300, South Africa*
Corresponding author e-mail address: crispin.mbulanga@nmmu.ac.za

1. Introduction

One application of semiconductors, namely solid state lighting technology, is destined for a bright future. In particular, ZnO nanostructures have gained substantial interest in the research community due to its requisite large direct band gap and the stability of the exciton (binding energy of 60 meV) even above room temperature. A reasonable understanding of the UV emission has been achieved [1 - 2], whereas the origin of the visible emission (green/yellow/orange/red luminescence) is still a source of controversy [3]. In this paper, the deep level emission (DLE) in solution grown ZnO nanorods after sequential annealing in different environments and for different times, is reported. In addition to photoluminescence (PL) spectroscopy, X-ray diffraction (XRD), X- ray photoelectron spectroscopy (XPS), Auger electron spectroscopy (AES), Time-of-Flight Secondary Ion Mass Spectroscopy (TOF-SIMS) and hydrogen plasma treatment have been used in order to understand the possible intrinsic defects in the material.

2. Results

Fig. 1a shows room temperature PL spectra of ZnO nanorods sequentially annealed at different temperatures in flowing argon for 30 min. From the behavior of the DLE with annealing temperature, three bands are deduced (see arrows). With increasing annealing temperature an interplay between these different DLE bands can be observed. In particular, while yellow/red luminescence (at ~570 nm and ~ 660 nm) is enhanced after annealing around 400 ^{o}C, these bands start to quench at higher annealing temperatures and after annealing at 800 ^{o}C a green band at ~500 nm dominates. The effect of annealing time (in oxygen) at even higher temperature (900 ^{o}C) is shown in Fig. 1b. The yellow/red luminescence decreases rapidly with annealing time and is accompanied by a strong increase in the green PL band. The observed behavior is suggested to be a result of the removal of surface adsorbed impurities, the activation and creation of various intrinsic defects, and the passivation of defects by hydrogen. In addition to the PL studies, supporting results from XRD, XPS, AES, TOF-SIMS and hydrogen plasma treatment will also be reported. Full details on the recombination bands and the possible identity of the defects contributing to the DLE are discussed in the paper.

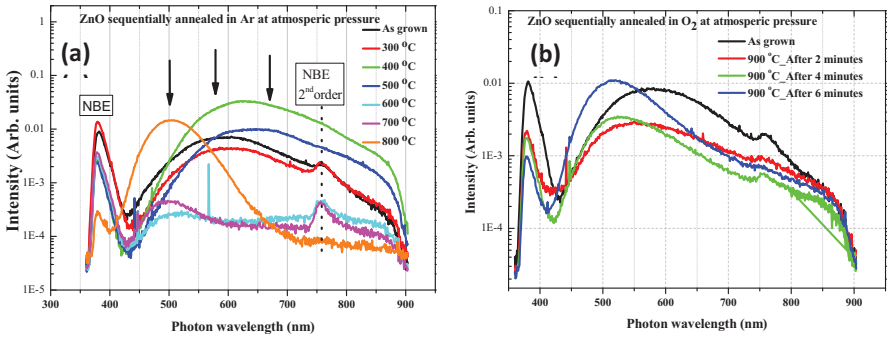

Figure 1. (a) PL spectra of solution grown ZnO nanorods on silicon substrate annealed sequentially in argon for 30 min. (b) PL spectra of similar samples annealed sequentially in O_2 at 900 ^{o}C.

3. References

1. C. F. Klingshirn *et al*., 'Zinc Oxide: From Fundamental Properties Towards Novel Applications', Springer series, (2010), 120.
2. V. Khranovskyy *et al*. 'Comparative PL study of individual ZnO nanorods grown by APMOCVD and CBD techniques,' Physica B, 407 (2012), 1538-1542.
3. T. Moe Børseth *et al*., 'Identification of Oxygen and Zinc vacancies optical signals in ZnO', Appl. Phys. Lett., 89 (2006), 262112.

[P28]

Influence of varying Cr^{3+} mol% in $MgAl_2O_4$:0.1% Eu^{3+}, x% Cr^{3+} $(0 \le x \le 0.15\%)$ nanophosphor synthesized by sol-gel process

Setumo V. Motloung[1], **Francis B. Dejene**[1], **Hendrik C. Swart**[2], **Odirileng M. Ntwaeaborwa**[2]

[1]*Department of Physics, University of the Free State (Qwaqwa campus), Private Bag X13 Phuthaditjhaba, 9866, South Africa*
[2]*Department of Physics, University of the Free State, P.O. Box 339, Bloemfontein, 9300 South Africa*
Corresponding author e-mail address: volksfmv@gmail.com

1. Introduction

Recently, many aluminate materials have been extensively studied as phosphors for the next generation of display and lighting devices. Among them, magnesium-aluminum oxide ($MgAl_2O_4$) spinel crystals with related transition dopants have received a great deal of attention due to its mechanical strength, high resistance to chemical attacks, and its outstanding dielectric and optical properties [1]. $MgAl_2O_4$ singly doped with Eu^{3+} and Cr^{3+} ions for the red and violet-green light phosphors, respectively, have been studied [1,2]. In this study, $MgAl_2O_4$ (hosts) and 0.1% Eu^{3+}, x% Cr^{3+} co-activated phosphor were successfully prepared at a relatively low temperature (~80 °C) using the sol–gel method. The co-activator (Cr^{3+}) mol% was varied at a range of $0 \le x \le 0.15$ mol%, while the Eu^{2+} concentration was kept constant at 0.1%. The samples were annealed at 800 ^{0}C in a furnace. The annealed samples were characterized by powder X-ray diffraction (XRD), scanning electron microscopy (SEM) and photoluminescence (PL) spectroscopy. The results showed that the emission color can be turned by varying the co-activator concentration.

2. Results

The XRD data revealed that all annealed samples consist of the pure cubic $MgAl_2O_4$ structure. The estimated crystallites size were in the range of 12.1 – 11.0 nm in diameter. SEM results showed that the dopant type and varying the Cr^{3+} concentration in the co-activated samples influences the surface morphology of the phosphor. The PL results showed that the host, 0.1% Cr^{3+} and Eu^{3+} activated nanophosphor emits at different wavelengths. Emission peak at 390 nm is attributed to the band-gap defects in the host material. Emission at 405 is attributed to arise from both the contribution from the host and Cr^{3+} ($^4T_1 \rightarrow {}^4A_2$ transition) emissions. The green emission peak at 565 nm is attributed to arise from either the host or Cr^{3+} ($^4T_2 \rightarrow {}^4A_2$ transition). An emission peak at 574 nm is attributed to the well-known orange emission from $^5D_0 \rightarrow {}^7F_1$ transition in Eu^{3+} ion, while the emission peak at 619 nm is assigned to the Eu^{3+} electric dipole from $^5D_0 \rightarrow {}^7F_2$ transition. An emission at 694 nm is attributed to the Cr^{3+} from $^2E \rightarrow {}^4A_2$ transition. Co-activating the host with Cr^{3+} ion quenches the host emission at 390 nm. The CIE color coordinates (see Fig. 2) shows that the emission color can be turned by varying the co-activator concentration.

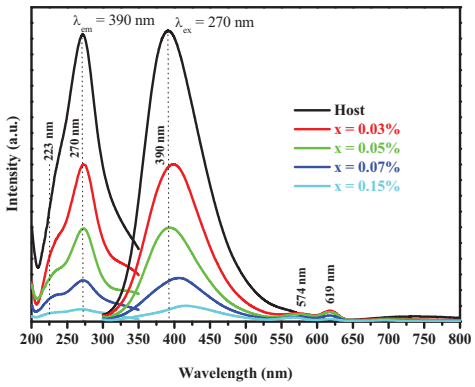

Fig. 1: The excitation and emission spectra of the $MgAl_2O_4$: 0.1% Eu^{3+},x% Cr^{3+} nano-phosphor.

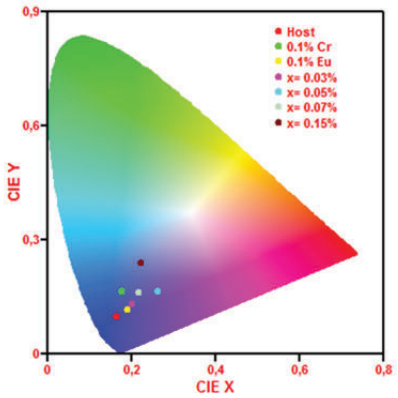

Fig. 2: CIE color coordinates for the host,singly and co-activated nano-powders.

3. References

[1] V. Singh, MD. M. Haque and Dong-Kuk Kim. *Bull. Korean Chem. Soc.* **28** (2007) 2477.
[2] P. Głuchowski, R. Pazik, D. Hreniak and W. Strek. *Chem. Phys.* **358** (2009) 52.

[P30]

Synthesis and Characterization of a Novel Rare-Earth Oxyorthosilicates (R_2SiO_5) (R = La, Gd, Y) Doped Dy^{3+} Nanophosphors

Simon N. Ogugua, Samy K.K. Shaat, Hendrik C. Swart, Odireleng M. Ntwaeaborwa*

Department of Physics, University of the Free State, Bloemfontein, ZA9300, South Africa
E-mail address: ntwaeab@ufs.ac.za*

1. Introduction

Nowadays, phosphors have found applications in solid state lighting, phototherapy, information display technologies, and solar cells, among other things. Rare earth oxyorthosilicates of the form R_2SiO_5 (R = La, Gd, Y) doped with rare earth elements, have been of interest for the past decades due to their wide band gap, fast decay times, high quantum efficiency, high density and minimal self-absorption. Using urea-assisted solution combustions method, we prepared both single and mixed rare-earth oxyorthosilicates doped with Dy^{3+} powder nanophosphors.

2. Results

The structures of our phosphors analysed using X-ray diffraction (XRD) confirmed that the phosphors crystalized in the pure monoclinic phases of La_2SiO_5, Gd_2SiO_5 and Y_2SiO_5 or in the mixture of any of the three compounds. We also analysed the morphologies, elemental composition, and the chemical and electronic states of our powders using field emission scanning electron spectroscopy (FE-SEM), energy dispersive X-ray spectroscopy (EDS) and X-ray photoelectron spectroscopy (XPS) respectively. The photoluminescence (PL) (Fig. 1) measured when the samples were excited using a 325 nm He-Cd laser showed broad blue emission assigned to self-trapped excitons in SiO_2 [1] (which were not observed in the PL spectra measured in phosphorescence mode when the samples were excited using monochromatic xenon lamp) and $^4F_{9/2} \rightarrow {}^6H1_{5/2}$ and $^4F_{9/2} \rightarrow {}^6H_{13/2}$ transitions of Dy^{3+} [2]. The colour purity of the samples calculated using the CIE coordinate calculator confirmed that the phosphors can emit tunable colours and white light. Furthermore, there was even distribution of the atomic and molecular ionic species on the surfaces of the samples as shown in the time-of-flight secondary ion mass spectrometer images in Fig 2.

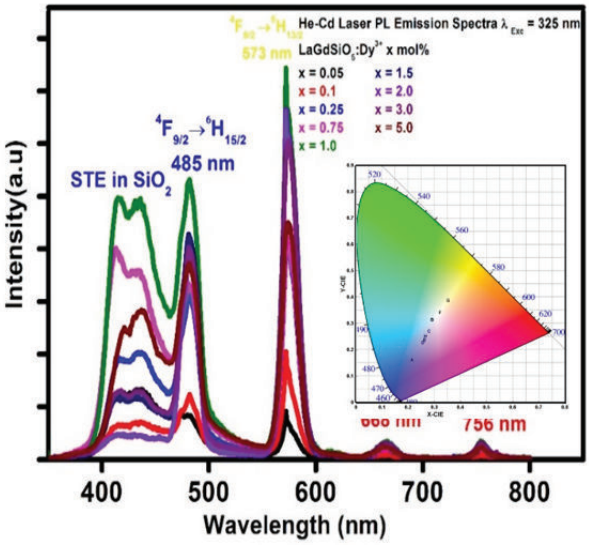

Fig.1: The PL emission spectra of $LaGdSiO_5:Dy^{3+}$ x mol% (x = 0.05, 0.1, 0.25, 0.75, 1.0, 2.0, 3.0 and 5.0) monitored using PL system with 325 nm He-Cd laser as excitation source. The inset is the corresponding CIE coordinates diagram.

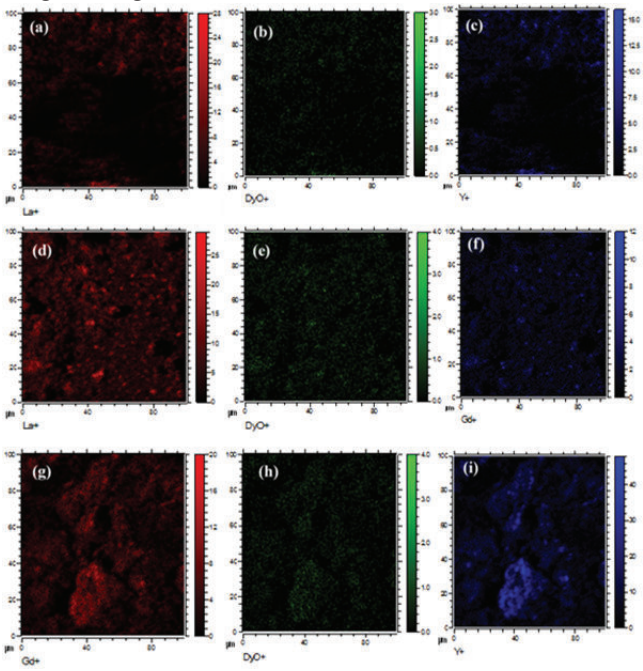

Fig.2:The positive ToF-SIMS images of (a) La^+, (b) DyO^+ and (c) Y^+ taken from $LaYSiO_5:Dy^{3+}$, (d) La^+, (e) DyO^+ and (f) Gd^+ taken from $LaGdSiO_5:Dy^{3+}$ and g) Gd^+, (h) DyO^+ and (i) Y^+ taken from $GdYSiO_5:Dy^{3+}$.

3. References

[1] C. Itoh, K. Tanimura, N. Itoh. *J. Phys. C. Solid State Phys.* **21**(1988) 4693.
[2] K.G. Sharma, N.R. Singh. *New J. Chem*. **37** (2013) 2784.

[P30]

Advances in phosphors based on purely organic materials for solid state lighting applications

Kashma Sharma, Vijay Kumar, Vinod Kumar, Hendrik C. Swart

Department of Physics, University of the Free State, P.O. Box 339, Bloemfontein, ZA 9300, South Africa
Corresponding author e-mail address: shama2788@gmail.com, swarthc@ufs.ac.za

1. Introduction

A brief overview is presented on light emitting diodes (LEDs) based on purely organic materials. Organic LEDs are of interest to industry and academia because of their properties and versatility [1]. Till now research and practical workers had a very limited number of organic phosphors (OPs) at their disposal.The organic materials based phosphors have several advantages with respect to inorganic materials such as the ease of synthesis, handling and very high emission quantum efficiency [2-3]. Thus, tremendous efforts are still going on in this direction to search for environmental friendly, safer and more energy efficient organic phosphors for use in the light emitting applications.
Various authors reported synthesis of yellow-green phosphors based on different organic materials. Organic phosphors based on 1,9-anthrapyridone, cationic dyes, 4-amino napthalic acid and other compounds have been utilized for day-light fluorescent pigments [3]. Electroluminescent properties of self-assembled polymer thin films have been reported by Tian et al. [4]. Comparison between devices made using different organic materials and their derivatives with respect to synthetic protocols, characterizations, quantum efficiencies, sensitivity, specificity and their applications in different fields have been discussed. This review also discusses basic requirement and scientific issues that arise in synthesizing cost-effective and environmental friendly organic light emitting diodes based on these luminescent materials. In addition, it offers avenues for new researchers for futuristic development in the area.

2. Results

We have previously synthesized purely OPs based on bis-pyrimidine skeleton for the first time [3]. The phosphor emits at 560 nm, which reflect purely yellow emission. It has also been found that the phosphor did not degrade after 24 h UV exposure. The newly synthesized material can be utilized in electronic displays and lighting with relatively low cost and chemical versatility of systems. Blue light emitting diphenylquinoline and its halogenated derivatives were well reported in literature [5-6]. A simple reaction scheme for the synthesis of quinolone derivatives is shown in Scheme 1. By using different solvents the maximum emission wavelength can be adjusted [6]. Moreover, poly(quinolines) and their copolymers were successfully used as electron-transporting and emitting materials in OLEDs, selective luminescent sensors and nonlinear optics [5-6]. It has been observed that the phosphorescence in organic materials is probably credited to heavy atom effects through intermolecular halogen bonding, in aromatic carbonyl compounds [3, 7]. We can perform color tuning by simply controlling the electron density of these organic materials. The room temperature phosphorescence of OPs in amorphous polymer matrices has also been reported [8]. The efforts to improve luminescent properties of OPs are still going on and hope that the overall performance in terms of emission quantum efficiency will further be enhanced.

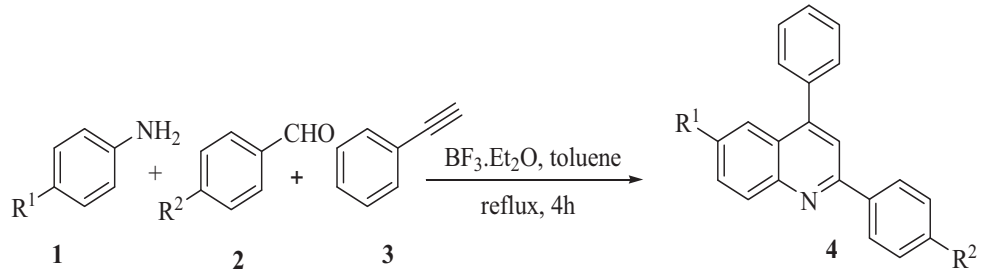

Scheme 1: Synthesis of quinolone derivatives

3. References

[1] A. Kohler and H. Bassler. *Mater. Sci. Eng.* **66** (2009) 71-109.
[2] S. P. Anthony, *Chem. Plus Chem* **77** (2012) 518.
[3] V. Kumar, M. Gohain, V. Kumar, J. H. Tonder, B. C. B. Bezuidenhoudt, O. M. Ntwaeaborwa, H. C. Swart. *J. Lumin.* **149** (2014) 61-68.
[4] Jing Tian, Chung-Chih Wu, Mark E. Thompson, James C. Sturm, Richard A. Register. *Adv. Mater.* **7** (1995) 395-398.
[5] S. B. Raut, S. J. Dhoble, R. G. Atram. *Adv. Mat. Lett.* **2** (2011) 373-376.
[6] D. M. Pimpalshendea and S. J. Dhoble. *Lumin.* **29** (2014) 451–455.
[7] O. Bolton, K. Lee, H.-J. Kim, K. Y. Lin, J. Kim, *Nat. Chem.* **3** (2011) 205.
[8] D. Lee, O. Bolton, B. C. Kim, J. H. Youk, S. Takayama and J. Kim. *J. Am. Chem. Soc.* **135** (2013) 6325−6329.

[P31]

Rare earth doped lanthanum strontium borate ($La_2Sr_3(BO_3)_4$: xTb^{3+}) polycrystalline green phosphors

D.V. Mlotswa[1], Roz M Madihlaba[2], M.O. Onani[2], B.F. Dejene[1], L.F. Koao[1]

[1]Department of Physics, University of the Free State, (Qwa-Qwa campus), Private Bag X-13, Phuthaditjhaba, 9866, South Africa
[2]Departments of Chemistry, University of the Western Cape, Private Bag X17, Bellville 7535, South Africa
Corresponding author e-mail address: dejenebf@qwa.ufs.ac.za

1. Introduction

Recently, great efforts have been made to develop efficient phosphor systems. Among these, a number of works have been carried out on investigations of the luminescent properties for borates, aluminates and gannets [1, 2]. Since the first white light emitting diodes(W-LED's) became commercially available, it have attracted great attention for their obvious advantages such as long lifetime, high luminescence efficiency, low power consumption and environmental friendliness, consequently they are expected to replace incandescent and fluorescent lamps for general lighting application in the future. Good glass host is very important for efficient luminescence of rare-earth ions. Borate glass is a suitable optical material with high transparency, low melting point, high thermal stability and good rare-earth ions solubility. Among them, $La_2Sr_3(BO_3)_4$, is one of the best candidates for the desired host materials of phosphors, and $La_2Sr_3(BO_3)_4$:xTb^{3+}, as a green phosphor could be possible used extensively in future in plasma display panels. Tb^{3+} - doped phosphors are considered more important due to their efficiency in the display of sharp and intense green emission at 544 nm due to an electronic transition of $^5D_4$-$^7F_5$. In this paper, we report combustion synthesis of some important, borate based, PL phosphors using commonly available fuels and oxidizers.

2. Results

The power X-ray diffraction pattern of synthesized $La_2Sr_3(BO_3)_4$: xTb^{3+} is shown in Fig. 1. It is in good agreement with the reference database JCPDS card 71-1485 of host lattice of $La_2Sr_3(BO_3)_4$. The average crystallite sizes of the nanoparticles were approximated from the most prominent XRD using Debye-Scherer's formula and it was found to be approximately 34 nm. The results also showed that varying the Tb^{3+} does not affect the crystal structure of the phosphor. The expected fluffy morphology of the particles was observed as normally obtained from the combustion synthesis studied using the scanning electron microscopy. However, these fluffy morphology breaks into irregular crystal-like structures with increasing concentration of Tb^{3+} ions. The emission spectrum under 209 nm excitation probing consists of four groups of emission lines located at about 490, 545,591 and 625 nm as shown in Fig. 2. These four groups are due to the $^5D_4$ - ^7F_j (j = 6, 5, 4, 3) transitions, respectively. The emission from the $^5D_3$ level of Tb^{3+} has not been observed even at low concentration. In fact, many Tb^{3+} activated materials show a blue emission from the $^5D_3$ level and a green emission from the $^5D_4$ level. However, if the surroundings offer high-frequency vibration, the probability for irradiative relaxation to the $^5D_4$ level is high and therefore the $^5D_3$ emission is difficult to observe.

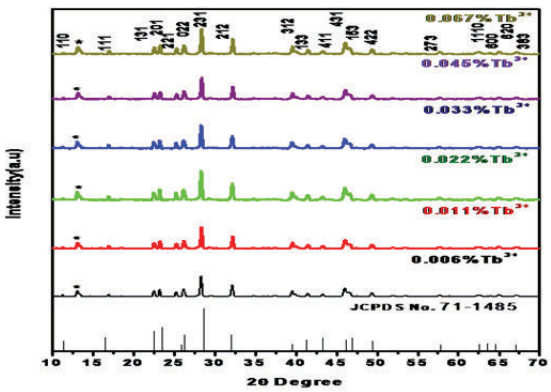

Fig. 1: XRD patterns of $La_2Sr_3(BO_3)_4$:xTb^{3+} with different Tb^{3+} doped concentration compared to the $La_2Sr_3(BO_3)_4$ (JCPDS card No.71-1485).

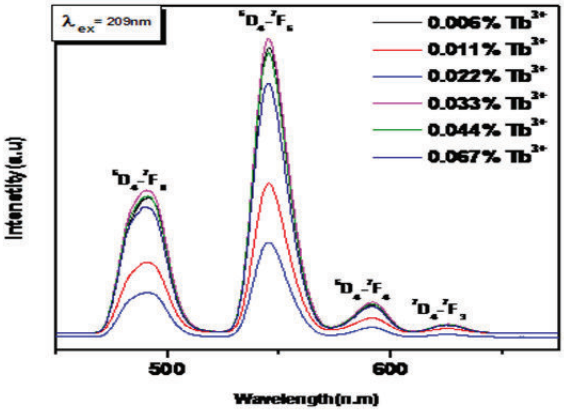

Fig. 2: Tb^{3+} concentration dependent PL emission spectra of emission spectra of $La_2Sr_3(BO_3)_4$:Tb3+ phosphor.

3. References

[1] G. Blasse, C.D donega, N. Efryushina, V. Dotsenko, I. Berezovskaya, Solid State Commun. 92 (1994) 687.
[2] R. Mlcak, A.H. Kitai, J. Lumin. 46 (1990) 391.
[3] L.E. Shea, R.K. Datta, J.J Brown, J. Electrochem. Soc 141 (1994) 1950.

[P32]

Structural and luminescence properties of $SrAl_2O_4:Eu^{2+}$, Dy^{3+}/Nd^{3+} phosphor thin films grown by pulsed laser deposition

Ali Wako[1], **Francis Dejene**[1] **and Hendrik C. Swart**[2]

[1] *Department of Physics, University of the Free State, QwaQwa Campus, Private Bag X13, Phuthaditjhaba 9866, South Africa*
[2]*Department of Physics, University of the Free State, P O Box 339, Bloemfontein, ZA-9300, South Africa*
Corresponding author e-mail address: wakoah@qwa.ufs.ac.za

1. Introduction

Long afterglow or persistent phosphors have the ability of absorbing energy from UV or sunlight and then release it slowly in the dark [1,2]. Inorganic phosphors doped with rare earth elements show broad band emission from blue to red which makes them suitable for a variety of industrial applications, such as luminescent pigments, fluorescent lamps, color display, plasma display panels (PDP), radiation dosimetry and X-ray imaging [3]. The type and duration of emission from a phosphor is affected by a number of parameters such as the type and amount of activators or dopants, the structure of the host lattice, the method of preparation or growth conditions and other post-treatments. These parameters play a significant role in inducing a crystal field effect within the host matrix which in turn influences the emission wavelength, its intensity and lifetime. The main task would therefore be to optimize these factors to obtain a phosphor that gives the best performance for the desired application. In this study thin films of $SrAl_2O_4:Eu^{2+}$, Dy^{3+}/Nd^{3+} were prepared using Pulsed Laser Deposition (PLD). The effect of varying argon gas pressure and substrate temperatures on the structure and photoluminescent (PL) properties of the $SrAl_2O_4:Eu^{2+}$, Dy^{3+}/Nd^{3+} thin films were investigated.

2. Results

X-ray diffraction (XRD) patterns of the $SrAl_2O_4:Eu^{2+}$, Dy^{3+}/Nd^{3+} phosphor thin films deposited on Si(100) in vacuum, 10, 20 and 30 mTorr argon partial pressure as compared with that of the as-prepared powder are shown in figure 1. The peaks fitted well with the powder and the JCPDS card number 74-0794 for the monoclinic $SrAl_2O_4$ of space group P1211 (4). It can be seen that with increasing the argon pressure the peaks in the (220) direction shifted to the lower 2-theta angles from 29.1° in vacuum to 27.9° in 30 mTorr argon partial pressure. Ar has a higher mass density and therefore tends to reflect lighter atoms in the plume more and these results in a film with big particles [4] which results in lattice expansion inducing crystal field effect in host lattice causing the XRD peak shift to lower angles. Figure 2 shows PL emission spectra recorded with He-Cd laser at excitation of 325 nm from $SrAl_2O_4:Eu^{2+}$, Dy^{3+}/Nd^{3+} thin films deposited under different argon atmospheres whereby emission peaks are observed to shift towards the higher wavelength side. Larger particles will cause lattice expansion and increase the crystal-field interaction of Eu^{2+} resulting in red shift.

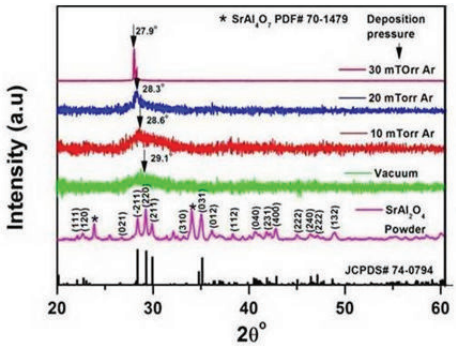

Fig. 1: XRD patterns of the $SrAl_2O_4:Eu^{2+}$, Dy^{3+}/Nd^{3+} phosphor thin films that were deposited in vacuum, 10, 20 and 30 mTorr argon partial pressure.

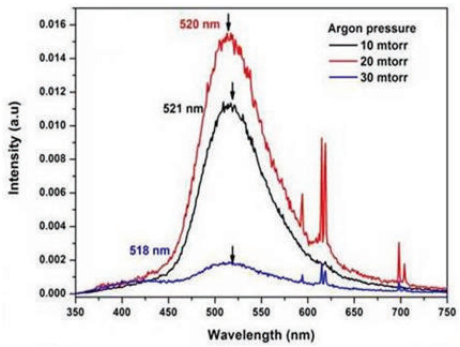

Fig. 2: Emission spectra for $SrAl_2O_4:Eu^{2+}$, Dy^{3+}/Nd^{3+} thin films showing variation of PL with argon partial pressure.

3. References

[1] S. Nagamani and B. S. Panighrahi. *J. Am. Ceram. Soc.* **93** (2010) 3832.
[2] P. Taylor, X. Duan, S. Huang, F. You and Z. Xu. *J. Exp. Nanosci.* **4** (2009) 169.
[3] V. Singh, J. Zhu and V. Natarajan. *Phys. Status Solidi* **203** (2006) 2058.
[4] S. T. Dlamini, H. C.Swart, J. J.Terblans and O. M. Ntwaeaborwa. *Solid State Sci.* **23** (2013) 65.

[P33]

Luminescence properties of CaO:Bi^{3+} phosphor

A Yousif [1,2], OM Ntwaeaborwa[1] and HC Swart[1]

[1] Department of Physics, University of the Free State, P.O. Box 339, Bloemfontein, ZA 9300, South Africa.

[2]Department of Physics, Faculty of Education, University of Khartoum, Khartoum, Sudan.

Corresponding author e-mail address: SwartHC@ufs.ac.za

1. Introduction

In recent years, there has been growing importance focused on research in light emitting diodes (LEDs) because of their long operation lifetime, energy-saving feature and high material stability [1, 2]. During the past few years, white LEDs fabricated using a near ultraviolet (n-UV) LED (380–420 nm) coupled with red, green, and blue phosphors have attracted much attention [2]. Accordingly, it is necessary to develop new blue phosphors that could be effectively excited in the near ultraviolet range especially for wavelengths of 400 nm [1]. The spectroscopic properties of the Bi^{3+} ion in different hosts have attracted much attention due to its emission wavelength that varies from the ultraviolet to the red region depending on the host matrix [3]. Therefore, with the appropriate matrix, the emission of Bi^{3+} ions can be used as a candidate for n-UV for LED applications. CaO:Bi^{3+} phosphor powder was successfully synthesized by the sol-gel combustion method. The structure, morphology and luminescent properties of the phosphor were characterized by X-ray diffraction (XRD), Scanning electron microscope (SEM), photoluminescence (PL) and cathodoluminescence (CL) techniques.

2. Results

The XRD results showed that, the CaO:Bi^{3+} has a single face-centered cubic crystal structure, and the phosphor particles were uniformly distributed. The phosphor excited by a 355 nm ultraviolet ray or 325 nm laser or electron beams emitted strong n-UV light with the wavelength of 395 nm ($^3P_1 \rightarrow {}^1S_0$ transition) (Figure 1). CL intensities were monitored as a function of the accelerating voltage (range of 1–3 keV with fixed filament current of 10 μA) and as a function of the filament current (in the range of 5–13 μA with accelerating voltage fixed at 2 keV) (Figure 2). For the CL intensity degradation study, the powder was subjected to an electron beam of current density of 39.2 mA cm^{-2}, with a working beam voltage of 2keV and a beam current of 10 μA. These results will be discussed in detail in this paper.

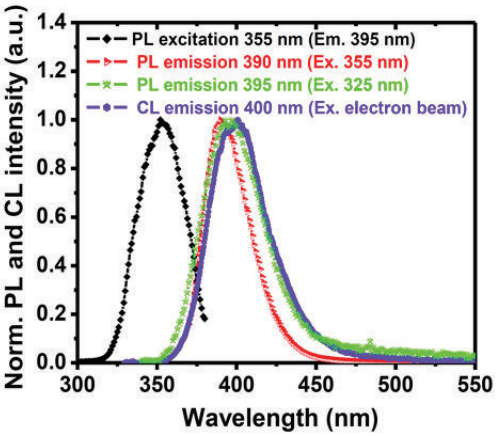

Fig. 1: Excitation and emission spectra of CaO:Bi^{3+} by using the xenon lamp monitored at 390 nm and 355 nm respectively. In addition, emissions of the CaO:Bi^{3+} by using a 325 nm He-Cd laser and electron beam with a working beam voltage of 2 keV and a beam current of 10 μA.

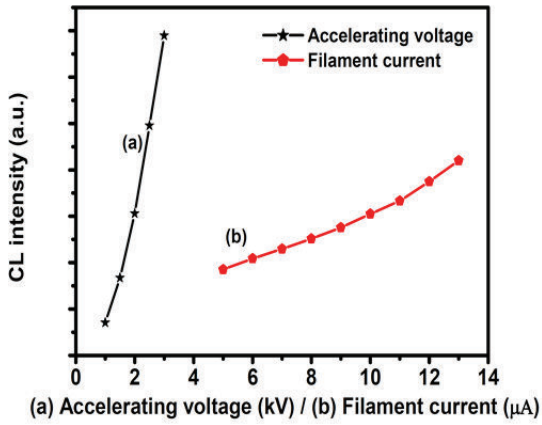

Fig. 2: The CL intensities of CaO:Bi^{3+} as a function of (a) accelerating voltage and (b) filament current.

3. References

[1] Y. Chiu, W. Liu, C. Chang, C. Liao, Y. Yeh, S. Janga, T. Chen, *J. Mater. Chem.* 20 (2010) 1755.

[2] P. Li, Z. Wang, Z. Yang, Q. Guo, *RSC* 4 (2014) 27708.

[3] A. Yousif, Vinod Kumar, H. A. A. Seed Ahmed, S. Som, L. L. Noto, O. M. Ntwaeaborwa, H. C. Swart, *ECS J. Solid State Sci.* 3 (11) (2014) R222.

[P34]

The effect of urea ratio on structural and luminescence properties of YVO_4:Dy phosphor

K.E Foka[1], B.F Dejene[1] and H.C Swart[2]

[1] Department of physics, University of the Fee State, Private bag x13, Phuthaditjhaba, 9866
[2]Department of Physics, University of the Free State, P. O. Box 339, Bloemfontein, 9300
Corresponding author e-mail address: fokake@gmail.com

1. Introduction

Although the luminescence characteristics of vanadates phosphors have been reported, yttrium vanadates (YVO_4) are good host materials for luminescence efficiency. Like Eu, Tm and other rare earth ions, Dy can also act as a useful activator. Many researchers have reported that YVO_4 can be modified by Eu to be used as red phosphor in colour television and cathode because of its high luminescence [1]. Besides europium, Dy ions is a good activator for YVO_4: Dy^{3+}. Synthesis of YVO_4 has previously been prepared by various methods. Here YVO_4:Dy was prepared by combustion method at initiation temperature of 600 ^oC. Combustion method is one of an ideal technique, because exothermic reaction was initiated at the ignition temperature and it generates heat which was manifested in a maximum temperature of 100-1650 K [2].

2. Results

Figure 1 shows the XRD patterns of the YVO_4:Dy powders synthesized by combustion method at initiation temperature of 600 ^{o} C with different mole ratios of urea. The phosphor powder showed that the peaks were due to YVO_4 tetragonal phase (JCPDS 17-0341). No other crystalline phase was detected on XRD spectra. Scanning electron microscopy results showed that when increasing ratio of urea the agglomeration of particles decreases and the nanorod-like shape structure starts to form. Figure 2 shows the emission spectra obtained from excitation of 282 nm. The emission spectra consist of two main peaks, yellow band at 573 nm corresponding to $^4F_{9/2}\rightarrow{}^6H_{13/2}$ and the blue band (482 nm) corresponds to the $^4F_{9/2}\rightarrow{}^6H_{15/2}$ transition. There is a very week band at 663 nm which correspond to $^4F_{9/2}\rightarrow{}^6H_{11/2}$ transition. The intensity of the yellow emission is stronger than that of blue emission, this is because when the Dy^{3+} ions is located at low symmetry local sites with no inversion centers, the $^4F_{9/2}\rightarrow{}^6H_{13/2}$ transition is prominent in its emission spectrum.

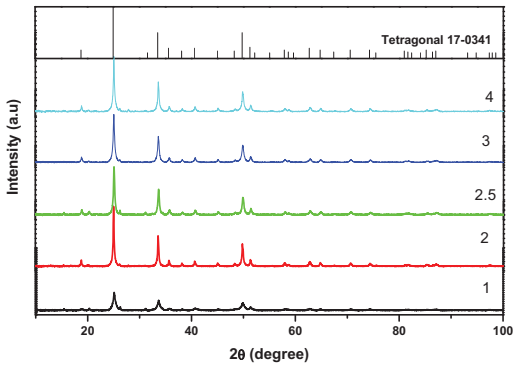

Fig.1: XRD patterns of YVO_4:Dy at different molar ratio of urea

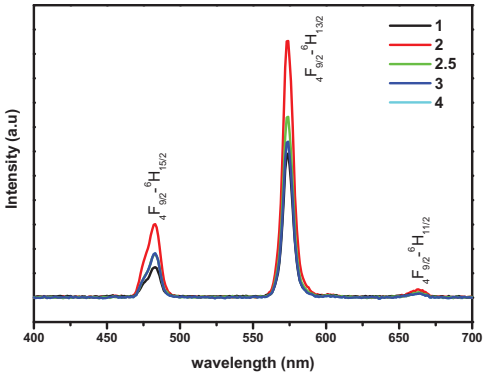

Fig.2: PL emission spectra of YVO_4: Dy with different ratio of urea

3. References

[1] J. Wang, Y. Xu, M. Hojamberdiev, Y. Cui, H. Liu and G. Zhu, *J. of Alloys and Compounds.* **479** (2009), 772-776.
[2] H. Zhang, X. Fu, S. Niu and Q. Xin, *J. of Alloys and Compounds*. **457** (2008) 61-65.

[P35]

Interaction mechanism for energy transfer from Ce to Tb ions in silica

H.A.A. Seed Ahmed[1,2], W.S. Chae[3], O.M. Ntwaeaborwa[1] and R.E. Kroon[1,*]

[1]Department of Physics, University of the Free State, Bloemfontein, South Africa
[2]Department of Physics, University of Khartoum, Khartoum, Sudan
[3]Korea Basic Science Institute (KBSI), Gangneung, Republic of Korea
**Corresponding author e-mail address: KroonRE@ufs.ac.za*

1. Introduction

Energy transfer phenomena can play an important role in the development of luminescence materials. For example, the green luminescence from Tb^{3+} doped silica can only be excited efficiently using very short wavelength ultraviolet light near 227 nm. However, the excitation wavelength can be shifted to a more accessible value of 325 nm by co-doping with Ce^{3+} ions which absorb at this wavelength and then transfer the energy to the Tb^{3+} ions [1]. Inokuti and Hirayama developed models for radiationless energy transfer that occurs via the exchange interaction or various types of multipole interactions [2]. In this work numerical simulations based on these theoretical models are compared to experimental results obtained for the energy transfer from Ce to Tb in sol-gel silica to identify the mechanism for energy transfer.

2. Results

The experimental results were obtained by exciting samples having a fixed Ce concentration (0.5 mol%) and varying the Tb concentration between zero and 0.8 mol%. Fig. 1 shows that for such co-doped samples excited at 325 nm (i.e. for the Ce ions) the emission intensity from Ce decreases, while that from Tb increases, with an increasing Tb concentration, as expected when Tb is effectively excited via energy transfer from the Ce ions. Energy transfer from the Ce donor to the Tb acceptor also resulted in a decrease in the Ce luminescence lifetime with increasing Tb concentration (Fig. 2). Analysis of the decrease in the Ce donor emission intensity as a function of the Tb co-doping concentration showed that it corresponded best with the energy transfer models based on the exchange and the dipole-dipole interactions. The critical transfer distance obtained from the fitting using both models was around 20 Å. Since the exchange interaction requires a distance shorter than 10 Å to occur, the mechanism for energy transfer was identified as the dipole-dipole interaction. This conclusion was supported by an analysis of the change in Ce donor lifetime data as a function of the Tb co-doping concentration.

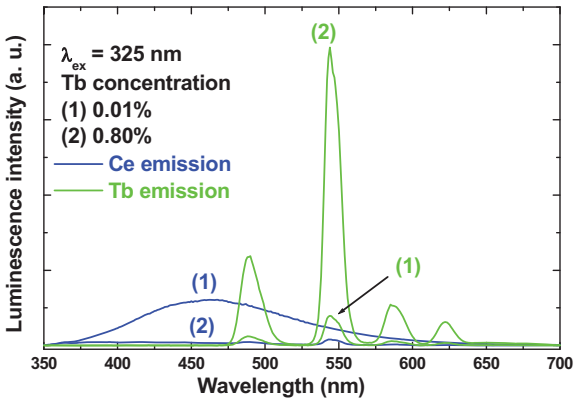

Fig.1: PL emission of (1) SiO_2:Ce(0.5%),Tb(0.01%) and (2) SiO_2:Ce (0.5%),Tb(0.80%). The Ce emission was recorded in fluorescence mode while the Tb emission was recorded in phosphorescence mode from the same samples.

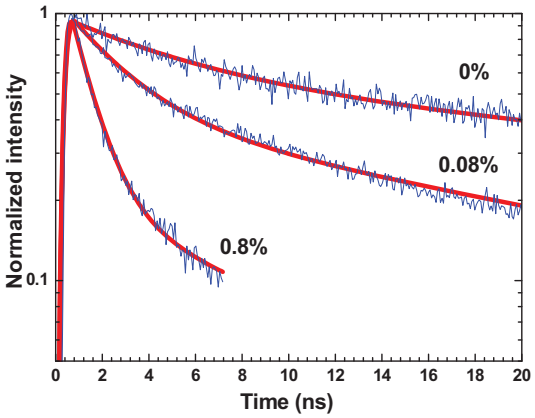

Fig. 2: The decay curve of the samples SiO_2:Ce (x%) where x is 0%, 0.08% and 0.8%. The blue curve is the measured data and the red points are the convolution of the fitted data.

3. References

[1] H.A.A. Seed Ahmed, O.M. Ntwaeaborwa and R.E. Kroon. *J. Lumin.* **135** (2013) 15.
[2] M. Inokuti and F. Hirayama. *J. Chem. Phys.* **47** (1967) 3211.

[P36]

Spectroscopic properties of Pr^{3+} ions embedded in lithium borate glasses

D. D. Ramteke[1, 2], **H. C. Swart**[2], **R. S. Gedam***[1]

[1] Department of Applied Physics, Visvesvaraya National Institute of Technology, Nagpur-440 010, India
[2] Department of Physics, University of the Free State, P.O. Box 339, Bloemfontein 9300, South Africa
E-mail: rupesh_gedam@rediffmail.com

The days have passed since glasses were remembered only as window and bottle material. The recent development makes the glasses most important material for Laser, optoelectronic devices, electro-chromic devises and solid state lighting [1-3]. Among all glasses, lithium borate glasses have many advantages such as simplicity in manufacturing, wide variety of possible compositions and good rare earth solubility [4]. Use of rare earths in the glasses make them feasible to design various optical devices with specific applications. Pr^{3+} differs from the rare earth family because of its unique energy levels. It offers the possibility of simultaneous blue and red emissions in the visible region for laser action and near infra-red emission at 1.3 μm for optical amplification [5]. Considering the technological importance of Pr^{3+} and lithium borate glasses, the glass samples with composition 27.5 Li_2O-(72.5-X) B_2O_3-X Pr_6O_{11} (X= 05, 1, 1.5 and 2) were prepared by a simple melt quench technique. These glasses were systematically characterized by optical absorption spectra, density, Fourier transformed infra-red and photoluminescence spectroscopy.

Fig. 1: Glasses with different mol % Pr_6O_{11}

Fig. 1 shows the optically polished Pr_6O_{11} containing lithium borate glasses for optical absorption measurements. It was observed that with the addition of Pr_6O_{11}, the glasses became green in color. The absorption spectra showed absorption bands at 443, 469, 481 and 589 nm which were assigned to transitions $^3H_4 \rightarrow {}^3P_{2,1,0}$ and and $^3H_4 \rightarrow {}^1D_2$ respectively [6]. Absorbance of these glasses increased and the optical absorption edge shifted towards longer wavelength with addition of Pr_6O_{11}. This red shift was due to structural changes which has a significant effect on the optical energy band gap of these glasses. It is also observed that the density and molar volume of the glasses increased with addition of the Pr_6O_{11}. The increase in density of the glasses might be due to the higher atomic weight of the Pr_6O_{11} as compared to the other oxides and creation of BO_4^- units. On the other hand the increase in molar volume could directly be related to the large ionic radius of the Pr^{3+} ions. The photoluminescence measurements at an excitation wavelength of 443 nm showed that these glasses are useful for solid state light applications.

References

[1] D. D Ramteke, R. S. Gedam. *J. Rare Earth*, 32 (2014) 389
[2] D. D Ramteke, R. S. Gedam. *J. Rare Earth*, 32 (2014) 1148
[3] D. D Ramteke, R. S. Gedam. *Spectrosc.Lett*. 48 (2015) 417.
[4] D. D Ramteke, R. S. Gedam. *Spectrochim. Acta A* 133 (2014) 19.
[5] K Biswas, AD Sontakke, J Ghosh, K Annapurna. *J. Am. Ceram. Soc*. 93 (2010) 1010
[6] W. T. Carnall, P. R. Fields, K. Rajnak, *J. Chem. Phys*., 49 (1968) 4424.

[P37]

$Zn_2SiO_4:Mn^{2+}$ co-doped with Tm^{3+} and other Re ions (Re = Rare-earth): Synthesis, Structure and Optical Properties

Pontsho Mbule[1], **Martin Ntwaeaborwa**[2], **Bakang Mothudi**[1] **and Mokhotjwa Dhlamini**[1]

[1]*Department of Physics, University of South Africa, PO Box 392, 0003, South Africa*
[2]*Department of Physics, University of the Free State, P.O.Box339, Bloemfontein, 9300 South Africa*
Corresponding author e-mail address: mbuleps@unisa.ac.za

1. Introduction

Zinc silicate (Zn_2SiO_4) is a good host lattice for luminescence centers such as rare-earth ions and transition metals (TM) to prepare light emitting materials (phosphors) that can emit blue, green and red light [1] upon excitation with high energy electrons or photons. In this work, combustion method was used to prepare undoped and manganese (Mn^{2+}) and thulium (Tm^{3+})–co-activated zinc silicate ($Zn_2SiO_4:Mn^{2+},Tm^{3+}$) nanoparticulate powder phosphors. In addition, a selection of Re ions (rare-earth ions) were used for co-doping to tune the emission colour. The structure, morphology and luminescence properties were investigated by X-ray diffractometer (XRD) and Field-Emission Scanning Electron Microscopy (FE-SEM) respectively , while the optical and luminescent properties were examined by Fourier Transform Infrared Spectroscopy (FTIR), ultraviolet visible (UV-vis) spectroscopy, Varian Cary-eclipse fluorescence spectrophotometer and 325 He-Cd laser equipped photoluminescence system.

2. Results

As shown in figure 1(a-b), the XRD patterns matching with the willemite structure of Zn_2SiO_4 were observed. However, there was additional secondary peak assigned to (101) diffraction of the hexagonal wurtzite structure of ZnO, suggesting that our material was an admixture of ZnO and Zn_2SiO_4. ZnO was either formed from the reaction of Zn^{2+} and O^{2-} during the combustion reaction in air or resulted from the incomplete decomposition of the precursors. A network of spherical (but faceted) agglomerated nanoparticles were observed from undoped, Mn^{2+}-doped and Mn^{2+}/Tm^{3+}-codoped Zn_2SiO_4 powders. The PL spectra recorded from $Zn_2SiO_4:Mn^{2+}$ nanophosphors with dopant concentration of Mn^{2+} ions ranging from 0.045 – 0.09 mol% show strong green-orange emission band at ~ 562 nm and a shoulder at ~523 nm and as the Mn^{2+} concentration increases the emission peak slightly shifted to the higher wavelength. This is a typical emission of Mn^{2+} in α-Zn_2SiO_4 and may be assigned to the electronic transition $^4T_1(^4G) \rightarrow {}^6A_1(^6S)$ [2]. Tuning of the emission colour by Tm^{3+} co-doping and other selected Re ions is demonstrated and will be discussed in detail. These nanophosphors have potential applications in nanoelectronics and optoelectronics.

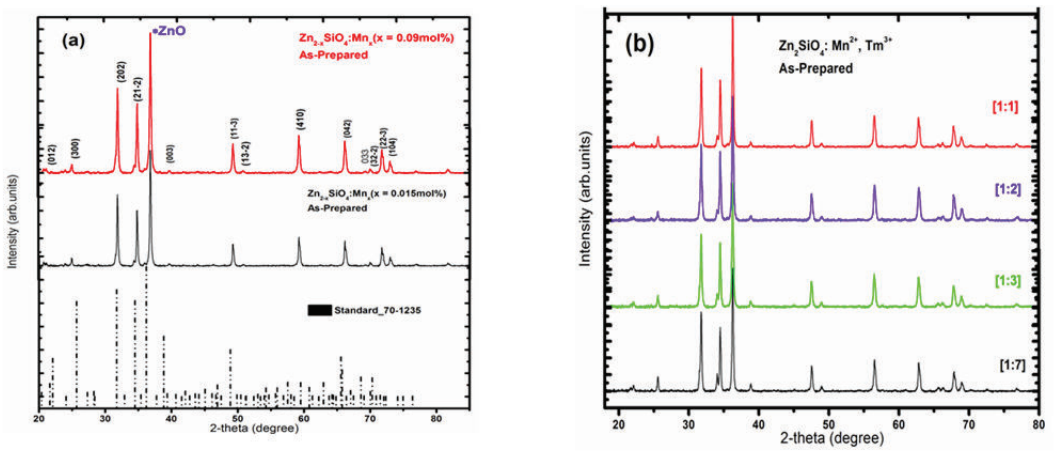

Fig. 1: XRD pattern of (a) $Zn_2SiO_4:Mn^{2+}$ and (b) $Zn_2SiO_4:Mn^{2+}, Tm^{3+}$

3. References

[1] J. El Ghoul, K. Omri, A. Alyamani, C. Barthou and L. J. El Mir, *J. Luminescence.* **138** (2013) 218.
[2] L. W. Yang, X.L. Wu, G. S. Huang, T. Qiu, Y. M. Yang and G.G. Siu, *Appl.Phys.* **81** (2005) 929.

[P38]

TOF SIMS Analysis, Structure and Photoluminescence Properties of Pulsed Laser Deposited CaS:Eu^{2+} thin films

Raphael Nyenge[1,2], Samy Shaat[1], Luyanda Noto[1], Puseletso Mokoena[1], Hendrik Swart[1], Martin Ntwaeaborwa[1]

[1]*Department of Physics, University of the Free State, P.O. Box 339, Bloemfontein, ZA 9300, South Africa*
[2]*Physics Department, Kenyatta University, P.O. Box 43844-0100, Nairobi, Kenya*
Corresponding author e-mail address: ntwaeab@ufs.ac.za

1. Introduction

Red-emitting alkali earth sulfide phosphor such as divalent europium (Eu^{2+}) doped calcium sulfide (CaS: Eu^{2+}) is a good material for blue pumped three-band phosphor-converted white LEDs since it has strong absorption in the blue region [1]. CaS: Eu^{2+} thin films were deposited on Si (100) substrates using the pulsed laser deposition technique to investigate the effect of Argon (Ar), Oxygen (O_2), and vacuum deposition atmospheres on the structural, morphological and photoluminescence (PL) properties of the thin films. The phosphor target was ablated using a 266 nm Nd: YAG laser. X-ray diffraction, Atomic force microscopy, scanning electron microscopy, energy dispersive X-ray, fluorescence spectrophotometry, and time-of-flight secondary ion mass spectrometry (TOF-SIMS) were used to characterize the thin films.

2. Results

The PL results for CaS: Eu^{2+} thin films deposited using different atmospheres are shown in Fig.1. Films prepared in Ar atmosphere showed better PL intensity than the films deposited in an O_2, while the least intensity was observed from the films prepared in vacuum. The emission observed at around 650 nm for all the films is attributed to the transitions from the excited $4f^6[^7F_0]5d^1(t_{2g})$ state to the ground state $4f^7(^8S_{7/2})$ of the Eu^{2+} [2] ions. The emission at 618 nm, which is more prominent in the film prepared in O_2, is ascribed to $^5D_0 \rightarrow {}^7F_2$ transitions in Eu^{3+} [3], suggesting that Eu^{2+} was unintentionally oxidized to Eu^{3+}. TOF-SIMS images indicated that Eu^{2+} ions were evenly distributed in the CaS host and that the thicknesses of the prepared thin films depend on the atmosphere in which the films were grown. The overlay of Fig. 2 shows Eu in the +3 state, observed as EuO^+ (m/z = 168. 8992) in the films prepared in an oxygen atmosphere. It is speculated that less oxidation of Eu^{2+} occurred during deposition in argon and vacuum atmospheres, since insignificant PL emission due to Eu^{3+} was observed.

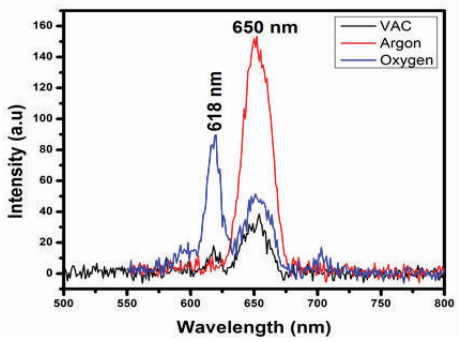

Fig. 1: The emission spectra for PLD CaS: Eu^{2+} thin films when excited at 250 nm.

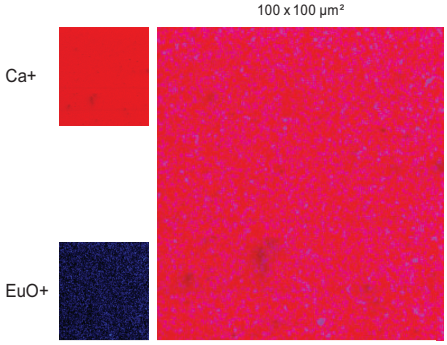

Fig. 2: Distribution of Eu^{3+}(observed as EuO^+)in thin films deposited in an oxygen atmosphere.

3. References

[1] Jia, X. Wang. *Opt. Mater*. **30** (2007) 375.
[2] H. K. Yang, K. S. Shim, B. K. Moon, B. C. Choi, J. H. Jeong, S. S. Yi and J. H. Kim. *Thin Solid Films* **516** (2008) 5577.
[3] P. Dorenbos. *J. Lumin.* **104** (2003) 239.

[P39]

Systematic Study of Up-Conversion Luminescence in $NaYF_4:Yb^{3+},R^{3+}$

Tero Laihinen[1,2], **Mika Lastusaari**[1,3], **Laura Pihlgren**[1], **Lucas C.V. Rodrigues**[4], **Jorma Hölsä**[1,3,4]

[1] *University of Turku, Department of Chemistry, Turku, Finland*
[2] *University of Turku Graduate School (UTUGS), Doctoral Programme in Physical and Chemical Sciences, Turku, Finland*
[3] *Turku University Centre for Materials and Surfaces (MatSurf), Turku, Finland*
[4] *Universidade de São Paulo, Instituto de Química, São Paulo-SP, Brazil*
Corresponding author e-mail address: tero.laihinen@utu.fi

1. Introduction

In up-conversion luminescence, the absorption of two or more low energy photons is followed by the emission of a high energy photon [1]. This phenomenon is usually more efficient when a sensitizer (*e.g.* Yb^{3+}) is used. The $NaYF_4$ material has been recognized as one of the most feasible hosts for efficient up-conversion luminescence, mainly due to the low phonon energy in $NaYF_4$ [2]. The up-conversion phosphors have many potential applications such as enhancing photosynthesis [3], solar cells and medical imaging [4].

In this work, $NaYF_4:Yb^{3+},R^{3+}$ (R: Pr, Nd, Sm, Eu and Tb - Tm) materials were obtained with the co-precipitation synthesis [5] to probe which lanthanides can be used as dopants with the Yb^{3+} sensitizer in the $NaYF_4$ host. The precipitates were annealed at 500 °C for 5 h in static N_2 + 10 % H_2 gas sphere to give the final products. The materials were studied with TG-DSC, FTIR and XPD methods. Up-conversion luminescence was obtained with NIR laser excitation at 976 nm which enables the excitation through the Yb^{3+} sensitizer.

2. Results

The DSC curves of the prepared materials show an exothermic signal at 400-500 °C due to the cubic-to-hexagonal phase transition of $NaRF_4$. The TG curves disclose small mass losses (*ca.* 2-4 %) during heating to 500 °C, attributed mainly due to the removal of water, ethanol and possible crystal water. The FTIR spectra do not reveal other impurities apart from water in the KBr discs. The XPD patterns confirm the hexagonal structure of the annealed materials. The up-conversion luminescence of Pr^{3+}, Nd^{3+}, Eu^{3+}, Tb^{3+}, Ho^{3+}, Er^{3+} and Tm^{3+} is observed in the presence of Yb^{3+}, although Nd^{3+}, Eu^{3+}, Tb^{3+} and Tm^{3+} do not have matching energy levels with Yb^{3+} (Fig. 1). The most intense luminescence is obtained with Er^{3+}, then with Ho^{3+} and Tm^{3+} doping (Fig. 2), as expected. The up-conversion luminescence is not obtained from Sm^{3+} and Dy^{3+}. This is probably due to efficient relaxation during the intermediate stages of stacking the NIR photons.

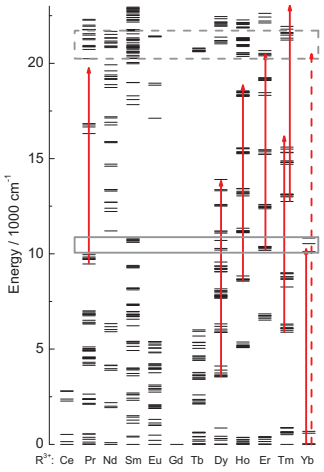

Fig. 1: Energy level schemes of the lanthanides (≤23000 cm^{-1}).

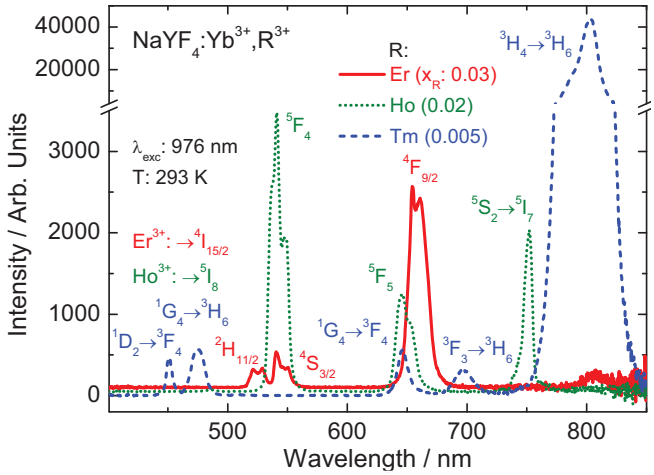

Fig. 2: Up-conversion luminescence spectra of the $NaYF_4:Yb^{3+},R^{3+}$ (R: Ho, Er or Tm) materials.

3. References

[1] F. Auzel. *Chem. Rev.* **104** (2004) 139.
[2] J. Zhao, Y. Sun, X. Kong, L. Tian, Y. Wang, L. Tu, J. Zhao and H. Zhang. *J. Phys. Chem. B* **112** (2008) 15666.
[3] T. Antal, E. Harju, L. Pihlgren, M. Lastusaari, T. Tyystjärvi, J. Hölsä and E. Tyystjärvi. *Int. J. Hydr. Energy* **37** (2012) 8859.
[4] M. Ylihärsilä, T. Valta, M. Karp, L. Hattara, E. Harju, J. Hölsä, P. Saviranta, M. Waris and T. Soukka. *Anal. Chem.* **83** (2011) 1456.
[5] G. Yi, H. Lu, S. Zhao, Y. Ge, W. Yang, D. Chen and L.-H. Guo. *Nano Lett.* **4** (2004) 2191.

[P40]

The influence of oxygen partial pressure on material properties of Eu^{3+}- doped Y_2O_2S thin films deposited by Pulsed Laser Deposition method

Abdub G. Ali[a*], Francis B. Dejene[a] and Hendrik C. Swart[b]

[a]Department of Physics, University of the Free State (Qwaqwa Campus), Private Bag X13, Phuthaditjhaba, 9866, South Africa.
[b]Department of Physics, University of the Free State, P.O. Box 339, Bloemfontein, 9300, South Africa.
* Corresponding author: E-mail: aliag@qwa.ufs.ac.za

1. Introduction

Eu^{3+}- doping has been of interest to improve the luminescent characteristics of thin-film phosphors. Europium-doped Y_2O_2S exhibits strong UV and cathode ray-excited luminescence, so it is widely used as red phosphors for low-pressure fluorescent lamps, cathode-ray tubes and plasma display panels [1]. Also, the hexagonal Y_2O_2S is a good host material for rare earth ions. In recent years, the Y_2O_2S: Eu has received much attention for its tremendous potential applications in optical display and lighting materials and basic science research on special luminescent spectra. Nanoscale and thin film Y_2O_2S: Eu has remarkably different luminescent properties from those of bulk samples: such as emission line broadens, lifetime changes and its spectra shift [2]. In this study Y_2O_2S: Eu thin films have been deposited with the pulsed laser deposition technique in an O_2 environment. The oxygen pressure was changed from 0 to 140 mtorr.

2. Results

The X-ray diffraction patterns (Fig.1) show mixed phases of cubic and hexagonal crystal structures. As the oxygen partial pressure increased, the crystallinity of the films improved. Further increase of the O_2 pressure to 140 mtorr reduced the crystallinity of the film. Similarly, both scanning electron microscopy and atomic force microscopy confirmed that an increase in O_2 pressure affected the morphology of the films. The average band gap of the films calculated from diffuse reflectance spectra using the Kubelka-Munk function was about 4.75 eV. The photoluminescence measurements (Fig.2) indicate red emission of Eu^{3+} doped Y_2O_2S thin films with the most intense peak appearing at 619 nm, which is assigned to the $^5D_0$-$^7F_2$ transition of Eu^{3+}. This most intense peak is totally quenched at higher O_2 pressures. This phosphor may be good promising material for applications in the flat panel displays.

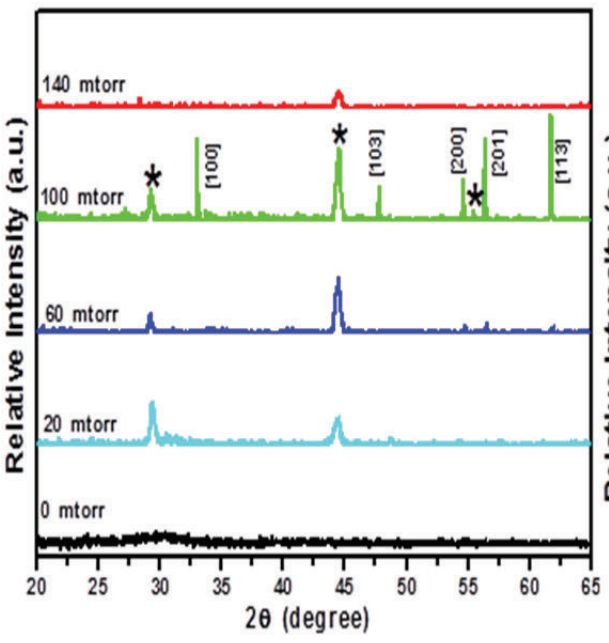

Fig.1: X-ray diffraction patterns of films deposited in vacuum and various O_2 partial pressures

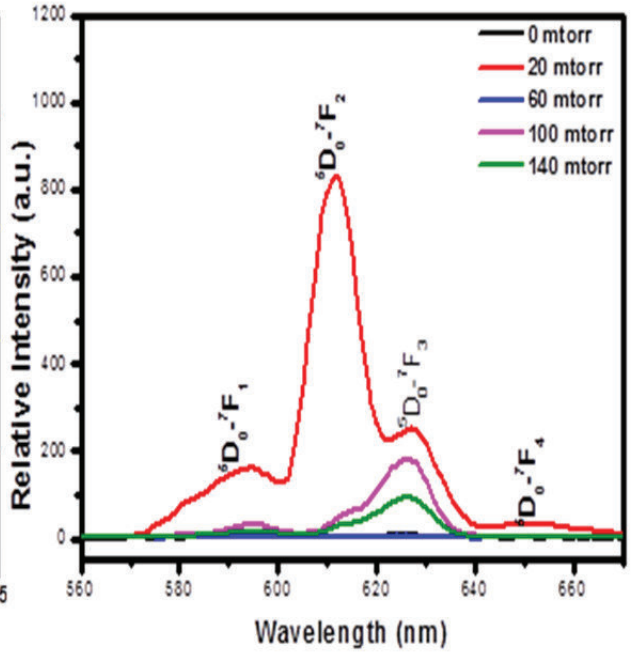

Fig. 2: Emission spectra for films deposited in vacuum and at various O_2 partial pressure

3. References

[1] H.T. Cui, G.Y. Hong, H.P. You, et al., J. Colloid Interface Sci. 252 (2002) 184.
[2] W. Kang, J. Park, D.K. Kim, K.S. Suh, Bull. Korean Chem. Soc. 22 (2001) 921.

[P41]

Interplay between Phase Transitions and Thermoluminescence in $BaAl_2O_4$

Mika Lastusaari[1,2], Lucas C.V. Rodrigues[1,3], Manu Lahtinen[4], Hermi F. Brito[3], Hendrik C. Swart[5], Jorma Hölsä[1-3]

[1]University of Turku, Department of Chemistry, FI-20014 Turku, Finland
[2]Turku University Centre for Materials and Surfaces (MatSurf), Turku, Finland
[3]University of São Paulo, Institute of Chemistry, São Paulo-SP, Brazil
[4]University of Jyväskylä, Department of Chemistry, Jyväskylä, Finland
[5]University of the Free State, Department of Physics, Bloemfontein, South Africa
Corresponding author e-mail address: jholsa@utu.fi

1. Introduction

The Eu^{2+} and R^{3+} (R: rare earth) doped alkaline earth aluminates (MAl_2O_4; M: Ca, Sr, Ba) are among the best persistent luminescence materials [1]. The most efficient is, however, $SrAl_2O_4:Eu^{2+},Dy^3$ – partly due to its emission in green to which the human eye is sensitive. Also the blue emitting $CaAl_2O_4:Eu^{2+},Nd^{3+}$ is more efficient than the barium one. All three materials should have similar properties since they have the stuffed tridymite (SiO_2) type structure. However, SiO_2 is known for polymorphism and MAl_2O_4 derived from this do not behave dissimilarly. Although $CaAl_2O_4$ seems to have only one form and $SrAl_2O_4$ two, for $BaAl_2O_4$ one knows one orthorhombic and two hexagonal [2] forms. These polymorphs are found at high temperatures quite far from the usual operating range (<200 °C) of persistent luminescent materials. Nevertheless, the role of possible low temperature phase transitions should not be excluded as a reason for the less good persistent luminescence performance of $BaAl_2O_4:Eu^{2+}(,R^{3+})$ [3,4]. Further studies are now carried out by using the high-temperature X-Ray Powder Diffraction (HT-XPD), Differential Scanning Calorimetry (DSC) and thermoluminescence (TL) methods.

2. Results

The HT-XPD patterns of $BaAl_2O_4$ (Fig. 1) at room temperature (RT) correspond to the hexagonal $P6_3$ form. Additional weak reflections may indicate symmetry decrease to *e.g.* orthorhombic but this needs further proof. The RT structure is not stable for more than some 50 °C before significant changes occur in the intensity of all reflections. Characteristic to these changes is that they occur over a wide temperature range and smooth changes seem to be the rule rather than the exception. The variation in intensity suggests displacement of atoms away from the reflection planes and changes may thus occur just in the space group. The DSC measurements were inconclusive since only a few broad signals and strong background variation were found instead of sharp signals. These features are in agreement with the slow and gradual nature of the changes in the XPD patterns. Both the HT-XPD and DSC results correlate well with the broad bands observed in the TL glow curves. When compared to the very simple (1 or 2 TL bands) glow curves of $CaAl_2O_4:Eu^{2+}$ or $SrAl_2O_4:Eu^{2+}$ (without R^{3+} co-doping), the five broad TL bands for $BaAl_2O_4:Eu^{2+}$ between 100 and 400 °C (Fig. 2) indicate a more complex trap structure with energies from 0.8 to 1.4 eV. Thus a reason for the inferiority of the $BaAl_2O_4$ host *vs.* $CaAl_2O_4$ and $SrAl_2O_4$ is clear: the close to continuous distribution of traps does not allow long-term storage of input energy but the bleaching of the traps occurs too rapidly. The persistent luminescence is then of short duration.

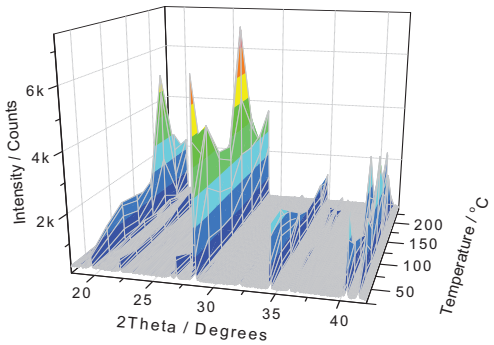

Fig. 1: The 3D XPD patterns of Eu^{2+} doped $BaAl_2O_4$ as a function of temperature from RT to 260 °C.

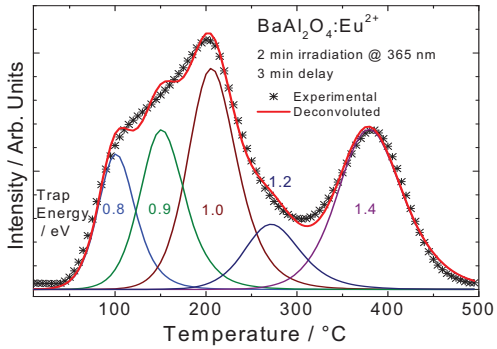

Fig. 2: The deconvoluted thermoluminescence glow curve for the Eu^{2+} doped $BaAl_2O_4$ showing a multitude, partially overlapping distribution of traps.

3. References

[1] H. F. Brito, J. Hölsä, T. Laamanen, M. Lastusaari, M. Malkamäki and L. C. V. Rodrigues. *Opt. Mater. Express* **2** (2012) 371.
[2] U. Rodehorst, M. A. Carpenter, S. Marion and C. M. B. Henderson. *Miner. Mag.* **67** (2003) 989.
[3] L. C. V. Rodrigues, J. Hölsä, J. M. Carvalho, C. C. S. Pedroso, M. Lastusaari, M. C. F. C. Felinto, S. Watanabe and H. F. Brito. *Physica B* **439** (2014) 67.
[4] B. M. Mothudi, M. A. Lephoto, O. M. Ntwaeaborwa, J. R. Botha and H. C. Swart. *Physica B* **407** (2012) 1620.

[P42]

Magneto-Optical Investigation of the Cyclic Redox $R_2O_2S \leftrightarrow R_2O_2SO_4$ (R: Eu, Tb) Reactions

Mika Lastusaari[1,2], Lucas C.V. Rodrigues[1,3], Cássio C.S. Pedroso[3], Rodrigo V. Rodrigues[3], Hermi F. Brito[3], Miroslav Maryško[4], Petriina Paturi[5], Jivaldo R. Matos[3], Jorma Hölsä[1-3]

[1]University of Turku, Department of Chemistry, FI-20014 Turku, Finland
[2]Turku University Centre for Materials and Surfaces (MatSurf), Turku, Finland
[3]University of São Paulo, Institute of Chemistry, São Paulo-SP, Brazil
[4]The Academy of Sciences of the Czech Republic, Institute of Physics, Cukrovarnická 10, CZ-162 53 Praha 6, Czech Republic
[5]University of Turku, Department of Physics and Astronomy, Wihuri Physical Laboratory, FI-20014 Turku, Finland
Corresponding author e-mail address: jholsa@utu.fi

1. Introduction

Impurities and dopants' inappropriate valences may deteriorate the performance of luminescent materials, cause waste of the high purity (rare earth) material and thus incur significant financial losses [1]. The methods used to detect elements' valence (XPS, Mössbauer and XANES) are not sensitive enough for low concentrations and EPR is not suitable for powders. Obtaining quantitative data leaves a lot to hope for, too. To make the things worse, the two most common rare earth dopants in phosphors, Eu^{3+} and Tb^{3+}, may exist in different oxidation states, Eu^{2+} and Tb^{IV} [1], as well. For the Eu^{3+} or Tb^{3+} doped R_2O_2S and $R_2O_2SO_4$, the Eu^{2+} or Tb^{IV} may be formed since the manufacture of these phosphors involve reducing and/or oxidizing conditions. The qualitative observation of Eu^{2+} can usually be made based on its intense luminescence due to the parity-allowed electric dipole $4f^6 \leftrightarrow 4f^5 5d^1$ transitions. In contrast, the Eu^{3+} line emission is weaker despite the high quantum yield. Tb^{IV} does not luminesce, but this species may absorb the emission of Tb^{3+} and, in addition, may facilitate non-radiative processes reducing the efficiency of Tb^{3+} doped phosphors even further [1].

2. Results

In this work, the comparison between the experimental and calculated temperature-dependent paramagnetic susceptibilities was used to obtain quantitatively the concentrations of the valence impurity in Eu_2O_2S (Eu^{2+}) and $Tb_2O_2SO_4$ (Tb^{IV}), both containing nominally only R^{3+}. The wave functions for the calculations were obtained from the analysis (Fig. 1) of the Eu^{3+} luminescence spectra [2,3]. Minute (ppm level) Eu^{2+} impurities could be defined due to the huge difference in the paramagnetic susceptibility of Eu^{2+} and Eu^{3+}. However, temperatures below 50 K are then needed (Fig. 2). In contrast, the Tb^{IV} impurity in the Tb^{3+} host can be determined already at higher temperatures but still with similar susceptibility measurements. The latter method is based on comparing the slopes of the Tb^{3+}/Tb^{IV} susceptibility *vs.* temperature curves. The results for the Tb^{3+}/Tb^{IV} couple are less sensitive than for the Eu^{2+}/Eu^{3+} one, however. Finally, the host independent temperature evolution of the paramagnetic susceptibility was calculated for Gd^{3+} (or Eu^{2+} or Tb^{IV}) to yield an analytical expression to be used universally.

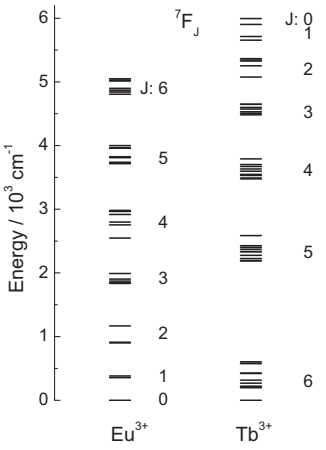

Fig. 1: The calculated ^7F_J (J = 0-6) energy level schemes for Eu^{3+} in Eu_2O_2S and Tb^{3+} in $Tb_2O_2SO_4$.

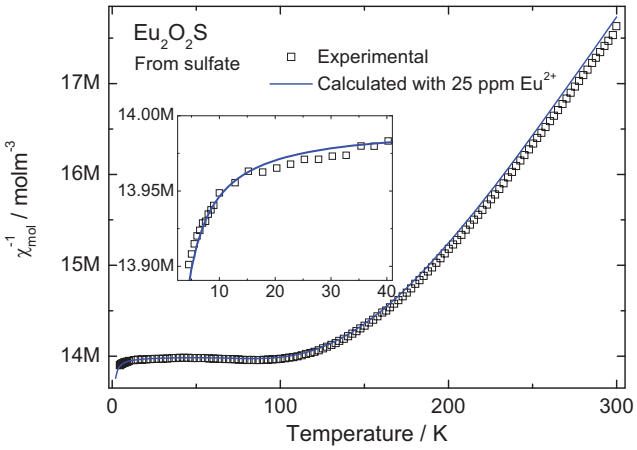

Fig. 2: The experimental and calculated paramagnetic susceptibilities of Eu_2O_2S with 25 ppm Eu^{2+}. Please note the y-scale.

3. References

[1] W. M. Yen, S. Shionoya and H. Yamamoto (Eds.). *Phosphor Handbook*, 2nd ed., (CRC Press, 2007).
[2] J. Sovers and T. Yoshioka. *J. Chem. Phys.* **51** (1969) 5330.
[3] P. Porcher, D. R. Svoronos, M. Leskelä and J. Hölsä. *J. Solid State Chem.* **46** (1983) 101.

[P43]

Pd doped ZnO nanostructures: Structural, luminescence and gas sensing properties

Gugu H. Mhlongo[1], **David E. Motaung**[1]
[1] *CSIR-National Centre for Nano-structured Materials, PO Box 395, 0001, South Africa*
Corresponding author e-mail address: gmhlongo@csir.co.za

1. Introduction

As a functional semiconductor, ZnO has been widely studied for various practical applications, including gas sensors [1]. Gas sensor is one of its important applications due to its high chemical and physical stability. It is well known that ZnO is n-type semiconductor and the responsible donors are usually identified as O vacancy (V_O), Zn interstitial (Zn_i), or complex defects [1]. Sensing properties of ZnO suffer from a lot of problems, such as high operation temperature, poor sensitivity, long response, and recovery time [2]. However, doping with different elements such Ag, Pd, Pt and so on [2], has long been verified to be an effective way to tailor the concentration of donors and acceptors in semiconductors, which is widely used to improve the gas sensing properties of metal oxide semiconductors. In this work, nanosized undoped and Pd (0.5 and 0.75 mol%) doped ZnO nanostructures were prepared using a sol-gel method. The microstructural, morphological and luminescent properties of the undoped and Pd doped ZnO nanostructures were conducted using XRD, XPS, SEM, and PL, respectively. The sensing behaviour of undoped, 0.5 and 0.75 mol% Pd doped ZnO nanostructured sensors towards NH_3 were also investigated at 200 ◦C.

2. Results

The SEM images of the undoped and Pd doped ZnO nanostructures (0.5 and 0.75 mol%) are shown in Fig. 1. SEM images obtained from both undoped and Pd-doped ZnO nanostructures (0.5 and 0.75 mol%) revealed similar morphology which indicates that the Pd doping has no major influence on the structures of ZnO. The changes in the current of undoped and Pd-doped ZnO nanostructured gas sensors upon exposure to NH_3 gas at 200◦C are shown in Fig. 2. As shown in figure 2, the current was shown to increase upon exposure to NH_3 gas, and then recovered to its initial value after NH_3 removal, indicating a good reversibility of these gas sensors.

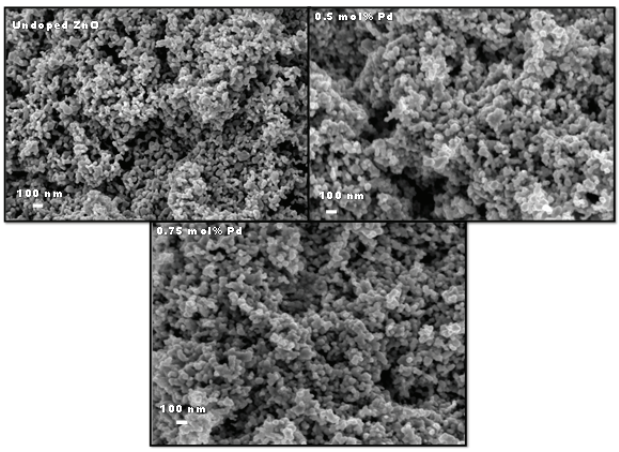

Figure 1

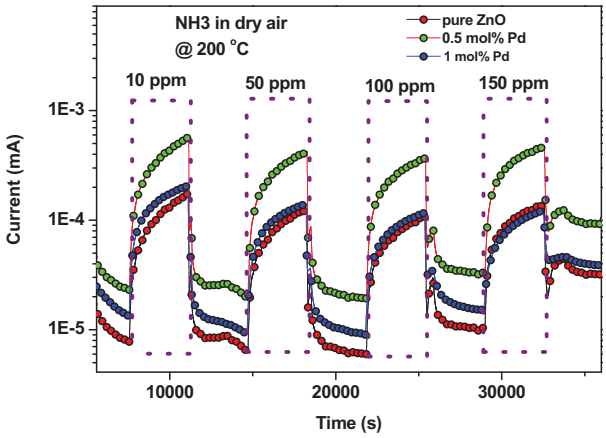

Figure 2

3. References

[1] G.J Kwak and K. J Yong *J. Phys. Chem.* C **112 (**2008) 3036
[2] L-L Xing, C-H Ma1, Z-HChen, Y-J Chen and X-Y Xue, Nanotechnology **22** (2011) 215501

Notes

Programme Overview
Morning Sessions

Time	Monday	Tuesday	Wednesday	Thursday	Friday
	4 May	5 May	6 May	7 May	8 May
5:30				GAME DRIVE	
7:00		BREAKFAST	BREAKFAST	BREAKFAST	BREAKFAST
8:00					
8:30		SESSION 1 Opening	SESSION 4 Notices		
8:40		André Vantomme	Rienk v Grondelle		
8:50					
9:00				SESSION 6 Notices	DEPARTURE
9:10		Kabongo	Tjaart Kruger	Ling	
9:20					
9:30		Carvalho			
9:40			David Cahen	Coelho	
9:50		Holtz			
10:00				Vinod Kumar	
10:10		Diale	DISCUSSION		
10:20				DISCUSSION	
10:30		DISCUSSION	TEA		
10:40				TEA	
10:50		TEA	SESSION 5 Hulicius	SESSION 7 Birch	
11:00					
11:10		SESSION 2 Adi Salomon			
11:20			Akande	Engelbrecht	
11:30					
11:40		Koao	Wamwangi	Aissa	
11:50					
12:00		Lee	Urgessa	Van Dyk	
12:10					
12:20		DISCUSSION	DISCUSSION	DISCUSSION	
12:30					
12:40		LUNCH	LUNCH	LUNCH	
12:50					
13:00					
13:10					

Programme Overview
Afternoon Sessions

Time	Monday	Tuesday	Wednesday	Thursday	Friday
	4 May	5 May	6 May	7 May	8 May
12:40		LUNCH	LUNCH	LUNCH	
12:50					
13:00					
13:10					
13:20					
13:20					
13:30		SESSION 3 Craciun	POSTER SESSION 2	SESSION 8 Hölsä	
13:40					
13:50				Abbass	
14:00	REGISTRATION	Janzén			
14:10				Pandey	
14:20		Omotoso			
14:30				Ayabei	
14:40		Tankio Djiokap			
14:50				DISCUSSION	
15:00		DISCUSSION	TEA	TEA	
15:10		TEA			
15:20		POSTER SESSION 1	POSTER SESSION 2 (Continued) 14:00 – 16:00	SESSION 9 Visser	
15:30					
15:40				Duvenhage	
15:50					
16:00				Mulwa	
16:10					
16:20			GAME DRIVE / Sundowners	Munyati	
16:30					
16:40				DISCUSSION	
16:50					
17:00					
15:20					
18:00	WELCOME (Restaurant)				
19:00	DINNER	DINNER	DINNER	DINNER	
20:30					

University of Pretoria
Department of Physics

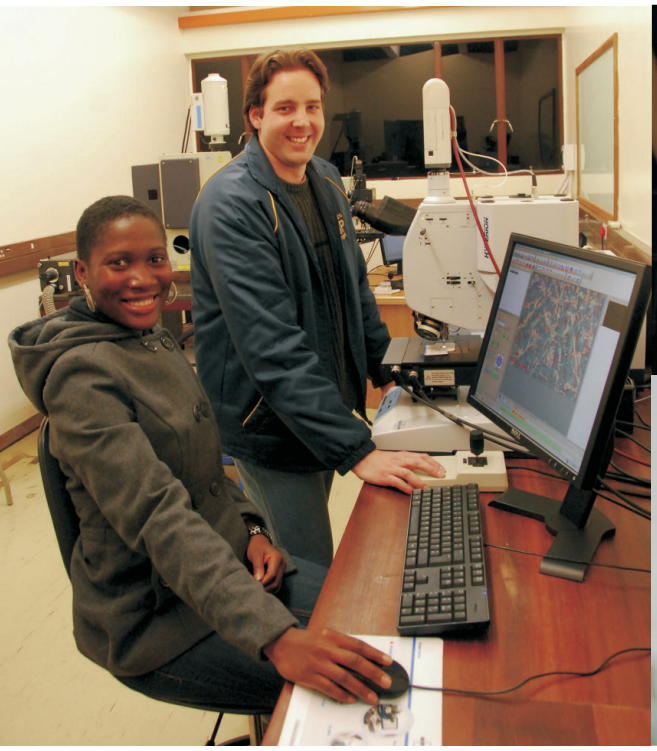
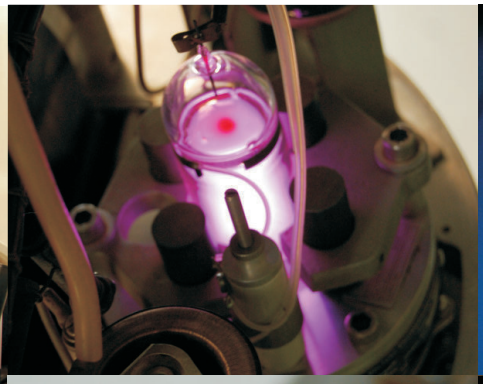
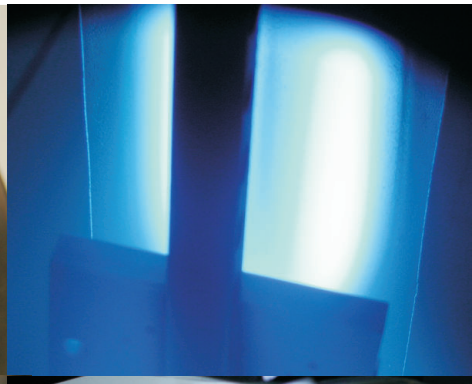
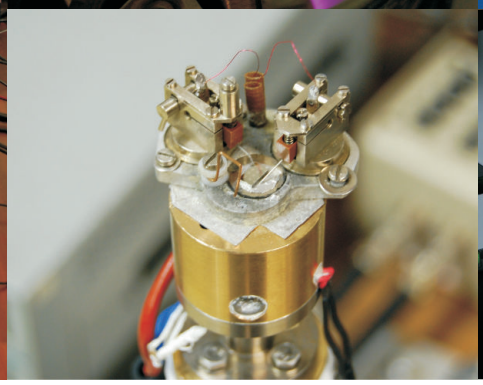


We offer postgraduate opportunities in the following research focus areas

Materials
- Nuclear applications
- Under irradiation
- Solar cells
- Opto-electronics
- Carbon-based
- Nano-magnetism

Theoretical Physics
- Mathematical physics
- High energy theory
- Quantum resonances theory
- Quantum information theory
- Computational solid state physics
- Symmetries and group theory

Astronomy

Biophysics

Physics Education

Enquiries about postgraduate studies

Head: Department of Physics
University of Pretoria
Private Bag X20, Hatfield, 0028

Email: Chris.Theron@up.ac.za
Tel: +27 12 420 2455
Fax: +27 12 362 5288
Web: **http://www.up.ac.za/physics**

UNIVERSITEIT VAN PRETORIA
UNIVERSITY OF PRETORIA
YUNIBESITHI YA PRETORIA
Faculty of Natural and Agricultural Sciences